Electrochemical Society

UNIV. OF MICHIGAN
NOV 10 1953
EAST ENGINEERING
LIBRARY

ELECTROCHEMICAL INDUSTRY

Canada

UNIVERSITY OF MICHIGAN LIBRARIES

Courtesy Ethyl Corporation

Chlorine ...

for antiknock compounds

Ethyl chloride, ethylene dichloride and ethylene dibromide play an important part in the manufacture of antiknock compounds for combustion engine gasolines.

Uniformly high quality GLC Graphite Anodes play an important part too—in helping the electrolytic industry meet the growing civilian and defense needs for chlorine and caustic soda.

ELECTRODE DIVISION

Great Lakes Carbon Corporation

Niagara Falls, N.Y. GLC Morganton, N. C.

Graphite Anodes, Electrodes, Molds and Specialties

Sales office: Niagara Falls, N.Y. **Other offices:** New York, N.Y., Oak Park, Ill., Pittsburgh, P

Sales Agents: J. B. Hayes, Birmingham, Ala., George O'Hara, Long Beach, Cal., Great Northern Carbon & Chemical Co., Ltd., Montreal, Can

DITORIAL STAFF

. M. Burns, *Chairman*
orman Hackerman, *Technical Editor*
uth G. Sterns, *Managing Editor*
ecil V. King, *Associate Editor*
. B. Thomas, *News Editor*
ary F. Murray, *Assistant Editor*

IVISIONAL EDITORS

. V. Petrocelli, *Corrosion*
ner Brenner, *Electrodeposition*
. C. Vosburgh, *Battery*
. C. Froelich, *Electronics*
. C. Gardiner, *Industrial Electrolytic*
. J. Sindeband, *Electrothermic*
ohn J. Chapman, *Electric Insulation*
arl Wagner, *Theoretical*
herlock Swann, Jr., *Electro-Organic*

EGIONAL EDITORS

oseph Schulein, *Pacific Northwest*
. C. Schumacher, *Los Angeles*
. W. Storey, *Chicago*
. W. Heise, *Cleveland*
aul S. Brallier, *Niagara Falls*
liver Osborn, *Houston*
arl A. Gulbransen, *Pittsburgh*
. C. Holm, *Canada*
. W. Cuthbertson, *Great Britain*
. L. Rama Char, *India*

DVERTISING OFFICE

ack Bain
dvertising Manager
45 Fifth Avenue
ew York 17, N. Y.
hone—*Murray Hill 2-3345*

Journal of the

Electrochemical Society

NOVEMBER, 1953 VOL. 100 · NO. 11

CONTENTS

Regional Features

Electrochemical Industry of Canada—Editorial. *A. F. G. Cadenhead* 293*C*
The Electrochemical and Electrometallurigcal Industries of Canada. *V. G. Bartram* 295*C*

Technical Papers

The Rate of Dissolution of Zinc and Cadmium in Chromic Chloride Solutions. *Cecil V. King and Natalie Mayer* ... 473
Some Properties of Tin-II Sulfate Solutions and Their Role in Electrodeposition of Tin, II. Solutions with Tin-II Sulfate and Sulfuric Acid Present. *Clarence A. Discher* 480
Electroplating on Titanium. *William H. Colner, Morris Feinleib, and John N. Reding* 485
An X-Ray Study of the Effect of Organic Compounds on the Crystal Growth of Nickel during Electrodeposition. *Francis Denise and Henry Leidheiser, Jr.* 490
Copper-Activated Zinc Sulfide Phosphors with Trivalent Substituents. *H. C. Froelich* 496
Electrical Conductivity and Density of Molten Cryolite with Additives. *Junius D. Edwards, Cyril S. Taylor, Lee A. Cosgrove, and Allen S. Russell* 508
Correlation of Limiting Currents under Free Convection Conditions. *C. R. Wilke, M. Eisenberg, and C. W. Tobias* ... 513
Thermodynamics of the Acid Weston Cell and the Acid Clark Cell. *Carl Wagner* 524

Technical Note

Iron Contamination of Storage Batteries. *E. Willihnganz* ... 527

Technical Review

On the Electrochemistry of Ion-Exchange Resins—A Review of Recent Work. *K. S. Spiegler* 303*C*

Current Affairs

Death of Colin G. Fink 317*C*
Division News 318*C*
Section News 318*C*
Personals 319*C*
New Members 319*C*
Letter to the Editor 320*C*
Book Reviews 320*C*
Recent Patents 321*C*
Literature from Industry 323*C*
New Products 324*C*
Employment Situations 324*C*

Published monthly by The Electrochemical Society, Inc., Mount Royal and Guilford Aves., Baltimore 2, Md., combining the JOURNAL and TRANSACTIONS OF THE ELECTROCHEMICAL SOCIETY. Editorial offices: 216 West 102nd Street, New York 25, N. Y. Statements and opinions given in articles and papers in the JOURNAL OF THE ELECTROCHEMICAL SOCIETY are those of the contributors, and The Electrochemical Society assumes no responsibility for them. Subscription $11.25 to members, $15.00 to nonmembers. Single copies $1.25 to members, $1.50 to nonmembers. Copyright 1953 by The Electrochemical Society, Inc. Entered as second-class matter November 15, 1947, at the Post Office at Baltimore, Md., under the act of August 24, 1912.

UNIVERSITY OF MICHIGAN LIBRARIES

SARGENT SLOMIN

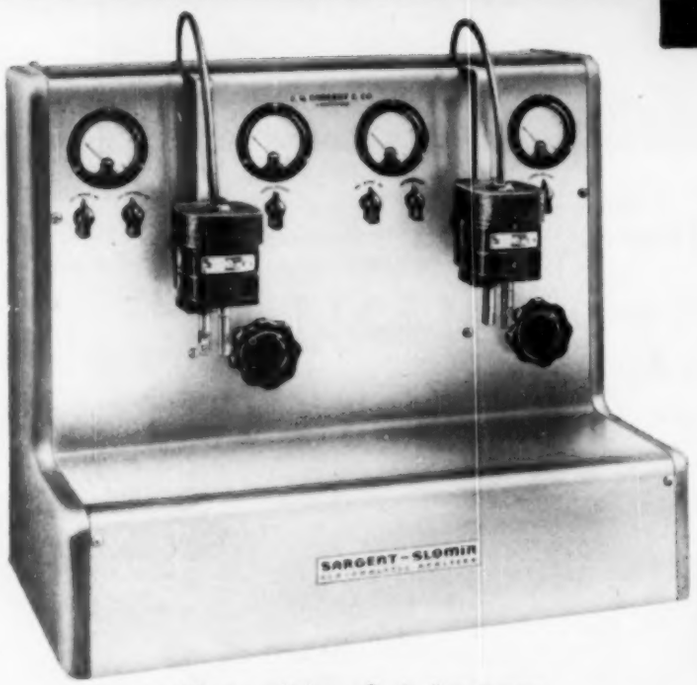

Motor-Stirred 5 Ampere

SARGENT HEAVY DUTY

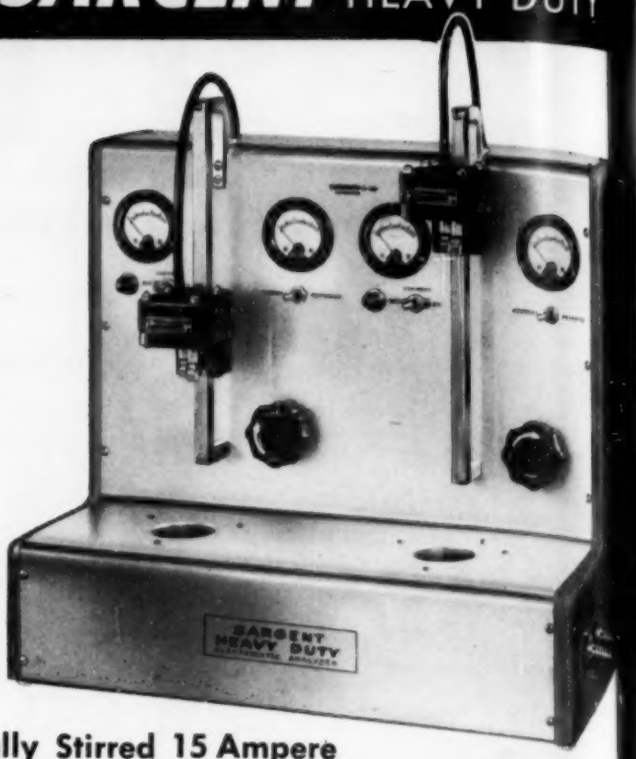

Magnetically Stirred 15 Ampere

Designed for continuous trouble-free performance, these electrolytic analyzers, manufactured by E. H. Sargent & Co., are durably constructed of the highest grade materials and component parts, including stainless steel front panel, cast aluminum end castings and stainless steel fittings.

Completely line operated, the Sargent analyzers employ self-contained rectifying and filter circuits. The deposition voltage between the electrodes is adjusted by means of auto-transformers, with meters indicating volts and amperes and controls on the panel. An easily replaceable fuse guards against circuit overload.

The Sargent-Slomin Analyzer stirs thorugh a rotating chuck operated from a capacitor type induction motor, motor having a fixed speed of 550 r.p.m. with 60 cycle A.C. current or 460 r.p.m. with 50 cycle A.C. current. Motors are sealed against corrosive fumes; are mounted on cast metal brackets, sliding on ½" square stainless steel rods, permitting vertical adjustment of electrode position over a distance of 4". Pre-lubricated ball-bearings support the rotating shaft.

The Sargent Heavy Duty Analyzer provides efficient stirring by the interaction between the cell current and the field established by a permanent magnet, tubular in shape and coaxial with the cell holder.

The Heavy Duty has recessed wells to hold the sample beakers, wells being 6¼" deep, designed to contain 250 ml electrolytic beakers. The wall of each well serves as an inner wall of the water jacket, for use in either heating or cooling. Two serrated nipples for rubber tubing connections for cooling or heating water are mounted on the right end casting. In plain copper analysis, 1 gram of copper may be deposited in 15 minutes with an accuracy of approximately 0.05% without the necessity of special techniques.

All electrolytic analyzers accommodate electrodes having shaft diameters no greater than 0.059 inch. Stainless steel spring tension chucks permit quick, easy insertion of the electrodes and maintain proper electrical contact. On the Heavy Duty Analyzer, the cathode chuck is eccentrically mounted, providing adjustability to accommodate electrodes up to 50 mm diameter. Special Sargent high efficiency electrodes are available for both analyzers.

Analyzers are complete with cord and plug for attachment to standard outlets. For operation from 115 volt, 50 or 60 cycle A.C. circuits.

	SARGENT-SLOMIN	HEAVY DUTY
Maximum D.C. current at each position	5 ampere	15 ampere
Maximum D.C. voltage at each position	10 volts	10 volts
Maximum power consumption	150* or 300 watts	400 watts
Height	18 inches	20¼ inches
Width	11¼* or 21 inches	21 inches
Depth	11¼ inches	11¼ inches
Net Weight	35* or 61 pounds	80 pounds
Shipping Weight	70* or 110 pounds	130 pounds

*One position unit

S-29459 ELECTROLYTIC ANALYZER — Motor Stirred, One Position, 5 Ampere, SARGENT-SLOMIN. (Not illustrated here) $275.00

S-29464 ELECTROLYTIC ANALYZER — Motor Stirred, Two Position, 5 Ampere, SARGENT-SLOMIN. (Illustrated above) $425.00

S-29480 ELECTROLYTIC ANALYZER — Heavy Duty, Magnetically Stirred, Two Position, 15 Ampere, Sargent. (Illustrated above) $575.00

(The Sargent-Slomin Analyzers are also available with integral, concealed heater unit.)

SARGENT

NEW SARGENT CATALOG — NOW AVAILABLE

SCIENTIFIC LABORATORY INSTRUMENTS · APPARATUS · SUPPLIES · CHEMICALS

E. H. SARGENT & COMPANY, 4647 W. FOSTER AVE., CHICAGO 30, ILLINOIS

MICHIGAN DIVISION, 1959 EAST JEFFERSON STREET, DETROIT 7, MICHIGAN

SOUTHWESTERN DIVISION, 5915 PEELER STREET, DALLAS 9, TEXAS

The Rate of Dissolution of Zinc and Cadmium in Chromic Chloride Solutions[1]

CECIL V. KING AND NATALIE MAYER

Department of Chemistry, New York University, New York, New York

ABSTRACT

The relative potentials of the zinc-zinc ion, chromous-chromic ion systems might lead one to expect smooth progress of the reaction $Zn + 2Cr^{+++} \rightarrow Zn^{++} + 2Cr^{++}$. However, various other reactions are possible, and the dissolution or corrosion process is complicated; it is electrochemical in nature, and, in some solutions, rapid enough to permit transport control of the rates. The dissolution rate is highly dependent on the form of chromic ion present, on pretreatment of the metal surface, in some solutions on the acidity, and, under some conditions, the main reaction is hydrogen evolution with little reduction of chromic ion.

INTRODUCTION

The dissolution of zinc in chromic chloride solutions was chosen for study for a number of reasons. The reduction of chromic ion to chromous does not require conversion of hydrogen ion to water as is usual with "depolarizers." The normal potentials of oxidizing and reducing couples are not dependent on hydrogen ion concentration; they are not widely different, but will allow essentially complete reaction:

$$Zn + 2Cr^{+++} \rightarrow Zn^{++} + 2Cr^{++} \qquad E^0 = 0.35 \text{ v.}$$

It was desired to compare the reaction kinetically with reactions of similar type, for example, the oxidation of copper and silver by ferric and ceric ions (1-3). Finally, it was hoped to compare the reaction of zinc with that of iron and cadmium, where the driving potentials are smaller; this aim has been only partly realized.

Several reactions can and do complicate the dissolution-reduction process. Chromic chloride solutions are acidic through hydrolysis, and, while pure zinc scarcely reacts with pure acid of such *p*H, catalytic hydrogen evolution becomes important in some solutions. Chromous salts are metastable in even slightly acid solutions:

$$2Cr^{++} + 2H^+ \rightarrow 2Cr^{+++} + H_2 \qquad E^0 = 0.05 \text{ v at } p\text{H} = 6.$$

Nevertheless, stable solutions of chromous salts can be prepared for analytical use by quantitative reduction of acidified chromic salts (or dichromate) by amalgamated zinc (4). Platinum and other substances catalyze the reaction with hydrogen ion, and the reversible Cr^{++}–Cr^{+++} potential cannot be established on a platinum electrode (5). Oxygen reacts rather rapidly and, eventually, completely with chromous ion, but even traces of oxygen make the reversible potential measurements difficult (5).

It is possible for zinc to carry the reduction to metallic chromium

$$Cr^{++} + Zn \rightarrow Cr + Zn^{++} \qquad E^0 = 0.05 \text{ v.}$$

There is no direct proof in the present research that this reaction takes place, since chromium was not identified as a product. However, hydrogen evolution with zinc and its absence with cadmium seems probably due to the formation of zinc-chromium couples.

The rate of dissolution is highly dependent on the form of chromic ion present. Aqueous chromic chloride solutions contain (6) the green dichlorotetraaquo ion $CrCl_2(H_2O)_4^+$ and the purplish-blue (violet when very dilute) hexaaquo ion $Cr(H_2O)_6^{+++}$. At equilibrium, all of the ion is in the purple form in solutions up to $0.6M$, while more concentrated solutions contain increasing amounts of the green form (42% at $8M$). Solutions freshly prepared from the green hydrated salt contain the green ion, which changes to the purple ion or the equilibrium mixture slowly, requiring 18 hours or more at 25°C. Acidity favors the purple form, but inhibits the attainment of equilibrium; if acid is added to a freshly prepared dilute green solution, it remains green indefinitely.

This rather complicated behavior is explained as follows (7): conversion of green ion to violet occurs in two stages, and requires the presence of hydroxyl ions

$$CrCl_2(H_2O)_4^+ + 2OH^- \rightleftharpoons Cr(OH)_2(H_2O)_4^+ + 2Cl^-$$
$$Cr(OH)_2(H_2O)_4^+ + 2H^+ \rightleftharpoons Cr(H_2O)_6^{+++}$$

[1] Manuscript received January 20, 1953. This paper was prepared for delivery before the Wrightsville Beach Meeting, September 13 to 16, 1953. From a Ph.D. thesis submitted by Natalie Heyman Mayer to the Graduate School of New York University, February 1953. Work done under Contract AT (30-1)-816 of the U. S. Atomic Energy Commission with New York University.

UNIVERSITY OF MICHIGAN LIBRARIES

The first reaction takes place slowly in dilute acid, not at all in more concentrated acid. The intermediate ion is green. If a small amount of base (not enough to precipitate the hydroxide) is added to a dilute green solution, displacement of chloride takes place rapidly; acidification after a few minutes gives the purple form at once.

The two forms have different hydrolysis constants (8): K (green) = 1.9×10^{-6}; K (purple) = 1.6×10^{-4} at 25°C. (These are for the first stage of hydrolysis, and the values vary considerably with ionic strength of the solution.) Formation of purple ion from green automatically slows down the conversion, since it increases the acidity.

Experimental

Cylinders of Special Purity zinc,[2] about 2.5 cm long and 2.0 to 1.6 cm in diameter (decreasing with use), were rotated in the solutions as in previous work (1–3). A few experiments with analytical grade zinc showed no significant difference except in hydrochloric acid alone. Some experiments were done with cadmium cylinders of similar dimensions; the metal was of best commercial grade.

All solutions were deaerated, and the experiments were carried out under nitrogen. The purple solutions were prepared by boiling, then cooling and storing under nitrogen until equilibrated (all solutions are green at the boiling point). Green solutions were prepared by dissolving the salt in, and diluting with, deaerated distilled water, with nitrogen continuously bubbling through.

Since the hydrated chromic chloride is hygroscopic, solutions were made at the approximate concentration desired, and analyzed. Stock solutions were made when possible, but many of the green solutions had to be used immediately. For analysis, the chromic ion was oxidized to chromate with sodium peroxide, excess being decomposed by boiling; then phosphoric acid and excess standard ferrous sulfate were added, and the remaining ferrous ion titrated with standard dichromate, using diphenylamine sulfonic acid as indicator. Mean concentrations are given below, and the actual concentrations were seldom more than 3 per cent different.

In some of the runs, a 600-ml beaker was used, and it was equipped with a plastic refrigerator bowl cover with close-fitting holes to admit the motor shaft, nitrogen inlet tube, etc. When it was desired to use small samples to be discarded after a few minutes, run, 65 to 100 ml of solution was placed in a small square bottle with neck slightly larger than the cylinder and Bakelite sleeve which covered the extended motor shaft. Nitrogen was admitted through a tube fitted into a hole in the side of the bottle. In both methods, air was largely, though not rigorously, excluded.

[2] New Jersey Zinc Sales Company, New York, N. Y.

At first, the temperature was maintained at 30° ± 0.1°C, but when the temperature coefficient was found to be low and the reproducibility of rates poor, most of the experiments were done at room temperature, between 25° and 30°C.

All rates were measured by weighing the cylinders, which were initially abraded and finally polished with No. 600 silicon carbide paper, or were etched after such polishing, as described below. Average weight losses per minute in short runs are plotted in the graphs. These may be taken as approximately "instantaneous" rates, except where the rate is obviously changing rapidly with time.

In the polarization experiments, current was supplied by dry cells and measured with calibrated meters. Electrical connection was made through mercury in a steel cup mounted on the motor shaft; a steel spring, fitted in a slot in the motor shaft extension, helped to make good contact with the metal cylinders. A platinum sheet 8 x 12 cm served as a second electrode.

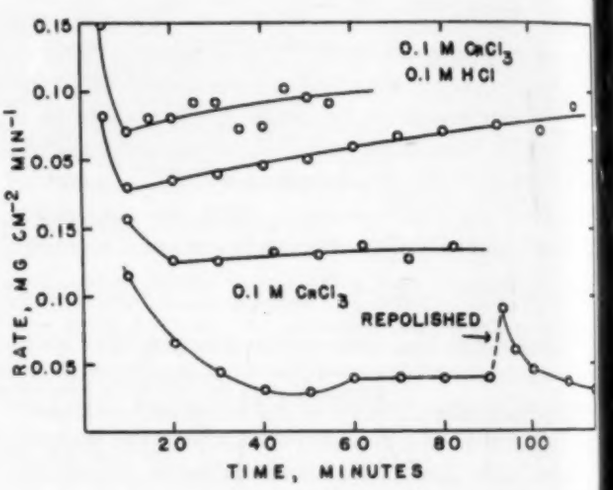

Fig. 1. Zinc cylinder (1.9 cm diameter) rotated in 500 ml purple chromic chloride solution at 2160 rpm, 30°C.

Experiments with Purple Solutions

The cylinders were rotated for periods of 2 to 15 min, at 2160 rpm (~12000 cm/min peripheral speed), in 500 ml of solution at 30°C. During this time, 6 to 20 mg zinc ordinarily dissolved; after weighing, the cylinder was reimmersed in the same solution. The metal was polished at the start of each series of runs; the surface soon became dull and, in time, developed a gray-black film. The rates behaved as shown in Fig. 1 and 2. Results in identical solutions were similar, but varied widely in successive runs, either with the same or with different cylinders. Different methods of polishing, including

bringing the zinc surface to a bright mirror finish in chromic acid etching baths, gave similar results.

Hydrogen evolution always accompanied the dissolution, and, even in runs of several hours duration, there was no evidence of reduction of chromic to chromous ion in the bulk of the solution. Low concentrations of added hydrochloric acid had little effect; larger amounts increased the rate appreciably, and diminished the amount of black film formation. In long runs, the cylinders developed a few deep pits. If not removed completely by abrading the cylinders, these developed further in subsequent runs; eventually a few new pits would appear.

Analysis of the gray-black film proved difficult. Enough was scraped from a cylinder to subject to x-ray analysis, but it showed no crystalline structure. The film was allowed to develop in several 3- to 5-hour runs, and removed each time in the same

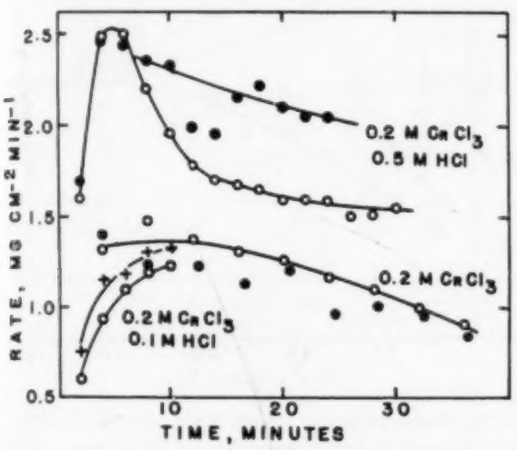

FIG. 2. Zinc cylinder (1.9 cm diameter) rotated in 500 ml purple chromic chloride solution at 2160 rpm, 30°C.

sample of dilute nitric acid. The solution was colorless and gave no test for any chromium salt.

When rotated, the metal acquires and maintains only a very thin film. When left stationary in the solution for 24 hours, a thicker film is formed. This is not removed by dilute nitric acid, but turns green in concentrated nitric acid. It can then be removed in boiling, dilute hydrochloric acid, and gives a green solution containing chromic chloride.

This seems to identify the initial black film as chromous oxide CrO, which does not dissolve in dilute acids, but is oxidized to Cr_2O_3 by concentrated nitric acid. Evidently hydrogen evolution at the zinc surface causes the *p*H to rise, and all chromous ion formed is precipitated as CrO. It is possible that chromic hydroxide or oxide is also formed, but this could not be proved.

A sample of 0.15*M* purple chromic chloride (50 ml) was run slowly through a Jones reductor column filled with dry, 20–30 mesh (unamalgamated) zinc; the *p*H of the solution increased from 2.3 to 3.9, but there was no apparent reduction. After thorough washing, dilute sulfuric acid was run through, and the emerging solution was intensely green in color. Evidently chromic hydroxide or a basic salt had been retained on the zinc. If either a chromous compound or metallic chromium was formed, it was not evident.

Initial rates (i.e., with the zinc repolished for each point) were now run, with a wide range of added hydrochloric acid; the results are shown in Fig. 3. The more acid solutions were green, since they were deaerated by boiling, and it was not known at the time that the presence of acid would prevent equilibration on cooling. Hydrogen evolution was copious, and the green solutions changed to purple in longer runs. This is due to the pronounced increase in *p*H at the zinc surface, which allows exchange of

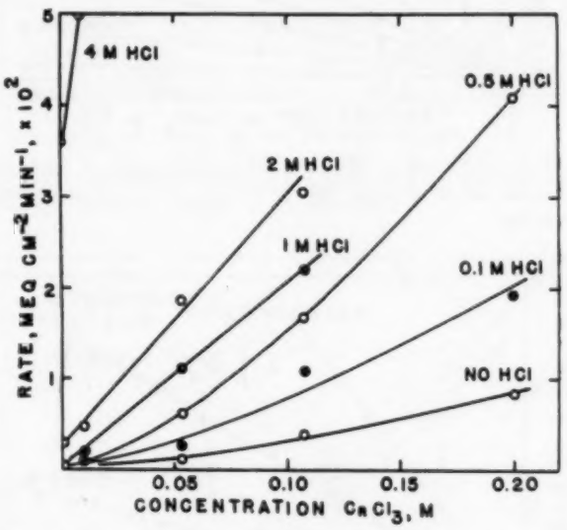

FIG. 3. Effect of HCl on dissolution rate of zinc cylinder at 2160 rpm, 25°–30°C, 65 ml chromic chloride solution.

hydroxyl for chloride in the green ion, with subsequent conversion to purple ion in the bulk of the solution.

In these runs the zinc surface always became gray, but definite films were not evident in the more acid solutions. Even in long runs the solutions did not change to the characteristic blue of chromous chloride, nor could chromous hydroxide be identified on the addition of base. There was no way of testing for metallic chromium on the zinc surface, although it was suspected that this was responsible for the hydrogen evolution.

For comparison, similar experiments were carried out with cadmium cylinders of similar dimensions. While cadmium can reduce chromic ion to chromous with the concentrations used here, it cannot carry the reduction to metallic chromium:

$$Cd + Cr^{++} \rightarrow Cd^{++} + Cr \qquad E^0 = -0.31 \text{ v.}$$

UNIVERSITY OF MICHIGAN LIBRARIES

The rates obtained are plotted in Fig. 4 and 5. Rates for both zinc (Fig. 3) and cadmium are given in milliequivalents to facilitate comparison.

Cadmium dissolves about half as fast as zinc under these conditions; no visible films are formed on the surface, no hydrogen is evolved, and, in longer runs (45 min or more), much of the chromic ion is reduced. The more acid green solutions change, not to purple, but to the characteristic blue of chromous chloride. Addition of sodium hydroxide precipitates

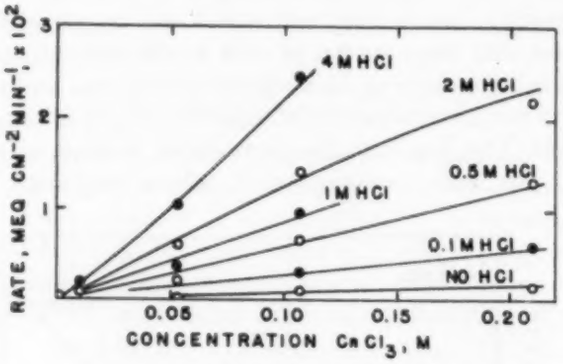

FIG. 4. Effect of HCl on dissolution rate of cadmium cylinder at 2160 rpm, 25°–30°C, 65 ml chromic chloride solution.

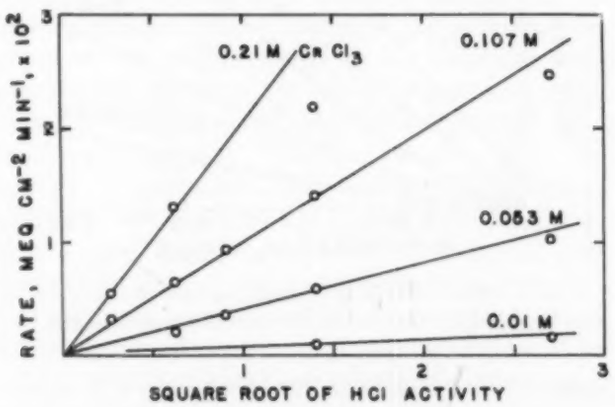

FIG. 5. The rates of Fig. 4 vs. square root of HCl activity

yellow-brown $Cr(OH)_2$, which slowly changes to blue-green $Cr(OH)_3$ in the air.

None of these rates are additive for acid and chromic ion. The difference in reactivity of zinc and cadmium in deaerated hydrochloric acid alone is very evident. Cadmium dissolves at a scarcely appreciable rate even in 4*M* HCl on the scale of Fig. 4; zinc dissolution increases exponentially with acid concentration.

Experiments with Green Solutions

The cylinders were rotated in 65-ml samples of solution for periods of ½ to 5 min, during which time 20 to 50 mg of zinc ordinarily dissolved. The rates increase as the zinc becomes etched, as shown in Fig. 6, levelling off in 15 to 40 min, depending on the concentration. The rates were more reproducible with etched zinc, but, if not used for a day or more, a cylinder had to be re-etched for some time to repeat the maximum rate.

The experiments described below were done with etched cylinders. The zinc surface became dull, but no corrosion film was apparent. Each cylinder consisted of only a few single crystals which were clearly visible. The surface remained smooth to the eye and touch, but under the microscope appeared very rough, each crystal looking somewhat like the surface of a corroded file. There was no pitting; in the course of the experiments some crystal faces dissolved more

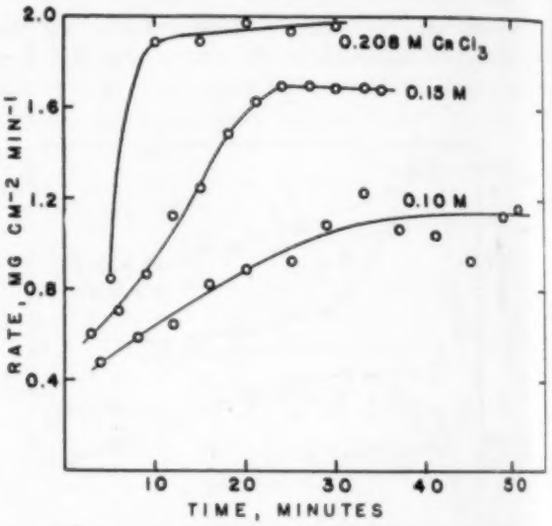

FIG. 6. Zinc cylinder (1.8 cm diameter) rotated in 65 ml green chromic chloride solution at 2160 rpm, 23°–25°C, fresh solution for each point. Another run in 0.15*M* $CrCl_3$ rose more slowly to 1.63 after 65 min.

than others, resulting in flattened spots on the cylinders.

Hydrogen evolution was visible in somewhat less than half these experiments, and began suddenly after a few minutes of rotation in the solution. It appeared to be a chance occurrence and showed no correlation with conditions or concentration. When hydrogen was evolved, the rates were less reproducible, but not distinctly low or high. In longer runs, the solutions changed to purple when hydrogen was produced, and there was no test for chromous ion; if no hydrogen was evolved, in 45 min or more the solution became blue and $Cr(OH)_2$ could be precipitated.

Fig. 7 shows the effect of rotational speed of the cylinder on the rate, and Fig. 8 gives more details of the dependence of rate on concentration. It will be shown below that most of these rates are in the range of diffusion (or transport) control, but it is obvious that this is not true for all concentrations and ro-

tational speeds, since, if it were, the rates would be linear with both variables.

Temperature Coefficients

Rates were measured in two green chromic chloride solutions at two rotational speeds, at temperatures between 10° and 70°C, and the results are shown in

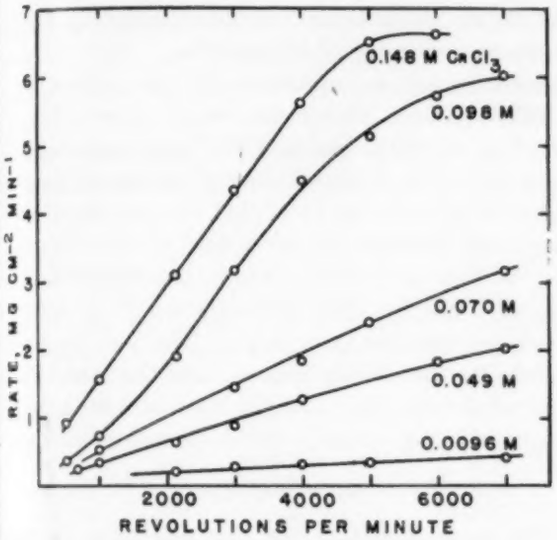

FIG. 7. Etched zinc cylinders rotated in 400 ml green chromic chloride at 27°C.

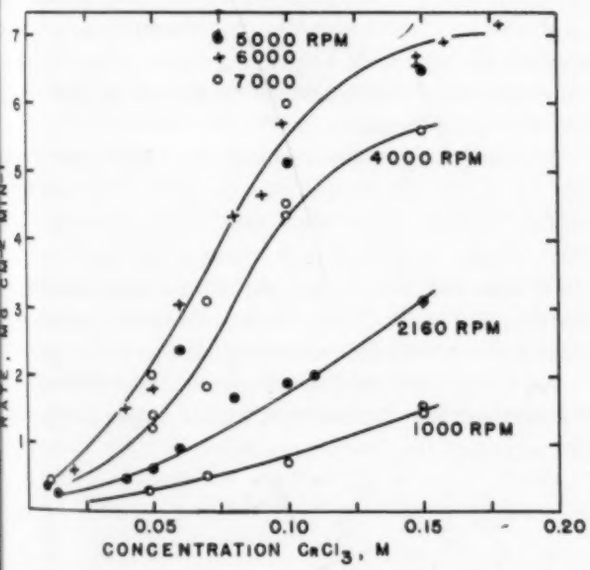

FIG. 8. Etched zinc cylinders rotated in 400 ml green chromic chloride at 27°C.

Fig. 9. The solutions used are permanently green at the boiling point, but change fairly rapidly to purple between 50° and 70°C. Consequently, a 400-ml sample was heated rapidly to the appropriate temperature and the rotating cylinder immediately immersed for a 30- or 60-sec period. The highest weight loss was 83 mg in 30 sec. Because of the method, the accuracy is not high.

The change in slope of the curves for 6000 rpm above 50°C indicates a change in mechanism rather than conversion to the purple ion, since it does not occur at 2160 rpm. The lower-temperature slopes give activation energies lying between 4000 and 6000 cal/equivalent, which is in the range of diffusion activation.

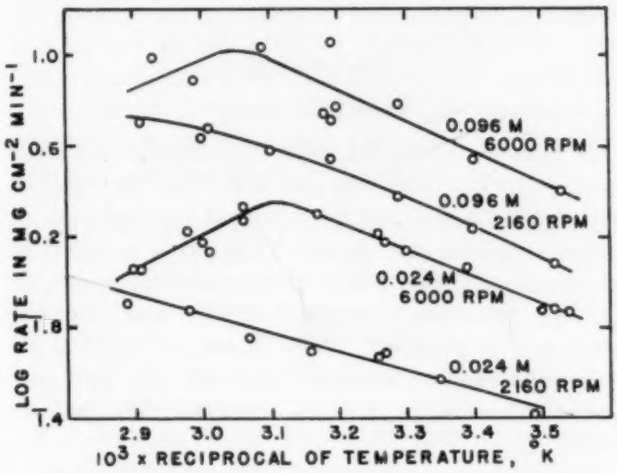

FIG. 9. Temperature coefficient in green chromic chloride solutions; zinc cylinders 1.8 cm diameter.

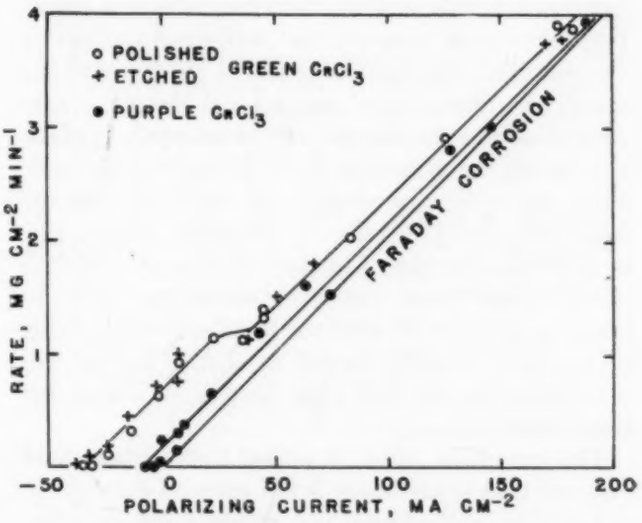

FIG. 10. Cathodic and anodic polarization of zinc cylinders 1.7 cm diameter, 2160 rpm, 27°C.

Polarization of the Zinc

Zinc cylinders rotating at 2160 rpm in 400 ml of solution were subjected to cathodic and anodic polarization (at ~27°C) in both purple and green solutions, using an auxilliary platinum electrode. The results are shown in Fig. 10. The metal is readily protected from corrosion by a cathodic current, about 8 ma/cm² being necessary in purple solutions, 30 to 40 ma/cm² in green solutions. The time of immersion was 5 min in purple, 3 min in green solutions for each measurement, and it is rather surprising that

UNIVERSITY OF MICHIGAN LIBRARIES

polished and etched zinc dissolves at nearly the same rate in the latter solutions when polarized. In view of the variability of rate measurements sometimes found, it is not certain whether the polarization curve should be drawn as shown in Fig. 10, or whether a straight line should be drawn through all the points for green solutions. In any case, there is probably some reduction in free corrosion on anodic polarization.

Discussion

Purple Solutions

It may be concluded from the observations with purple chromic chloride solutions that the rate of zinc dissolution is never controlled by transport of chromic ion to the surface. The main reaction is hydrogen evolution and is electrochemical in nature in that permanent, separate anodic and cathodic areas are established. There is some reduction to chromous, and, at low acidities, CrO is formed and partially blocks the surface, accounting for the low rates.

Free hydrogen evolution requires either the formation of metallic couples or catalytic reduction of hydrogen ion by the chromous ion formed. Lack of hydrogen evolution with cadmium, although reduction takes place, suggests that deposition of metallic chromium on the zinc is responsible for the cathodic areas. The formation of couples and the entire rate control seems to be determined "accidentally" (which may mean the exact condition of the zinc surface), hence the rates vary widely from run to run, change with time, etc. The behavior resembles that of zinc in acidified solutions of methylene blue (9), which is slowly reduced with "catalytic" evolution of 30 to 40 times as many equivalents of hydrogen, and pitting of the zinc. Possibly metal impurities in the dye deposit on the zinc and form couples, as is assumed here for chromium.

The enormous effect of added hydrochloric acid suggests that chromic ion is not reduced directly by either zinc or cadmium, but rather by atomic hydrogen on the metal surface. The dissolution of zinc is complicated, but reaction with cadmium proceeds smoothly, probably with quantitative reduction of chromic ion. In the latter case, the rates, as shown in Fig. 4 and 5, can be approximately represented by the equation:

$$dn/dt = kC_{Cr^{+++}}a_{HCl}^{1/2}$$

where a_{HCl} is the hydrochloric acid activity (10).

It is important in such a case to estimate the maximum rate at which chromic ion could reach the cadmium surface by convective-diffusive transport if the surface process were very rapid. One way to do this is by means of an equation developed by Wagner (11) for the rotating cylinder-turbulent flow experimental system:

$$dn/dt = 0.010\ cv(D/\nu)^{0.83}. \qquad (I)$$

This equation is based on the method of dimensionless group analysis (12) to correlate previous experimental work (13); the values 0.010 and 0.83 are constants, v is the peripheral speed of the cylinder, D the diffusion coefficient of the reagent, and ν the kinematic viscosity of the solution.

Substituting in equation (I) the values: $c = 0.107M$ (107×10^{-6} moles cm^{-3}), $v = 12000$ cm min^{-1}, $\nu = 0.0090$ cm^2 sec^{-1} for dilute aqueous solutions, $D = 7.4 \times 10^{-6}$ cm^2 sec^{-1}, estimated from the value for ferric ion at 15°C (14), the calculated maximum rate becomes $dn/dt = 3.5 \times 10^{-2}$ meq cm^{-2} min^{-1}. This is less than twice the highest experimental value for this concentration (Fig. 5). It is concluded that the lower rates in Fig. 5 are controlled mainly by the surface process, and that the highest points fall below the straight lines because a partial concentration gradient is set up (mixed rate control).

Green Solutions

The over-all picture for zinc dissolving in green chromic chloride solutions is that the rate process hovers between chemical (or electrochemical) and diffusion control. With polished cylinders, the former is slower and rate-controlling; as the surface becomes etched its real area becomes greater, the chemical rate increases, and transport to the surface becomes the slowest process.

At the lowest concentrations of Fig. 8, the rates are not at maximum values, since they increase with concentration faster than the latter. Above 6000 rpm, there is little if any increase in rate, and, at 4000 rpm and above, the rates approach maximum values at $0.15M$ $CrCl_3$. At intermediate values one can expect transport-controlled rates.

An alternative method of testing observed rates is to calculate the "effective diffusion layer thickness" by means of the Nernst equation:

$$\delta = \frac{DAc}{dn/dt} \qquad (II)$$

and compare the values found with those for known transport-controlled reactions. Table I gives values of δ calculated from the rates of Fig. 7 for 5000 rpm. These may be compared with values ranging from 4.0×10^{-4} to 4.4×10^{-4} cm found previously for acetic and hydrochloric acids with similar cylinders rotating at 5000 rpm (15).

Values of δ vary somewhat with D, as can be seen by combining equations (I) and (II), but this is unimportant. The two low values of Table I, corresponding to higher rates than expected, are perhaps

due to greater roughness of the surface at the higher concentrations. A "roughness factor" can be inserted in equation (I) and is necessary, if increased turbulence is caused at the metal interface (11). It is also possible that these high rates were caused by dissolution with hydrogen evolution in addition to chromic reduction.

It would be of interest to study rates in the green solutions with added acid. If there were no hydrogen evolution, all rates of chromic reduction should be transport-controlled, since the chemical rates would no doubt be increased. If hydrogen evolution started (as by "accidental" deposition of chromium), the rates should be higher and dependent on the acidity,

TABLE I. *Effective diffusion layer thickness* $D = 7.4 \times 10^{-6}$ cm² sec⁻¹, 5000 rpm, cylinder diameter 1.9 cm

C_{CrCl_3}, M	Rate, meq cm⁻² min⁻¹	δ, cm, $\times 10^4$
0.0096	0.010	4.2
0.049	0.047	4.6
0.070	0.072	4.3
0.098	0.156	3.5
0.148	0.198	3.3

but extremely variable from one experiment to another.

Conclusions

In this work with zinc and cadmium dissolution in chromic chloride solutions, three rate-controlling processes have been found operative under suitable conditions.

1. Transport of chromic ion, by convection and diffusion, to the metal surface. This process is rate-controlling with zinc in the green solutions, provided the chemical rate is sufficiently high, as with an etched surface and probably with enough hydrogen ion present (although this factor was not tested). Also, accidental hydrogen evolution may vitiate the transport control.

2. Simple chemical control, as with cadmium in the purple solutions with added acid. The dissolution of zinc in the same solutions is probably partly under the same type of chemical control, but the process is complicated by simultaneous hydrogen evolution, and the over-all rates are considerably greater.

3. An electrochemical process in which chromium is probably deposited on the zinc, forming couples; hydrogen evolution is then the main reaction, and the rates vary in accidental fashion. Since hydrogen ion is used up, the *p*H rises at the zinc surface and varying amounts of chromous oxide, perhaps chromic oxide or hydroxide, are formed. Precipitation of these solids, with indefinite amounts of chromium, leads to great variation in the dissolution rates.

Any discussion of this paper will appear in a Discussion Section, to be published in the June 1954 issue of the Journal.

References

1. H. Salzberg and C. V. King, *J. Electrochem. Soc.*, **97**, 290 (1950).
2. C. V. King and F. Lang, *J. Electrochem. Soc.*, **99**, 295 (1952).
3. H. Salzberg, *J. Electrochem. Soc.*, **98**, 31 (1951).
4. J. J. Lingane and R. L. Pecsok, *Anal. Chem.*, **20**, 425 (1948).
5. G. S. Forbes and H. W. Richter, *J. Am. Chem. Soc.*, **39**, 1140 (1917).
6. F. Ephraim, "Inorganic Chemistry," 5th ed., (P. C. L. Thorne and E. R. Roberts, Editors) pp. 302–4, Interscience Publishers, New York (1949).
7. A. B. Lamb, *J. Am. Chem. Soc.*, **28**, 1710 (1906).
8. A. B. Lamb and G. R. Fonda, *J. Am. Chem. Soc.*, **43**, 1154 (1921).
9. C. V. King, *Trans. N. Y. Acad. Sci.*, II, **10**, 262 (1948).
10. H. S. Harned and B. B. Owen, "The Physical Chemistry of Electrolytic Solutions," p. 547, Reinhold Publishing Corporation, New York (1943).
11. C. Wagner, Private communication.
12. A. C. Riddiford and L. L. Bircumshaw, *J. Chem. Soc.*, **1952**, 701; *Quart. Revs., London*, **6**, 157 (1952).
13. C. V. King, *J. Am. Chem. Soc.*, **57**, 828 (1935); C. V. King and P. L. Howard, *Ind. Eng. Chem.*, **29**, 75 (1937).
14. International Critical Tables, V, p. 65.
15. C. V. King and M. M. Burger, *Trans. Electrochem. Soc.*, **65**, 403 (1934).

UNIVERSITY OF MICHIGAN LIBRARIES

Some Properties of Tin-II Sulfate Solutions and Their Role in Electrodeposition of Tin

II. Solutions with Tin-II Sulfate and Sulfuric Acid Present[1]

CLARENCE A. DISCHER

Rutgers University, The State University of New Jersey, College of Pharmacy, Newark, New Jersey

ABSTRACT

Density, refractive index, surface tension, viscosity, freezing point depression, conductivity, transference number, and the electrode potential to pure tin and hydrogen, respectively, have been measured for a range of tin-II sulfate-sulfuric acid solutions. The effects of the sulfuric acid on these properties are noted. Relationships between concentration and the magnitude of these properties and various derived properties are determined. Possible structural species existing in the solutions are suggested.

INTRODUCTION

Some physical properties of aqueous tin-II sulfate solutions have been reported in a previous paper (1). In the present paper the same properties are studied for the aqueous system, tin-II sulfate-sulfuric acid. Using the information given in the two papers as a basis for comparison, a study of physical properties of similar solutions containing addition agents should enable one to determine which of these physical properties, if any, vary in the presence of effective addition agents. The work on addition agents will be reported in the next paper of this series.

EXPERIMENTAL

The procedures and equipment have been previously reported (1). It was necessary to substitute a low-temperature thermometer, graduated in 0.1°C divisions, for the differential thermometer in the freezing point work.

Since the properties studied are a function of both the molar concentration of the tin-II sulfate present and its mole fraction,[2] it was thought best to confine the major part of the experimental work to a series of concentrations at the same mole fraction. The mole fraction selected was 0.32. However, additional baths, sufficient in number to indicate the effect of varying mole fraction, were run.

RESULTS

Molar concentrations are given in Table I, together with experimental values of the physical properties measured. Experimental values for the electrical properties measured are given in Table II.

[1] Manuscript received December 15, 1952. This paper was prepared for delivery before the Montreal Meeting, October 26 to 30, 1952.

[2] Mole fraction, as used in this paper, is defined as the number of moles of tin-II sulfate divided by the total number of moles of tin-II sulfate and sulfuric acid.

Refractive index measurements are plotted vs. the molar concentration of tin-II ion in Fig. 1. The effect of mole fraction variation is shown by the family of curves. While the 0.32 mole fraction series is the only one studied in detail, it is apparent that refractive indices for other mole fractions arrange

TABLE I. *Some physical properties of* $SnSO_4$-H_2SO_4 *solutions*

Concentrations		Density (g/ml)	Refractive index	Viscosity (poise)	Surface tension (dynes/cm)	Freezing point (°C)
Moles tin-II sulfate/liter	Moles sulfuric acid/liter					
0.028	0.065	1.006	1.3343	0.0090	72.7	−0.18
0.060	0.131	1.017	1.3363	0.0092	72.5	−0.58
0.112	0.234	1.032	1.3390	0.0095	—	−0.99
0.172	0.373	1.052	1.3426	0.0099	73.2	−1.65
0.225	0.506	1.070	1.3460	—	73.7	−2.38
0.262	0.529	1.079	1.3471	0.0105	—	−2.47
0.340	0.769	1.109	1.3530	0.0115	73.3	−3.91
0.405	1.029	1.134	1.3566	0.0120	73.9	−5.19
0.462	1.039	1.146	1.3590	0.0124	74.7	−5.57
0.519	1.180	1.167	1.3623	0.0137	74.7	−6.57

TABLE II. *Some electrical properties of* $SnSO_4$-H_2SO_4 *solutions*

Moles tin-II sulfate/liter	Specific conductivity (mhos)	$E_{Sn,Sn^{++}}$ (volts)	E_{H_2,H^+} (volts)	Transference No. Sn^{++}	Transference No. H^+
0.028	0.0325	0.2266	0.0655	0.07	0.65
0.060	0.0652	0.2263	0.0520	0.05	0.79
0.112	0.1088	0.2243	0.0384	0.06	—
0.172	0.1797	0.2240	0.0284	0.00	0.72
0.225	0.2342	0.2240	0.0284	−0.12	0.82
0.262	0.2429	0.2270	0.0301	−0.09	0.66
0.340	0.2246	0.2269	0.0125	−0.05	0.26
0.405	0.2809	0.2252	0.0165	−0.04	0.21
0.462	0.3357	0.2224	0.0138	+0.07	0.58
0.519	0.4435	0.2276	0.0193	−0.03	0.66

themselves in the order of mole fraction. In regard to the 0.32 series curve, it is to be noted that there is a break at about 0.27 moles per liter. For comparison purposes the curve for pure tin-II sulfate ($n = 1.00$) solutions has been included (1). While the plot is not presented, the molar refraction curve shows a gradual increase in the magnitude of molar refraction up to $0.3M$ tin-II sulfate. Above $0.3M$, this curve levels off at a value of about 24.

A graph of the density data is not presented because the curves resemble those for refractive index. There is a marked inflection in the 0.32 mole fraction curve at approximately the same concentration of tin-II ion as in the corresponding refractive index plot.

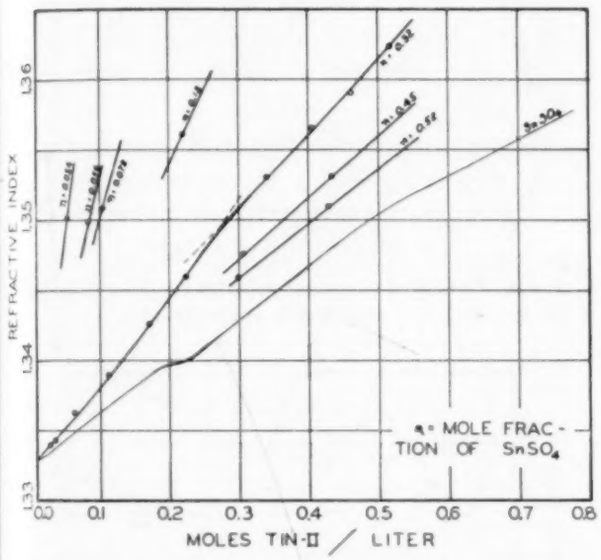

FIG. 1. Variation of refractive index of $SnSO_4$-H_2SO_4 solutions with molar concentration of $SnSO_4$ for various mole fractions of $SnSO_4$.

The surface tension measurements are given in Table I, but are not presented in graphic form. However, the following points may be significant. For all solutions studied the surface tension is greater than that of pure water (71.8 dynes/cm). This indicates that the molecular species present in the solutions are, at least partially, in the ionic form. Macleod's constant (2) was calculated at each concentration; the plot obtained is similar to that shown in Fig. 1.

Absolute viscosity data are plotted in Fig. 2. The curves for sulfuric acid (3) and tin-II sulfate solutions are included for comparison. The points for mole fractions other than 0.32 mole fraction are omitted in this and the following plots since in all cases they arrange themselves in the order of mole fraction as shown in Fig. 1. The dotted line represents the theoretical viscosity of tin-II sulfate-sulfuric acid solutions. It was obtained by summation of the contributions of tin-II sulfate and sulfuric acid, respectively, no interaction between these substances being assumed. Relative viscosity and specific viscosity were calculated for each concentration of

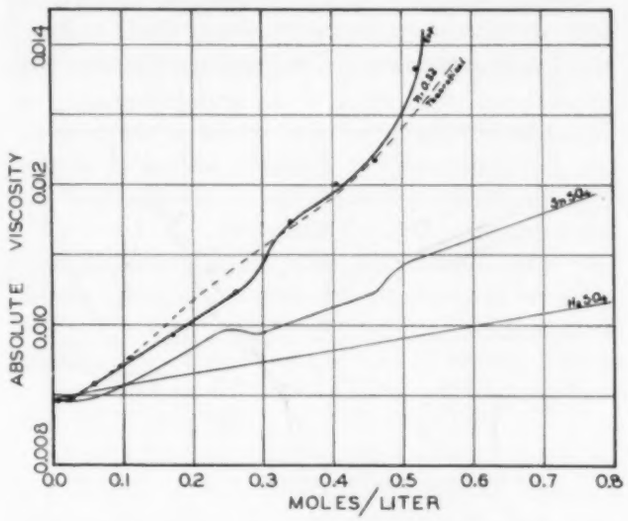

FIG. 2. Variation of absolute viscosity (poises) with concentration of $SnSO_4$ for the 0.34 mole fraction $SnSO_4$ series. The curves for pure $SnSO_4$ and H_2SO_4 solutions are shown for comparison. The theoretical viscosity, assuming additivity of viscosity of the constituents, is shown as a broken line.

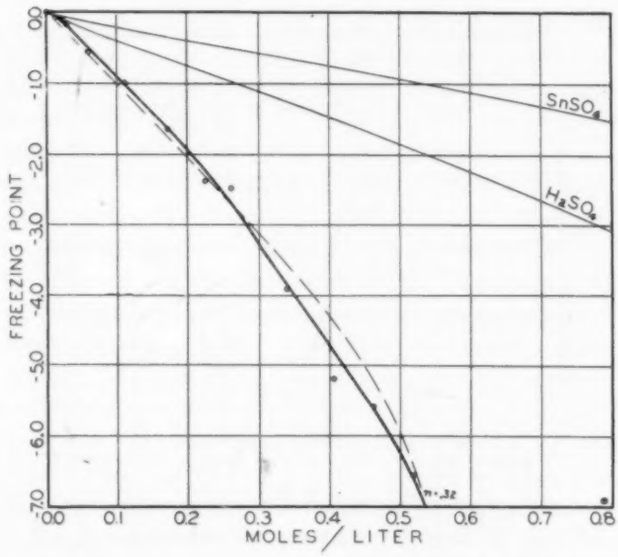

FIG. 3. Variation of the freezing points (°C) of the 0.34 mole fraction series of solutions with concentration of $SnSO_4$. The $SnSO_4$, H_2SO_4, and theoretical 0.34 mole fraction series curve are shown for comparison.

tin-II ion. These two plots are not shown since they duplicate the general features shown in Fig. 2.

Freezing point data are presented in Fig. 3. It is noteworthy that for the 0.32 mole fraction series the theoretical curve, obtained by summing contributions of tin-II sulfate and sulfuric acid, closely parallels the experimental curve to about 0.2 M tin-II sulfate.

UNIVERSITY OF MICHIGAN LIBRARIES

At higher concentrations the experimental depressions are greater than theoretical. The values for van't Hoff's i increase steadily with increasing concentration in the 0.32 mole fraction series.

Specific conductivity and equivalent conductivity data are plotted vs. concentration of tin-II in Fig. 4 and Fig. 5, respectively. Conductivity variation with

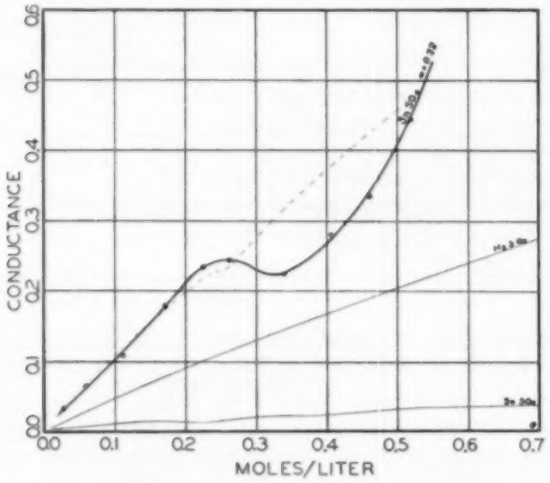

FIG. 4. Variation of the specific conductance of the 0.34 mole fraction series of solutions with concentration of $SnSO_4$. The $SnSO_4$, H_2SO_4, and theoretical 0.34 mole fraction series curve are shown for comparison.

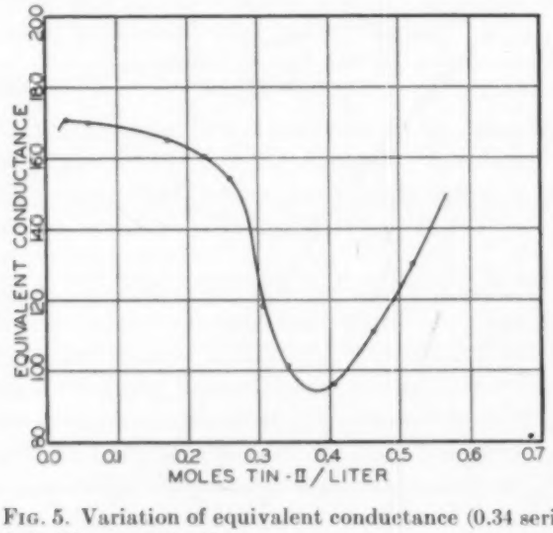

FIG. 5. Variation of equivalent conductance (0.34 series) with $SnSO_4$ concentration.

change in concentration of sulfuric acid and vs. total sulfate was also studied. The plots obtained indicate that conductivity follows tin-II concentration more closely than acid or total sulfate concentration, especially at higher total concentrations. Using Onsager's equation, the equivalent conductance at infinite dilution was calculated for each concentration of tin-II ion, and the values plotted. Two straight lines result, one ranging from 0.03M to 0.3M, and the other from 0.3M to 0.6M tin-II ion.

Transference data are presented in Fig. 6. The transference number for tin-II is small and positive until nearly 0.2M tin-II. At higher concentrations it is negative, reaching a minimum value at about 0.23M and increasing slightly thereafter. The curve for transference number for hydrogen ion practically duplicates that for equivalent conductance. This is expected since hydrogen ion is the predominant

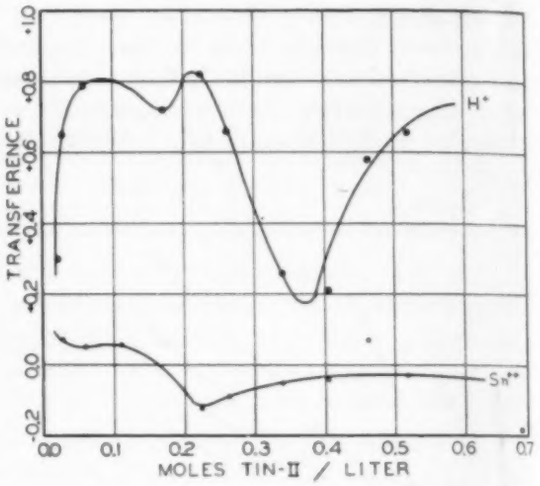

FIG. 6. Variation of transference by tin-II and hydrogen ions, respectively, with $SnSO_4$ concentration.

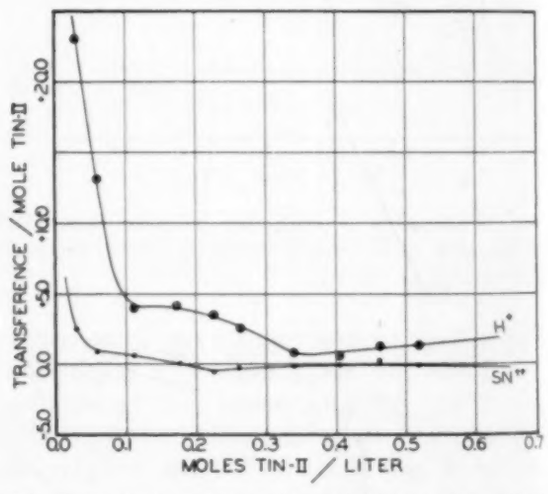

FIG. 7. Variation of the ratio of transference number to the molar concentration of tin-II with $SnSO_4$ concentration.

carrier of the current in these solutions. As found with conductivity, the transference by hydrogen ion seems to vary as a function of the tin-II concentration, rather than the concentration of sulfuric acid or total sulfate. In Fig. 7 the ratio of the transference of each of the ions to molar concentration of tin-II is plotted vs. molar concentration of tin-II.

Electrode potentials are plotted vs. tin-II concentration in Fig. 8. Activity coefficients, based on these measurements, are shown in Fig. 9. The plots for activity are not shown, but the curve obtained for

hydrogen ion is similar to that for specific conductivity.

The plating behavior as expected is unsatisfactory. In general, increasing the acid ratio increases the brightness of the crystals, while increasing the tin-II ratio increases the grayness of the deposits. At lower current densities, especially in the still bath, there is a tendency to give gray powdery deposits, the clumps

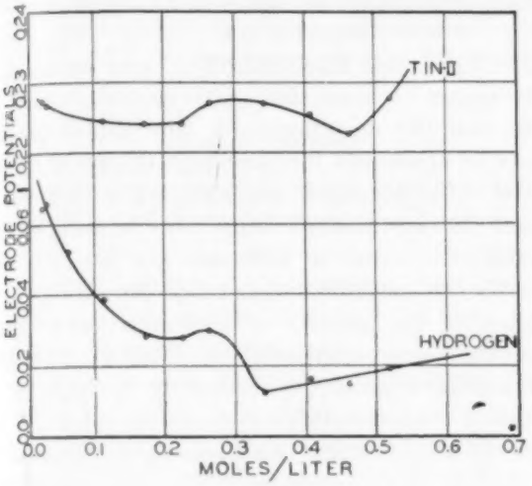

FIG. 8. Variation of single electrode potentials (volts) with concentration of $SnSO_4$.

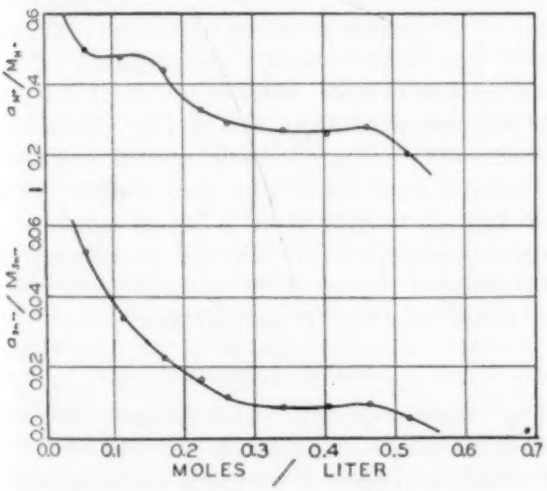

FIG. 9. Variation of activity coefficients of hydrogen and tin-II, respectively, with $SnSO_4$ concentration.

of powdery crystals becoming tighter with increasing electrolyte concentration. Increasing current density and concentration result in increasingly longer branched needles, the branching becoming progressively less with increasing concentration. There is, as expected, severe gassing at high current densities and low tin-II concentrations.

Discussion

This discussion must be concerned primarily with the 0.32 mole fraction tin-II sulfate series of solutions, since this series is the only one in which a reasonably complete range of concentrations was studied. A study of the plots presented indicates two general concentration ranges of consistent behavior: the first, 0.0–0.2*M* tin-II sulfate and, the second, from approximately 0.3–0.6*M* tin-II sulfate. For concentrations between these ranges, that is, 0.2–0.3*M*, the curves obtained by plotting property vs. molar concentration show a break or pronounced change in slope. It may also be noted that when the theoretical curves obtained by summation of the effects of pure tin-II sulfate and pure sulfuric acid are plotted, the deviation from the experimental value changes sign between 0.20–0.30*M*. The conclusion drawn is that there are two areas of behavior for solutions of 0.32 mole fraction tin-II sulfate-sulfuric acid. Consequently the molecular species present must be different in each, with a transition between species falling between 0.2–0.3*M*.

Concentration range 0.0–0.2M.—In this range the contributions of tin-II sulfate and sulfuric acid to a given property are very nearly additive. This indicates that, for the most part, the two components are acting independently of one another. This range represents those concentrations of sulfate ion in which the tin-II exists either as simple ions, molecules, or the complex $Sn[Sn(SO_4)_2]$ depending upon concentration as presented in the previous paper (1).

As shown in Fig. 6, the transference number of tin-II is positive in this concentration range. It decreases steadily with increasing concentration, becomes zero at about 0.18*M* tin-II; it is negative at higher concentrations. This is indicative of the presence of free tin-II ion, the number of free tin-II ions decreasing with concentration. The gradual decrease in concentration of free tin-II ion is also indicated by the activity coefficient of tin-II. The numerical value of this latter property decreases with increased concentration in the concentration range under study.

Freezing point data also give some light as to the nature of the molecular species present in solutions within the 0–0.2*M* tin-II range. With reference to Fig. 3 it is seen that the theoretical curve obtained by summing contributions of tin-II sulfate and sulfuric acid, if one assumes no appreciable interreaction, closely parallels the curve obtained from the experimental data. This indicates that tin-II exists in ultimate particles similar to those in pure tin-II sulfate solutions of corresponding concentration. That is, the tin-II sulfate exists in low concentrations as tin-II ions, sulfate ions, and tin-II sulfate molecules, with the relative amounts of each changing in favor of the molecular form with increasing concentration.

Theoretical freezing points may also be calculated

UNIVERSITY OF MICHIGAN LIBRARIES

by use of concentration data in Table I and activity data derived from the electrode potentials given in Table II. Using the concentration of free ions, as given by the activity, and the concentration of molecules, as given by the difference between molar concentration and activity, the following freezing points may be calculated for the respective solutions in this concentration range: −0.31°, −0.61°, −1.05°, −1.63°C. The calculated value for the 0.225*M* solution is −1.98°C. The corresponding experimental freezing points are −0.18°, −0.58°, −0.99°, −1.65°C; −2.38°C for the 0.225*M* solution. This correspondence between calculated and experimental values further supports the view that within this concentration range the tin-II exists in varying ratios of simple tin-II ions and tin-II sulfate molecules, the actual ratio being a function of the concentration of the solution. Above 0.2*M* the theoretical freezing points agree with the experimentally determined values only on the assumption of the existence of the tin-II in complex negative ions.

Molar refraction does not vary linearly with concentration in this region. This also lends support to the supposition that a change in ratio of the various particles is taking place.

On the basis of the evidence presented it seems probable that simple molecules and ions of tin-II sulfate and sulfuric acid exist in the lower part of the concentration range. As concentration increases the molecular tin-II sulfate increases at the expense of the simple tin-II ions, possibly followed by the appearance of some $[Sn(SO_4)_2]^=$ complex ion.

Concentration range 0.3–0.6M.—In this range the existence of the tin-II in complex ions is indicated. Transference by tin-II is negative (Fig. 6). The activity coefficient levels off at very low values (Fig. 9). Theoretical values for specific conductance obtained by summing contributions by each component are much larger than the experimental, indicating heavy complex ions (Fig. 4).

The existence of one fundamental species of particle in solutions in this concentration range is indicated by the nearly constant values for the ratios of a given property to the concentration of tin-II ions, that is the contribution per mole of tin-II ion to a given property becomes constant or nearly so. This is ordinarily possible only if the ultimate particle of the substance in solution remains constant. The slight slope of some of the lines obtained on plotting these molar quantities vs. tin-II concentration may be explained by slight changes in ionization of the complex acids present, Plots of this type are shown for transference and activity in Fig. 7 and 9, respectively. Molar refraction becomes practically constant at a value of 24 in this concentration range. The ratio of specific viscosity to tin-II concentration is also practically constant. Equivalent conductance (infinite dilution) as calculated using Onsager's equation, gives a straight line in this concentration range.

Two sulfatostannite ions may be postulated, $[Sn(SO_4)_2]^=$ and $[Sn(SO_4)_3]^=$. Calculation of freezing points, assuming the former, yields theoretical values much below experimental. Only by using $H_4[Sn(SO_4)_3]$ and $H_2Sn[Sn(SO_4)_3]$, and assuming a high degree of ionization of these sulfatostannous acids, can the experimentally determined freezing points be accounted for. The high degree of ionization of sulfatostannous acid assumed in such calculations is inconsistent with the experimentally determined values of hydrogen ion activity. Apparently the measurement as made cannot be a true measure of the activity of hydrogen ion in these relatively concentrated solutions. That a high degree of ionization is present is verified by the high values of surface tension in this concentration range.

Miyamoto (4) made conductivity measurements on $SnSO_4$–H_2SO_4 systems. He postulated the $H_2Sn(SO_4)_2$ and $H_2Sn_2(SO_4)_3$ systems as most probable.

Mole fractions other than 0.32.—No thoroughgoing study of other mole fractions has been undertaken. However, a range of samples to give mole fraction values of 0.034, 0.056, 0.072, 0.129, 0.40, 0.44, and 0.52 was prepared. As shown by Fig. 1, families of curves result. These curves arrange themselves in the order of mole fraction of tin-II sulfate. For the high acid electrolytes there is better agreement in many properties, e.g., transference by hydrogen ion, if the property is plotted vs. total sulfate concentration rather than tin-II concentration.

Acknowledgment

The author is grateful to the Rutgers University Research Council for funds for the employment of Mr. Abel Dominguez to conduct the vast amount of routine laboratory work necessary for this paper.

Any discussion of this paper will appear in a Discussion Section, to be published in the June 1954 issue of the JOURNAL.

REFERENCES

1. C. A. DISCHER, *J. Electrochem. Soc.*, **100**, 45 (1953).
2. D. B. MACLEOD, *Trans. Faraday Soc.*, **19**, 38 (1923).
3. International Critical Tables, **1**, 107; **4**, 254, 464; **5**, 11; **6**, 241, 310, McGraw-Hill Book Company, Inc. (1933).
4. S. MIYAMOTO, *Bull. Chem. Soc. Japan*, **7**, 56 (1932); *C. A.*, **26**, 2916 (1932).

Electroplating on Titanium[1]

WILLIAM H. COLNER, MORRIS FEINLEIB,[2] AND JOHN N. REDING

Armour Research Foundation of Illinois Institute of Technology, Chicago, Illinois

ABSTRACT

A method for obtaining adherent electrodeposits on titanium is described. It consists in subjecting titanium to an anodic etch prior to plating, under controlled conditions. Bath composition and operating variables are discussed, and photomicrographs showing the mechanical nature of the bond are given. Conditions for electropolishing titanium are also reported.

INTRODUCTION

Titanium has recently emerged from the class of rare metals, and is in the process of becoming an important structural material. Its outstanding properties are a high strength-to-weight ratio and excellent corrosion resistance to a great number of chemicals at room temperature.

The need for electroplating on titanium may arise for several reasons, such as decorative plating, improved resistance to high-temperature gases, improved mechanical properties of the surface, or joining of titanium parts.

Titanium is an extremely active metal. Its high corrosion resistance is due to the fact that the metal becomes covered with an impervious and tightly adherent oxide film. This film, however, makes it very difficult to obtain adherent electrodeposits on the metal. Conditions required to remove the oxide are usually so drastic that the metal reacts violently once the surface film is dissolved; under such conditions it becomes very hard to apply a sound electroplate, or even a strike, to the titanium.

A survey of the literature cast little light on the problem. Some mention was made by Couch and Brenner (1) of obtaining adherent deposits on titanium using a dry lithium hydride, ethyl ether, etc. However, this technique was considered impractical insofar as the present problem is concerned. Conventional methods for plating on common metals were tried on titanium; these met with no success. Such methods include straight pickling in HF, "nickel pickle" (simultaneous cathodic pickling and nickel deposition), or immersion plates (which yield adherent electrodeposits on aluminum or magnesium).

It was apparent that the activity of the titanium surface was so great in aqueous solutions that an oxide-free surface could not be maintained. In order to reduce the reactivity of the titanium metal, yet maintain it oxide-free, nonaqueous solutions were investigated.

Some plate adherence was achieved by subjecting the metal, prior to plating, to a cathodic treatment in a bath whose main constituent was ethylene glycol, and which also contained a zinc salt, HF, and a small amount of water. This will be discussed below.

The most successful approach to the problem of obtaining adherent electrodeposits on titanium was to subject the metal to an anodic etch prior to plating. This procedure is described in detail below.

EXPERIMENTAL

Raw material.—The bulk of the experiments were carried out with commercially pure titanium sheet.[3] Several lots of RC-55 (Rem-Cru) and Ti75-A (Titanium Metals Corporation), 0.025–0.065 in. thick, were used. A few tests were performed with RC-130 B (Rem-Cru) alloy.[3]

Preparation before plating.—Titanium sheet specimens 2.5 in. x 1 in. were used. They were cathodically cleaned (when required) in a solution of 20 g/l of sodium orthosilicate at 70°C, and rinsed. This was followed by pickling in a solution containing 185 cc/l of 48 per cent HF and 8.6 cc/l of 70 per cent HNO_3 until the specimen looked clean, and drying. The metal was next subjected to the anodic etching treatment.

Plating.—After anodic etching, specimens were rinsed and then given a copper strike at room temperature, without stirring, in the following solution: CuCN, 23 g/l; NaCN, 34 g/l; Na_2CO_3, 15 g/l. The current was first brought up to 50 amp/ft² (5.4 amp/dm²), then brought back to about 15 amp/ft² (1.62 amp/dm²) after a few seconds. Plating was continued for 3 to 5 minutes.

The copper strike, after another rinse, was followed

[1] Manuscript received November 5, 1952. This paper, was prepared for delivery before the Montreal Meeting, October 26 to 30, 1952.

[2] Present address: Division of Metallurgical Research, Kaiser Aluminum and Chemical Corporation, P.O. Box 1451, Spokane, Washington.

[3] RC-55: C—0.05–0.2%; O, N, Fe—few hundredths to few tenths % each; other elements—trace.

Ti75-A (nominal): Fe—0.1%; N—0.02%; O—trace; C—<0.04%; W—<0.08%.

RC-130B (nominal): Mn—4%; Al—4%; O, N, Fe—same as RC-55.

UNIVERSITY OF MICHIGAN LIBRARIES

by a copper plate at room temperature, with stirring, from the following bath: 448 g/l $Cu(BH_4)_2$ [sp gr 1.36]; HBF_4 to *p*H 0.6. Plating was carried on at 50 amp/ft² (5.4 amp/dm²) for about 10 minutes in most cases (about 0.0005 in.). For heavy plates (about 0.005 in.), plating time was 40 minutes at 100 amp/ft² (10.8 amp/dm²).

Testing.—The mechanical properties of electroplates were tested by scraping them with a knife. If no detachment could be observed, the specimen was clamped in a vise and bent by hammering through a 180° angle. The adherence of the plate in the bent areas was then examined.

In the later stages of the work, a more severe test was substituted for the bend test. One end of the specimen was again clamped in a vise, and then subjected to repeated flexing, using both a bending and a twisting motion. Again, the plate was examined for detachment. The bend and flex tests were naturally most severe when performed on heavy electroplates.

The final test of adherence was the solderability test (which was most severe on thin electroplates). This test consisted of soldering a copper strip onto the electrodeposit, then pulling off the strip. If the joint broke wholly in the solder, the specimen passed the test. In other cases, portions of the copper plate would be pulled off; the size of these areas was a measure of the quality of the plate.

The Anodic Etch

Under proper conditions, anodic etching prior to plating yielded fully adherent copper electroplates (0.0005–0.005 in. thick), which passed the bending, flexing, and solderability tests. Good results were obtained with commercially pure titanium as well as RC-130 B alloy. Etching was carried out in an essentially nonaqueous bath.

Mechanism

The anodic etch, under the right conditions, leads to a rough surface that provides mechanical keying of the electrodeposits. Fig. 1 to 3 clearly show the pockets and reentrant angles created by anodic etching. The surface roughness of these specimens may be as high as 50 microinches root mean square. Plating on this rough surface takes place with good throwing power, and the pockets appear to be completely filled with the plated metal. At the same time, the electroplate surface becomes increasingly smooth as plating proceeds, until it is almost comparable to that of a metal electrodeposited on a smooth base. Even with 0.0005 in. of copper, a fairly smooth plate surface is obtainable.

The mechanical nature of the bond is best illustrated in Fig. 1 to 3. It is supported by the fact that no substance other than titanium metal was found on the surface of anodically etched specimens by spectrographic and electron diffraction techniques,

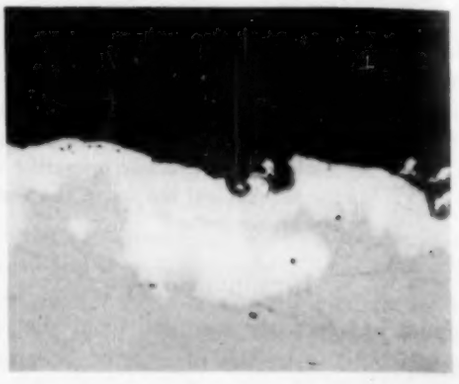

Fig. 1. Anodically etched titanium. × 500. Unetched. (In the photomicrographs illustrating this paper, the titanium base metal is the phase in the lower portions. The specimens shown in Fig. 1, 2, and 4 were plated with nickel for metallographic polishing purposes.)

Fig. 2. 0.5-mil copper plate on anodically etched titanium. × 500. $H_2O + H_2O_2 + NH_4OH$.

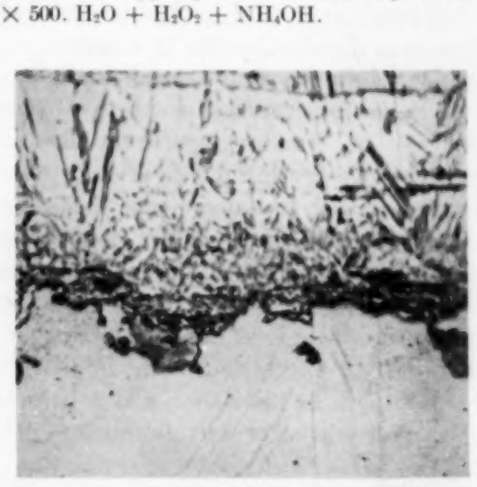

Fig. 3. 5-mil copper plate on anodically etched titanium. × 500. $H_2O + H_2O_2 + NH_4OH$.

which means that no special chemical compound is formed by this etching. Furthermore, the degree of roughness of the surface bears a definite relationship to the adherence of electrodeposits. Under proper conditions, many etching baths can be operated so

as to yield a very smooth, electropolished surface on titanium (Fig. 4); plates on such a smooth surface have never been adherent. With improper current distribution, etching can take place in low current density areas and polishing in high current density areas *on the same specimen*; subsequent electroplating yields adherent deposits in the etched areas only.

Anodizing Conditions

When titanium is made anode in a bath in which it is reactive (e.g., a bath containing HF), several possible reactions may take place:

1. The current may be insufficient to prevent local (chemical) action, with the evolution of hydrogen. In extremely active baths, it may be altogether impossible to stop this local action at any reasonable current density. The type of surface obtained under such conditions varies from an even, clean, uniformly etched metal to a fairly smooth

FIG. 4. Electropolished titanium. × 500. Unetched

grayish or blackish film. Such surfaces do not lead to adherent plates.

2. In low activity baths, an anodic treatment may lead to the formation of an impervious oxide film, which is usually colored, the color depending upon the applied voltage. This is comparable to the anodizing of aluminum. The passivated anode offers a high resistance to the passage of current, which drops to a low value. Again, the adherence of electrodeposits on such a base is very poor.

3. It is in baths of intermediate activity that the anodizing of titanium yields the type of etched surface desired for electroplating. In such a bath, if increasing current is applied (starting from zero), several effects may be observed. At first, the main result is a decrease in the local chemical action (which takes place with displacement of hydrogen). Until local action has stopped completely, the weight of metal dissolved from the anode per unit time decreases, even though an increasing amount of anodic current is applied. When a certain value of current density has been reached, which varies with bath composition, temperature, etc., the local action is eliminated, and the anodic dissolution of titanium continues without gassing (see Fig. 5). Under such conditions, it is possible to obtain the type of etched surface desirable for electrode deposition, or, by varying operation conditions, an electropolished surface (Fig. 4). The volume of the experimental baths was about 300 cc. During the course of experiments, the composition of the bath was altered slightly by evaporation and hydrogen evolution. As evidenced by the data in Fig. 5, the weight loss per unit time in the range of local action was highly sensitive to the changes in composition. Since the reproducibility in the range of local action was poor the curves

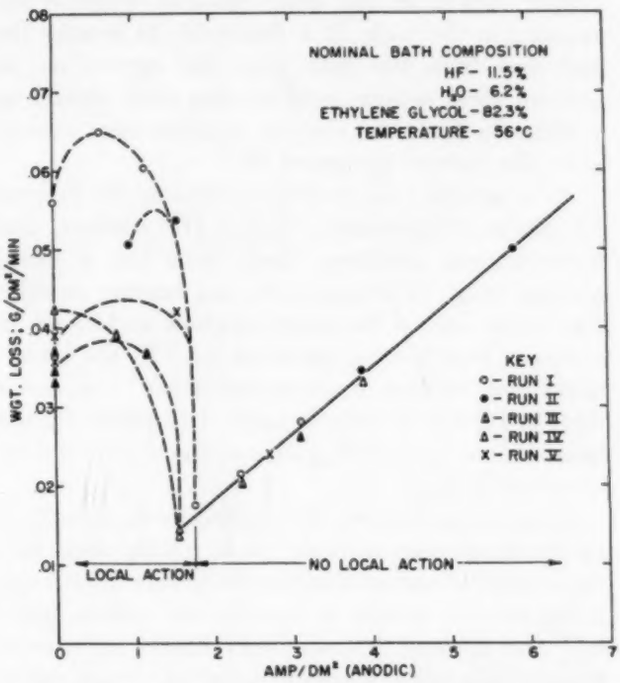

FIG. 5. Weight loss of titanium during anodic treatment vs. current density.

connecting the points in that range are merely conjecture, and are drawn with broken lines. In general, with increasing use of the bath, the weight loss in the range of local action decreases. The only effect in the range of no local action with prolonged use of the bath is to decrease the severity of the etch. The apparent valence change of titanium during anodic dissolution was determined from weight loss measurement, on the assumption that the metal dissolves at 100 per cent current efficiency (in the range of no local action). The values found were somewhat in excess of 3, and were slightly higher for electropolishing than for etching. Such determinations are complicated by possible side reactions at the anode, such as the oxidation of Ti^{++} and Ti^{+++} compounds or of hydrogen bubbles.

UNIVERSITY OF MICHIGAN LIBRARIES

Operating Variables

A number of solutions with low water content were investigated. Best results were obtained with baths based on ethylene glycol and HF. A typical composition would be the following: 15 per cent by weight HF; 6 per cent H_2O; 79 per cent ethylene glycol. Such a bath should be operated at 55°–60°C, at 50 amp/ft² (5.4 amp/dm²), or slightly less. The required etching time is 15 to 30 minutes. When applying current, it is recommended that it be brought up above the desired value (to help stop local action), then brought back to the operating level. Agitation or circulation of the solution is helpful, if not essential. Cathodes may be graphite, copper, nickel, or any other material which is not reactive in the bath. It is preferable to remove the specimen from the bath with the current on, to prevent local action; certainly the work should be withdrawn from the etching solution very rapidly after the current is turned off.

As a general rule, etching conditions are favored by higher temperatures, higher HF content, and lower current densities. Each bath has a useful etching range of temperature and current density. The upper limit of the temperatures would be set by excessive local action, the lower limit by the transition from etching to electropolishing. The lower limit of current density is again determined by the onset of local action (Fig. 5), and the upper limit by electropolishing.

As mentioned before, electrodeposits do not adhere to electropolished surfaces. It is readily seen that the control of current distribution is very important; if the current density is excessive on certain areas, they may become electropolished. Also, if the current density falls below a critical value at certain spots, they are no longer protected against local action, and the adherence of plates is poor at these points.

The useful range of etching current densities is greater at higher temperatures, as well as at higher HF concentrations, as long as local action is prevented.

Bath composition may influence not only the etching range, but also the severeness of the etch. Thus, at increasing water content, the etch may become deeper, but the etching range is reduced in favor of local action, making control more difficult.

It was found that these baths did not deteriorate on standing; however, some loss in activity was noted with use. Partial rejuvenation was obtained by small additions of HF. Extensive study of these factors was not undertaken.

Fairly good results have been obtained from a wholly inorganic bath based on phosphoric acid: 53.9 per cent by weight H_3PO_4; 12.5 per cent HF; 15.5 per cent NH_4HF_2; 18.1 per cent H_2O. This bath is more active than the one based on ethylene glycol but more difficult to control. Its useful etching range was 35°–45°C, with current densities of 30–50 amp/ft² (3.23–5.4 amp/dm²). This shows that it may be possible to use a number of different solutions for the anodic etching of titanium and its alloys before plating.

Electropolishing

Electropolishing of titanium was a side product of the research on anodic etching for plating.

A solution based on HF and ethylene glycol, but slightly lower in HF than the etching solution, may be recommended for electropolishing, e.g., 6 per cent by weight HF; 6 per cent H_2O; 88 per cent ethylene glycol. This bath should be operated at room temperature or slightly above (up to 40°C), at current densities in excess of 50 amp/ft² (5.4 amp/dm²), and preferably around 75–100 amp/ft² (8.1–10.8 amp/dm²). Better electropolishing solutions than the above can probably be compounded, and the above composition is given mainly as a guide. However, even from the above bath, very smooth finishes (as low as 2.5 microinches rms) were obtained.

Zinc Strike

Cathodic treatment of titanium in a bath consisting of ethylene glycol, HF, a small amount of water, and a zinc salt showed that, on application of current, zinc deposited on the cathode at first, but soon redissolved even though no interruption of current occurred. If the specimen was removed before the redissolution of the zinc, the deposit could easily be scraped off. During and after dissolution of the zinc, a black film formed on the titanium surface. Deposition of copper on this black film gave adherent coatings. The electrodeposits adhered to the extent of passing the bend test when the deposits were 0.5 mil in thickness. These deposits did not pass the solderability test and heavier deposits, 3.0 mils to 5.0 mils in thickness, would not pass the bend test. The conditions required for formation of the black film differed greatly between the lots of commercially pure grades of titanium and titanium alloys used. Because of the difficulty of control and the inability to obtain satisfactory adherence, this approach was discarded.

Summary and Conclusions

Conventional methods used to obtain adherent electrodeposits on other metal fail in the case of titanium.

However, fully adherent copper electroplates (up to 0.005 in. thick) on titanium are obtained when the material is anodically etched, prior to plating, in a solution based on HF and ethylene glycol, under controlled conditions of temperature and current density. Metallographic examination indicates that the bond between plate and basis metal is a mechanical one, due to interlocking between the etched surface of the titanium and the plated metal which appears to "throw" well into the cavities created by the etch.

Under different operating conditions, an anodic treatment of titanium will yield an electropolished surface, which is not good for adherent plating.

Acknowledgment

The authors wish to acknowledge the help of the Watertown Arsenal Laboratories, Watertown, Massachusetts, who sponsored the research described herein, and their kind permission to publish this material.

Any discussion of this paper will appear in a Discussion Section, to be published in the June 1954 issue of the JOURNAL.

REFERENCE

1. D. E. COUCH AND A. BRENNER, *J. Electrochem. Soc.*, **99**, 234 (1952).

UNIVERSITY OF MICHIGAN LIBRARIES

An X-Ray Study of the Effect of Organic Compounds on the Crystal Growth of Nickel during Electrodeposition[1]

FRANCIS DENISE AND HENRY LEIDHEISER, JR.

Virginia Institute for Scientific Research, Richmond, Virginia

ABSTRACT

X-ray diffraction analyses were made of nickel electrodeposits prepared in the presence of organic compounds. The compounds varied in their ability to alter the grain size and the degree and/or type of preferred orientation. Compounds most effective in increasing the cathode potential during deposition both decreased the grain size and changed the type of preferred orientation to a type other than (100) or to a random distribution of the crystals. Compounds of lesser effectiveness in increasing the cathode potential reduced the grain size, but had no effect on the preferred orientation. Brittle deposits were characterized by an orientation other than (100), and the ductile deposits were characterized by a (100) preferred orientation. The results of this study and the work of other authors indicate that a major fraction of mirror-bright nickel electroplates exhibit no preferred orientation.

INTRODUCTION

A comprehensive study of the interaction of organic compounds with a nickel surface during electrodeposition is being carried out. As part of this study, x-ray diffraction analyses have been made of deposits prepared in the presence of 29 different organic compounds in order to determine the effects of these compounds on crystal growth.

EXPERIMENTAL

All plating experiments were carried out in a bath commonly referred to as the Watts bath, with the following composition: $NiSO_4 \cdot 6H_2O$ 240 g/l, $NiCl_2 \cdot 6H_2O$ 45 g/l, and H_3BO_3 30 g/l. A large stock solution was prepared and was purified in the conventional manner by treatment with $NiCO_3$, H_2O_2, and activated carbon. The *p*H was adjusted in all experiments to 4.0 with HCl. The exact plating conditions used in the individual experiments will be described later.

The cathode consisted of a polycrystalline sphere of copper, $\frac{5}{8}$ in. in diameter, with a small shaft for handling. The cathode was used in the spherical form because of the ability to secure uniform current density distribution over the surface, and because of the ease in making x-ray analysis. The cathode was electrolytically polished in 42.5 per cent by volume phosphoric acid before insertion in the plating bath. The anode consisted of a cylindrical nickel sheet resting on the periphery of a 400-ml beaker used as the plating cell. X-ray analysis indicated that the polycrystalline copper cathodes themselves exhibited no preferred orientation. Thus, any preferred orientation observed in the nickel electroplate resulted solely from the deposition, and not from a continuation of preferred orientation of the copper substrate.

X-ray analyses were made with copper radiation at a specimen-film distance of 3.0 cm. No filter was used since the nickel deposit served to filter out the majority of the beta radiation. The x-ray beam was directed tangentially to the surface of the deposit. The sphere was inserted in a special holder and its position was adjusted so that, when viewed with a telescope, exactly one-half of the x-ray beam intersected the surface of the specimen. This method was adopted because it was possible to obtain x-ray information about the deposit without stripping it from the base metal or without special sectioning techniques. The type of preferred orientation was determined directly by measuring the angle between the center of the intense arcs on the rings and the vertical plane. A knowledge of the angles between the various crystal planes in a face-centered cubic structure enables one to identify immediately the type of orientation.

The grain size of the deposit was typified by the terms large or small. Large grains were considered to be those having a mean diameter larger than 10^{-2} mm. Such grains yield spotty diffraction rings. Small grains were considered to be those having a mean diameter in the range 10^{-2} to 10^{-4} mm. Within this range, the diffraction rings are sharp and continuous. Grains smaller than 10^{-4} mm yield diffuse diffraction rings, and the breadth of the rings can be used in the determination of the grain size. However, in the 10^{-2}- to 10^{-4}-mm range, the x-ray method is not sensitive to differences in grain size. All deposits examined in this study had grains larger than about 10^{-4} mm.

[1] Manuscript received January 3, 1953. This research was sponsored by the Harshaw Chemical Company, Cleveland, Ohio.

Results

The nickel deposit formed in an unadulterated[2] Watts bath at current densities in excess of 1 amp/dm² and at temperatures of 20°–70°C exhibited a grain size larger than 10^{-2} mm and moderately strong (100) preferred orientation. At current densities below 1 amp/dm², either no preferred orientation or a (110) orientation was detected. The typical diffraction pattern obtained at current densities above 1 amp/dm² is given in Fig. 1. The diffraction rings consist of well-defined spots, indicating a grain size larger than 10^{-2} mm; intensity maxima occur 55° from the vertical on the (111) ring and at the meridial position on the (200) ring. A (100) preferred orientation is thus indicated. Similar results were obtained many times over a period of several years in baths prepared from different batches of nickel sulfate, nickel chloride, and boric acid.

It was next of interest to determine the effect of a number of organic compounds added singly to the Watts bath. A few preliminary experiments were carried out in order to choose a set of experimental conditions for the plating operation, and it was found that the results were essentially independent of current density between 2 and 10 amp/dm². Further experiments were then carried out under the follow-

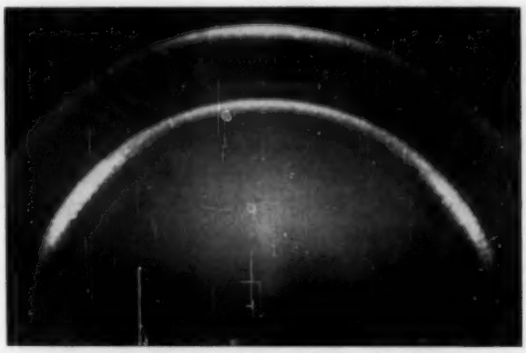

FIG. 1. X-ray diffraction photograph of nickel deposit formed in unadulterated Watts bath. Spotty nature of rings indicates a grain size larger than 10^{-2} mm; moderate (100) preferred orientation.

TABLE I. *The effect of 29 organic compounds on the appearance, ductility, grain size, and preferred orientation in nickel electrodeposits*

Organic compound	Conc. in moles/l	Appearance of deposit	Ductility	Grain size*	Preferred† orientation
None	—	Grainy, matte	Ductile	Large	mod (100)
m-Aminophenol	0.0025	Semibright	Brittle	Small	mod (211)
p-Aminosulfonic acid	0.004	Semibright	Ductile	Small	sl (100)
Aniline	0.001	Dull, gray	Brittle	Small	Random
Benzaldehyde	0.002	Grainy, matte	Brittle	Large	Random
Benzaldehyde *m*-sulfonate (Ni salt)	0.008	Very bright	Brittle	Small	sl (100)
m-Benzenedisulfonic acid (Ni salt)	0.016	Bright	Ductile	Small	s (100)
Benzoic acid	0.0025	Matte	Ductile	Small	mod (100)
Benzonitrile	0.0005	Semibright	Brittle	Small	sl (311)
Ethanolamine	0.01	Grainy, matte	Ductile	Large	mod (100)
Ethanol	0.01	Grainy, matte	Ductile	Large	mod (100)
Ethylamine	0.01	Matte	Ductile	Large	mod (100)
Ethylenecyanohydrin	0.0012	Bright	Brittle	Small	Random
Ethylenediamine	0.002	Matte, gray	Brittle	Small	Random
Naphthalene-2,7-disulfonate (Na)	0.008	Bright with haze	Ductile	Small	s (100)
Naphthalene-1,3,6-trisulfonate (Na)	0.01	Bright with haze	Ductile	Small	s (100)
1-Napthylamine-4,8-disulfonic acid	0.0002	Bright one side Matte other side	Brittle	Small	Random
Nitrobenzene	0.001	Matte, gray	Brittle	Small	Random
Phenol	0.01	Grainy, matte	Ductile	Large	mod (211)
p-Phenolsulfonic acid	0.01	Grainy, matte	Ductile	Large	(100)
Piperidine	0.01	Matte	Ductile	Large	mod (100)
Propionitrile	0.003	Matte	Brittle	Large	sl (211)
Pyridine	0.001	Matte, white haze	Brittle	Small	Random
Quinaldine ethiodide	0.0005	Semibright	Brittle	Small	sl (210)
Quinoline ethiodide	0.001	Bright	Brittle	Small	mod (211)
Saccharin	0.0007	Semibright	Ductile	Small	s (100)
Succinonitrile	0.0005	Bright	Brittle	Small	(221) and (310)
Thianaphthene dioxide	0.0002	Bright, hazy	Ductile	Small	s (100)
Thiourea	0.003	Bright	Brittle	Small	sl (100)
p-Toluenesulfonamide	0.001	Bright, hazy	Ductile	Small	s (100)

* Large refers to grains larger than 10^{-2} mm, and small to grains less than 10^{-2} mm.
† Sl—slight, mod—moderate, s—strong, random—no detectable preferred orientation.

[2] An "adulterated" Watts bath is defined as one to which organic compounds have been added.

UNIVERSITY OF MICHIGAN LIBRARIES

ing conditions: 6 amp/dm², 60°C, *p*H of 4.0, stirring by a 2-blade propeller rotating at 300 rpm. The concentration of addition agent used was determined, in part, by the maximum concentration which did not cause the deposit to crack or to peel. The cathode potential results (1) were of great assistance in choosing a representative concentration.

The results of this study are summarized in Table I. In a few cases, several different concentrations of the agent were used with identical results, but, for brevity, only a single concentration is listed in the table. The appearance of the deposit was noted and described by the terms grainy, matte, dull, semi-bright, bright with haze, or bright. A very qualitative measure of the ductility of the deposit was made by holding the deposit on the supporting wire up to the ear, bending the wire through an angle of 45°, and listening for a cracking sound. If cracking was heard, the deposit was termed brittle; if none was heard, the deposit was termed ductile. No attempt was made to grade the deposits in degree of ductility. The type of preferred orientation is given in the sixth column along with a qualifying phrase such as strong, moderate, or slight. The term "random" is used in cases where the rings appeared of uniform intensity to the naked eye over the entire arc. Several typical diffraction patterns are given in Fig. 2–5.

During this study, approximately 200 nickel electrodeposits were examined by x-ray diffraction. Since these deposits were prepared over a period of several years, all the deposits could not be examined visually at the same time. However, in several cases, lots of about 20 specimens were examined within a short period, and the surface appearance could be compared immediately with the x-ray diffraction photograph. The generalization soon emerged that there was no direct relationship between the degree or type of preferred orientation and the brightness of the surface. Both matte and bright deposits were noted with strong, preferred orientations and with complete absence of any detectable orientation. A survey of Table I shows the lack of correlation between brightness, and degree and type of preferred orientation. These results are in accord with those obtained by Clark and Simonsen (2) and by Smith, Keeler, and Read (3). On the other hand, approximately 50 per cent of the mirror-bright deposits exhibited no detectable preferred orientation when examined by x-ray diffraction. A mirror-bright deposit is considered to be one which shows no visible imperfection

FIG. 2. X-ray diffraction photograph of nickel deposit formed in presence of 0.002 mole/l of ethylenediamine. No detectable preferred orientation.

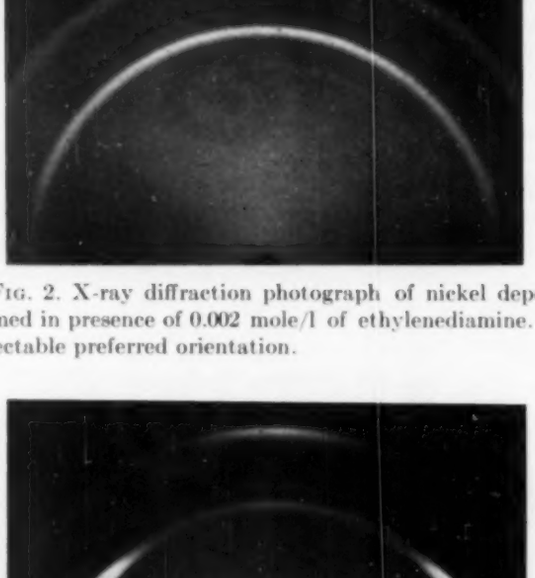

FIG. 3. X-ray diffraction photograph of nickel deposit formed in presence of 0.0007 mole/l of saccharin. Grain size less than 10^{-2} mm; strong (100) preferred orientation.

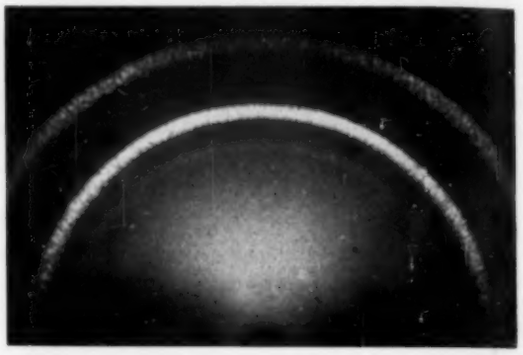

FIG. 4. X-ray diffraction photograph of nickel deposit formed in the presence of 0.003 mole/l of propionitrile. Grain size larger than 10^{-2} mm; slight (211) orientation.

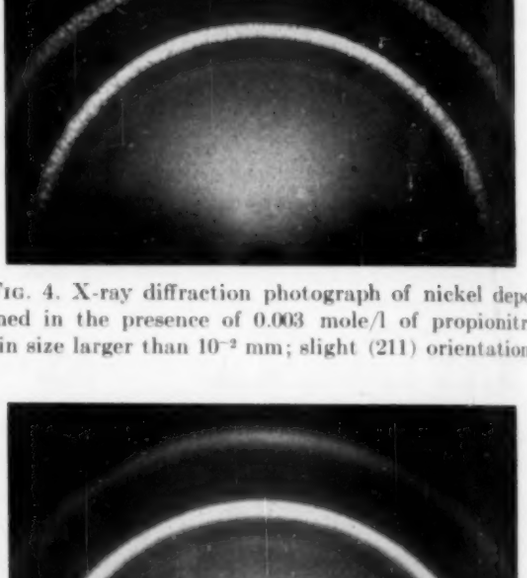

FIG. 5. X-ray diffraction photograph of nickel deposit formed in the presence of 0.008 mole/l of nickel benzaldehyde *m*-sulfonate. Grain size less than 10^{-2} mm; slight (100) orientation.

in shininess when examined in a well-lighted room and in the direct beam of a flashlight in a dark room. Many bright deposits exhibit a strong haze when examined carefully in a dark room.

In order to test the foregoing conclusion, the following experiments were performed. Nine commercial, bright plating baths were obtained and were formulated according to the directions furnished by the manufacturer. Nickel was electrodeposited on the electrolytically polished copper spheres at 50°–60°C and at current densities of 2 and 6 amp/dm^2. Mirror-bright deposits were obtained from each of the nine baths, although three of the deposits contained many pits on the surface. Four of the deposits exhibited no detectable preferred orientation, two of the deposits exhibited very slight preferred orientation, and two of the deposits exhibited slight orientation. These results furnish additional support for the conclusion that a large number of mirror-bright nickel electroplates show no preferred orientation.

Discussion

In the absence of organic additives and under the conditions used in this study, the Watts bath yielded a deposit with a (100) preferred orientation. A similar orientation has been reported by other workers (4). It is known that, when nickel is electroplated from the same bath on electrolytically polished single crystals of copper and nickel, the deposit occurs as a single crystal on the (100) faces (5). For some unknown reason, the Watts solution promotes the formation of a deposit with the (100) planes parallel to the substrate. This behavior is not characteristic of the nickel deposit alone, since a (211) orientation is observed in the all-chloride bath of Wesley (6), and, as shown in this study, small amounts of organic impurities can change the type of preferred orientation completely. An understanding of the driving force for the (100) type of preferred orientation in the Watts bath is an intriguing problem.

Twenty-three of the 29 organic compounds tested had an effect on the crystal growth of the deposit as evidenced by their ability to reduce the grain size or change the type and/or degree of preferred orientation, as compared to the deposit obtained in the unadulterated Watts bath. These compounds are classed in groups 2–5 given below. Five of the compounds yielded deposits which were similar in all respects to the deposits obtained in the unadulterated Watts bath. These five compounds thus had no effect on the crystal growth of the deposit and are classed in group 1.

Group 1. The presence of the organic compound resulted in the formation of a deposit with a grain size larger than 10^{-2} mm and with moderate to strong (100) preferred orientation.

Group 2. The presence of the organic compound resulted in the formation of a deposit with a grain size larger than 10^{-2} mm and with a preferred orientation other than (100).

Group 3. The presence of the organic compound resulted in the formation of a deposit with a grain size smaller than 10^{-2} mm and with moderate to strong (100) preferred orientation.

Group 4. The presence of the organic compound resulted in the formation of a deposit with a grain size smaller than 10^{-2} mm and with only a slight (100) preferred orientation.

Group 5. The presence of the organic compound resulted in the formation of a deposit with a grain size smaller than 10^{-2} mm and with a preferred orientation other than (100), or with no detectable preferred orientation.

The compounds falling in each of these five groups are listed in Table II.

An excellent correlation exists between the effects of the addition agents on crystal growth and the effects of the same compounds on the cathode potential (1). The following discussion is given in relation to results reported in Reference (1).

The compounds which were ineffective in changing the grain size or preferred orientation in the deposit (group 1) had a negligible effect on the cathode potential, whereas the compounds which both decreased the grain size and changed the type or degree of preferred orientation (groups 4 and 5) had a moderate to great effect on the cathode potential. The compounds which were only effective in decreasing the grain size and did not change the type or degree of (100) preferred orientation (group 3) had a small to moderate effect on the cathode potential, and yielded cathode potential curves which leveled off with further increases in concentration of the organic compound. Two of the compounds classed in group 2 (benzaldehyde and propionitrile) increased the cathode potential greatly, whereas phenol had a negligible effect on the cathode potential. The grouping of the compounds in relation to their effect on the cathode potential is given in Fig. 6 for convenience in a different form than given in Reference (1).

It appears from this correlation that the compounds which interfere only moderately with the deposition of nickel, as evidenced by a small to moderate effect on the cathode potential, are capable of reducing the grain size greatly, but are ineffective in changing the type of preferred orientation. Compounds which interfere to a great extent with the deposition of nickel are capable of both decreasing the grain size and changing the type of preferred orientation.

The compounds classed in group 3 are characterized by either acidic groups, such as the sulfonate

UNIVERSITY OF MICHIGAN LIBRARIES

or carboxyl, or by groups which are neither strongly acidic nor strongly basic, such as the sulfone and sulfonamide groups. The compounds classed in groups 4 and 5 are characterized by the presence of basic groups, such as nitrogen in conjugated ring, nitrile, and amine. The similarity of results obtained with aniline and nitrobenzene in the cathode potential and x-ray diffraction experiments suggests strongly that the nitro group is reduced under the conditions used. The greater effectiveness of the basic groups in interfering with crystal growth is not unexpected, since these compounds would presumably be attracted to the cathode by virtue of their positive charge in solution.

TABLE II. *The grouping of organic compounds according to their effects on the grain size and orientation of the deposit*

Group 1. Large grain size, (100) preferred orientation

Ethanol	Piperidine
Ethanolamine	*p*-Phenolsulfonic acid
Ethylamine	

Group 2. Large grain size, orientation other than (100)

Benzaldehyde
Phenol
Propionitrile

Group 3. Small grain size, strong (100) orientation

m-Benzenedisulfonic acid (Ni salt)	Saccharin
Benzoic acid	Thianaphthene dioxide
Naphthalene-2,7-disulfonate (Na salt)	*p*-Toluenesulfonamide
Naphthalene-1,3,6-trisulfonate (Na salt)	

Group 4. Small grain size, slight (100) orientation

p-Aminosulfonic acid
Benzaldehyde *m*-sulfonate (Ni salt)
Thiourea

Group 5. Small grain size, random or orientation other than (100)

m-Aminophenol	Nitrobenzene
Aniline	Pyridine
Benzonitrile	Quinaldine ethiodide
Ethylenecyanohydrin	Quinoline ethiodide
Ethylenediamine	Succinonitrile
1-Napthylamine-4,8-disulfonic acid	

Fifteen of the 30 deposits recorded in Table I were graded brittle and 15 were graded ductile. In the case of the brittle deposits, 13 exhibited no preferred orientation or a preferred orientation other than (100), and two exhibited slight (100) preferred orientation. In the case of the ductile deposits, 14 exhibited (100) preferred orientation and only one exhibited another type. It appears that the compounds which were sufficiently active at the surface to change the type of preferred orientation also had a great tendency to impart brittleness to the deposit.

No correlation between brittleness and grain size was detected. A large grain size did not necessarily confer ductility to the deposit, and a small grain size did not necessarily confer brittleness. Ductile and brittle deposits were both observed with grain sizes smaller and larger than 10^{-2} mm.

The primary interest of this study was to determine the effect of individual organic compounds on the crystal growth of nickel during electrodeposition. The results, however, are also of value in assessing any relation between preferred orientation and brightness. Results with over 200 electrodeposits indicated conclusively that there is no correlation between preferred orientation and brightness. How-

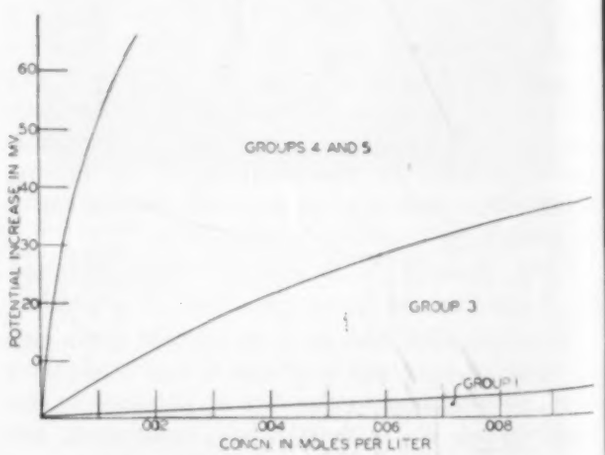

FIG. 6. Correlation of the effects of organic compounds on the cathode potential at 1 amp/dm² with their effects on crystal growth (see Table II).

ever, it was noted that a high fraction (roughly 50% in this study) of the mirror-bright deposits exhibited no detectable preferred orientation. Clark and Simonsen (2) made a similar observation, but they did not stress the fact. These workers examined 86 nickel deposits, of which 15 were bright. Eleven (73%) of these 15 bright deposits had, in their words, "a random distribution of crystals." The results of Smith, Keeler, and Read (3) are more difficult to evaluate on this basis because they compared the line intensities obtained by back reflection in order to detect orientation. These workers examined 33 nickel deposits prepared in the presence of various organic agents, of which eight deposits were considered bright by visual examination. Six of these deposits yielded line intensity ratios the same or only slightly different from that obtained from a recrystallized nickel sheet, which presumably exhibited no preferred orientation. Only two of the deposits exhibited line intensity ratios greatly different from the nickel sheet. It is thus concluded that six (75%) of the eight bright deposits studied by Smith, Keeler, and Read showed no preferred orientation.

Even though it appears true that a high fraction of bright nickel plates exhibit no preferred orientation, it is also true that the absence of preferred orientation does not necessarily lead to a bright plate. Many of the dullest plates observed in this study also showed no detectable preferred orientation. The results with 1-naphthylamine-4,8-disulfonic acid afford an excellent example. The specimen was bright on one side and matte on the other, yet the x-ray diffraction photographs in both areas were identical: neither area exhibited preferred orientation and both areas had grain sizes between 10^{-2} and 10^{-4} mm.

The great majority of bright nickel electroplates formed in the presence of organic compounds have a small grain size, as pointed out by Zentner, Brenner, and Jennings (7). However, a small grain size does not necessarily lead to a bright deposit, as shown by Clark and Simonsen (2).

It is interesting to note that bright nickel plates can be obtained with no detectable preferred orientation and a small grain size, as well as with complete orientation and a very large grain size (single crystal), as is the case when deposition is carried out on the (100) face of copper or nickel single crystals (5). Bright plates can thus be obtained at both ends of a scale of grain size and orientation.

The lack of any preferred orientation in a high fraction of mirror-bright deposits indicates that one function of an addition agent is to minimize the differences between crystal faces at the surface. It appears that crystal growth is no longer controlled during bright plating by the nickel surface but by a film adjacent to the surface, since it is known from studies carried out by Gwathmey and coworkers at the University of Virginia and studies carried out in this laboratory that, when the rate of reaction is controlled by the surface, the reaction occurs at different rates on the various crystal faces.

Acknowledgment

The authors wish to express their deep appreciation to the laboratory staff of the Harshaw Chemical Company and especially to Mr. Andrew Aylies for their cooperation and sympathetic interest in this research.

Any discussion of this paper will appear in a Discussion Section, to be published in the June 1954 issue of the Journal.

REFERENCES

1. C. C. Roth and H. Leidheiser, Jr., to be published.
2. G. L. Clark and S. H. Simonsen, *J. Electrochem. Soc.*, **98**, 110 (1951).
3. W. Smith, J. H. Keeler, and H. J. Read, *Plating*, **36**, 355 (1949).
4. C. S. Barrett, "Structure of Metals," p. 439, McGraw-Hill Book Company, New York (1943).
5. H. Leidheiser, Jr., and A. T. Gwathmey, *J. Electrochem. Soc.*, **98**, 225 (1951).
6. W. A. Wesley and J. W. Carey, U. S. Pat. 2,316,303, April 13, 1943.
7. V. Zentner, C. W. Jennings, and A. Brenner, *Plating*, **39**, 865 (1952).

UNIVERSITY OF WISCONSIN LIBRARIES

Copper-Activated Zinc Sulfide Phosphors with Trivalent Substituents[1]

H. C. Froelich

Lamp Development Laboratory, General Electric Company, Cleveland, Ohio

ABSTRACT

With increasing concentrations of Cu and Al in H_2S-fired Zn(Al)S:Cu phosphors, the emission spectrum is shifted from green to orange under 3650 Å excitation. The emission of these triple sulfides consists of three sub-bands of such relative intensities that the presence of a single band is simulated. The bands have different temperature, decay, and excitation characteristics. Among other substituents, the elements Sc, Ce, Pr, and Nd are of interest, as they produce infrared stimulability even with high activator concentrations.

When fired in H_2S with oxide additions, the phosphors with Al emit only green light and become strongly electroluminescent. The green emission persists at all frequencies from 60 to 15000 cps. Phosphors prepared with 0.1 to 0.4 per cent Cu and with 0.25 to 2.5 moles Al/mole Cu are nearly equally bright. The mole ratio Cu:Al in the brightest NaCN-washed phosphors is near 1:1.

The results lend strong support to Kroeger's theory of charge compensation. The complexity of the emission spectra leads to the conclusion that several species of Cu atoms must be present in the phosphors. The electroluminescent response is attributed to oxide barriers in, or on, the phosphors.

Introduction

According to Kroeger and Dikhoff (1), blue and green emitting ZnS:Cu phosphors of high brightness are obtained when trivalent cations such as Al are introduced into the phosphor in place of monovalent halide ions. These results have been interpreted with the principle of charge compensation. Assuming that copper is monovalent, the incorporation of Cu into the ZnS lattice should be facilitated if pairs of monovalent copper and trivalent aluminum ions are introduced rather than copper alone, to replace pairs of divalent zinc ions at lattice sites.

Kroeger and Dikhoff's results are reported for copper concentrations from zero up to 10^{-4} gram atoms Cu per mole ZnS, or about 0.0065 per cent Cu in the phosphor. Their results are readily reproduced with these and the lower concentrations of Cu and Al. An extension of this work to much higher Cu and Al contents, however, has disclosed the existence of a new phosphor system with emissions extending into the orange. Already summarized briefly (2), the results are reported below in greater detail. They lend even stronger support to the contention that true triple sulfides are formed on the basis of the principle of charge compensation. However, interpretation is rendered more difficult due to the complexity of the observed emission spectra and to the dual role of activator and of base modifier which copper is now found to assume in the phosphors. This, in turn, may be related to the fact that, in previously studied phosphor systems, copper has not been found to be an effective activator when present in concentrations as high as 0.5 per cent Cu or more.

[1] Manuscript received January 20, 1953. This paper was prepared for delivery before the New York Meeting, April 12 to 16, 1953.

Characteristics of Phosphors Fired in Pure H_2S

Experimental

The phosphors were prepared and fired in the manner described in a previous paper (3). Copper and the trivalent elements were introduced in form of several salts such as chlorides, nitrates, sulfates, etc., with equally consistent results. Most of the phosphors were fired at 1100°C for ½ to 1 hour. Minor changes in the firing temperature did not produce characteristic changes in phosphor emission. When fired at 1000°C, the brightness was generally lower; when fired at 1200°C, the phosphors were coarser compared with the 1100°C materials. The presence of small amounts of air or gaseous oxides in the firing atmosphere caused relatively minor changes in emission characteristics in some cases, and very striking changes in other cases, notably those involving aluminum as the substituent. For this reason, the phosphors prepared in pure H_2S are considered separately from the phosphors fired in the presence of oxide additions. The phosphors with aluminum have so far been given more detailed consideration. Most of the emphasis in this report is, therefore, on materials with aluminum additions.

The emission curves were obtained with a recording spectroradiometer. In order to emphasize rela-

tive changes more clearly, all emission curves have been normalized at the peak positions. Unless otherwise noted, all activator concentrations refer to the amounts of Cu and Al, etc., in per cent by weight of ZnS, that were introduced in the raw batch mixture. The excitation source was a BH4 lamp.

Zn(Al)S *Phosphors*

Pure precipitated ZnS, fired in pure H_2S, did not give a fluorescent response with optical excitation. The introduction of aluminum into pure ZnS resulted in a weak to medium-bright emission with 3650 Å excitation. This is shown in Fig. 1 for two concentrations of Al. Of the two fairly well resolved bands, the greener one at about 5000 Å became more prominent at the higher Al concentration when excited at room temperature. At the temperature of liquid nitrogen, the samples with Al showed only a faint to weak blue emission in the 4500 Å band. At room temperature, the sample with low Al content gave a fairly long lasting green phosphorescence, while the sample with the higher Al concentration had a very short decay.

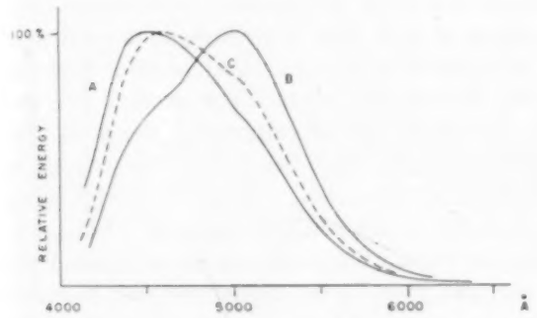

FIG. 1. Emission of H_2S-fired Zn(Al)S phosphors. Curve A—0.32% Al; curve B—1.7% Al with 3650 Å excitation; curve C—1.7% Al with cathode ray excitation.

It is not clear whether the emission is due to zinc or to aluminum atoms or ions in the Zn(Al)S base material.[2] As is well known from the system SrS–Ce_2S_3, solid solutions of trivalent sulfides in divalent sulfides are capable of existence up to certain molar proportions, and without formation of thio-spinells. This appears to be the case also with ZnS–Al_2S_3. Almost all of the Al_2O_3 that was formed or introduced in the raw material mix appears to have been converted into Al_2S_3 during the firing. The phosphor with 0.3 per cent Al was almost completely soluble in dilute HCl, while the material with 1.7 per cent Al left only a small amount of insoluble residue. The latter had to be calcined at 700°C in order to give the x-ray diffraction pattern of Al_2O_3. The formation of Al_2S_3 took place only when the aluminum compounds were in contact with ZnS; pure Al_2O_3, fired in H_2S at 1200°C, was not converted into Al_2S_3. The phosphors did not hydrolyze with water to give H_2S, and the washed materials retained their luminescence unimpaired. This is taken as indirect evidence that a solid solution was formed. X-ray diffraction work is in progress to determine the phase relationships.

The optical excitation of the phosphors was due to a weak absorption band in the near u.v. at about 3800 Å. As shown in Fig. 2, this band became slightly stronger with increasing Al concentration. The phosphors did not respond to infrared stimulation or to electroluminescent excitation. Under cathode ray excitation, the same blue and green emission bands were obtained as with u.v. excitation, but in different relative, and very low absolute intensities. The blue band was the stronger of the two with both Al concentrations.

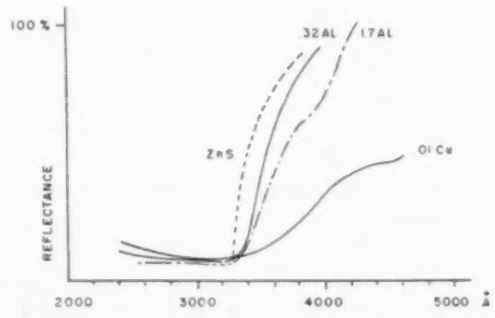

FIG. 2. Reflection spectra of H_2S-fired ZnS phosphors

Zn(Al)S:Cu *Phosphors*

In order to study the combinations of Cu and Al in ZnS, several different series of phosphors were prepared. For each concentration of Cu several concentrations of Al were used, representing deficiencies, equal amounts, and amounts in excess over the molar equivalents of Cu. The changes in emission that resulted from these substitutions are surveyed in the curves of Fig. 3 for 3650 Å excitation.

With copper concentrations up to about 0.05 per cent, all emissions at room temperature were substantially green, regardless of the amounts of Al introduced. This is shown by curves *A*, *B*, and *C* in Fig. 3. Curves *B* and *C* are identical despite a tenfold increase in Al content. They are slightly displaced compared with curve *A* due to a tenfold increase in the Cu activator content and the resulting suppression of the blue emission. At low Cu concentrations, therefore, Al is not a very effective modifier

[2] The abbreviated notation used for these zinc-aluminum sulfide phosphors was chosen to suggest that the exact manner in which Al is incorporated in the ZnS matrix is still uncertain, and that Al probably acts chiefly as a base modifier, especially in the system with additional copper.

PRINCETON U. MICROBIAL LIBRARIES

of the emission spectrum. At the lowest Cu concentration, curve *A*, the usual blue band appears individually and in low intensity.

With increasing concentration of Cu, the blue band disappeared and the peak of emission shifted further toward longer wave lengths. At 0.3 per cent Cu the shift became still stronger and the effect of Al became more characteristic. Thus, curve *E* for 0.3 per cent Cu and 0.069 per cent Al (mole ratio 1:0.54) peaks at 5400 Å, curve *F* for 0.32 per cent Al (mole ratio 1:2.5) peaks at 5550 Å, and curve *G* for 0.69 per cent Al (mole ratio 1:5.4) peaks at 5740 Å in the yellow. Simultaneously the curves broaden

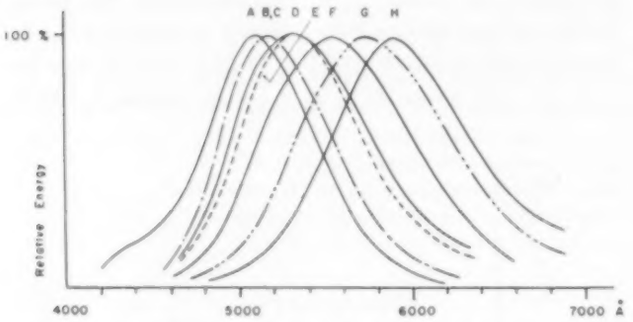

FIG. 3. Emission of H_2S-fired Zn(Al)S:Cu phosphors with 3650 Å excitation.

Curve	% Cu	% Al	Moles Al per mole Cu
A	0.005	0.0114	5.4
B	0.05	0.069	3.2
C	0.05	0.69	32.0
D	0.1	0.23	5.4
E	0.3	0.069	0.54
F	0.3	0.32	2.5
G	0.3	0.69	5.4
H	0.6	1.37	5.4

to a considerable extent, such that the half width of curve *G* is about 40 per cent greater than that of curve *A*. Curve *H* shows the emission spectrum of a phosphor with 0.6 per cent Cu and 1.37 per cent Al (mole ratio 1:5.4) which peaks at 5900 Å. With still higher Cu contents, the emission spectrum did not appear to deepen further appreciably, and the intensity of emission became too low for the spectrum to be recorded. Phosphors made with 1 per cent Cu or more (and corresponding amounts of Al) did not fluoresce at room temperature. They fluoresced only at low temperatures with u.v. excitation, and were olive colored in daylight.

Those phosphors which were prepared with molar deficiencies of Al compared with Cu contained excess free copper sulfide, which was readily removed by means of NaCN. The phosphors with molar equivalents or excess of Al over Cu did not contain any appreciable amounts of free copper sulfide. Likewise, they did not contain any free Al_2S_3 as they were not decomposed by water or weak acetic acid. However, they contained some Al_2O_3 which separated out when the phosphors were dissolved in dilute HCl.

While the amount of acid-insoluble Al_2O_3 increased with increasing molar excess of Al over Cu, the amount of readily soluble Al was much higher than the actual Cu equivalent. For example, three phosphors, prepared with 0.3 per cent Cu and with 2.2, 5.4, and 21.6 moles added Al per mole added Cu, gave 2.1, 3.9, and 15.8 moles soluble Al per mole Cu, as found by analysis for acid-insoluble Al_2O_3. Thus the amount of soluble Al increased in both relative and absolute amount compared with the constant amount of Cu.

It is uncertain, however, whether all acid-soluble Al was due to Al_2S_3 or at least in part to some Al_2O_3. In other words, the amounts of Al that were readily soluble in acid do not necessarily represent only the amounts of Al_2S_3 that were present in solid solution in ZnS, but they may also contain some acid-soluble Al_2O_3. The source for the latter product may be the excess Al_2O_3 in the phosphor itself (part of it being soluble and part of it being insoluble in acid) or, as a further complication, a possible solid solution of Al_2O_3 in ZnS which could also provide a homogeneous phosphor phase. The identification of separate phases in the phosphors, such as Al_2O_3, if any, is currently being attempted by x-ray diffraction. Preliminary work has shown only the diffraction lines characteristic of the ZnS wurtzite structure.[3]

Whether or not the conversion of the added aluminum salts into Al_2S_3 stops exactly at the mole ratio Cu:Al = 1:1, or continues beyond, there is a definite effect of excess Al upon the emission spectrum. This is shown by curves *E* to *G* in Fig. 3 where Al becomes increasingly more effective after the 1:1 mole ratio has been overstepped.

The phosphors with equivalent amounts or excess of Al turned out with white to yellow to olive body colors which did not change when the materials were washed with NaCN. The depth of color increased with increasing Cu concentrations. The phosphors appeared to contain all added Cu incorporated in solid solution. Chemical analysis for retained Cu content (after an NaCN wash) showed full recovery, within the experimental error, of all added Cu in the phosphors prepared with a molar excess of Al. Thus the phosphors appeared to represent complete solid

[3] (*Added in print*) According to a recent paper by H. Hahn and G. Frank [*Z. anorg. u. allgem. Chem.*, **269**, 227 (1952)], a compound of composition $ZnAl_2S_4$ was also found to have the wurtzite structure of ZnS when prepared above 1000°C, and the spinell structure when prepared at lower temperatures, the transformation being reversible.

solutions of (presumably) Cu_2S in the base material to form true triple Zn-Al-Cu sulfides. Expressed differently, the solubility of copper sulfide (Cu_2S) is considerably higher in zinc-aluminum sulfide than in pure zinc sulfide.

In some respects, the new Zn(Al)S:Cu phosphor system is reminiscent of the (Zn,Cd)S:Cu system, in which an increase of the substituting sulfide produces a shift of the ZnS:Cu emission toward longer wave lengths. However, the efficiency of the yellow-orange emitting Zn(Al)S:Cu phosphors was only about one-half of that of (Zn,Cd)S:Cu phosphors of similar color. The greener materials approached the brightness of the phosphors with cadmium, while at the longer wave length side the brightness fell off much more rapidly. However, there are other characteristic differences.

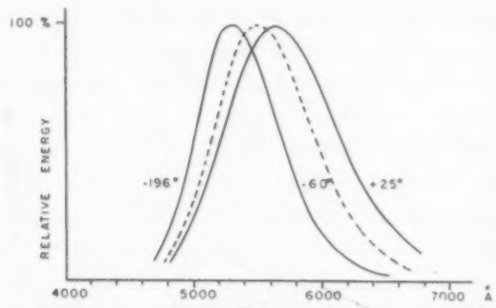

FIG. 4. Emission of phosphor *G* in Fig. 3 with 3650 Å excitation at different temperatures.

The (Zn,Cd)S:Cu system requires very small amounts of Cu activator (less than 0.01%), while the Zn(Al)S:Cu system requires up to 100 times as much Cu to produce corresponding colors. In this system, the substituting sulfide is actually a double sulfide, the pair Cu_2S-Al_2S_3 apparently replacing 4 ZnS in the lattice just as 4 CdS replace 4 ZnS in the phosphors with cadmium. Hence the peculiar situation in these new phosphors where copper performs a dual role, namely, that of a matrix constituent and modifier, and that of an activator as well.

Further differences with the (Zn,Cd)S:Cu system were found in the phosphorescent decay, which is rather long and strong in this system, but comparatively brief in Zn(Al)S:Cu. Also, the phosphors with cadmium are quite temperature stable, while the phosphors with aluminum lost brightness very rapidly at elevated temperatures. They were practically extinct at temperatures of 100°–150°C. On cooling to low temperatures, they all increased in brightness and changed to green, as shown, for example, in Fig. 4 for a phosphor with 0.3 per cent Cu and 0.69 per cent Al. While the peak of emission shifted from 5740 to 5300 Å, the intensity of emission increased, and the half width decreased again by nearly 40 per cent. Even the phosphor with 1 per cent Cu and 1.37 per cent Al was fairly bright green when excited at −196°C with 3650 Å radiation.

The emission bands give the impression of being true single bands which are displaced with increasing matrix substitution, as in the case of (Zn,Cd)S:Cu. This is not so, however. It can be demonstrated that the emission consists of three sub-bands of such relative intensities that the presence of a single band is deceptively simulated.

The change in color and attendant greater change in half width with low temperature excitation are taken as one indication of a multiple band emission at room temperature. A second point is the fact that the emission spectrum is dependent upon the intensity of the exciting u.v. radiation, as shown in Fig. 5 for the phosphor with 0.3 per cent Cu and

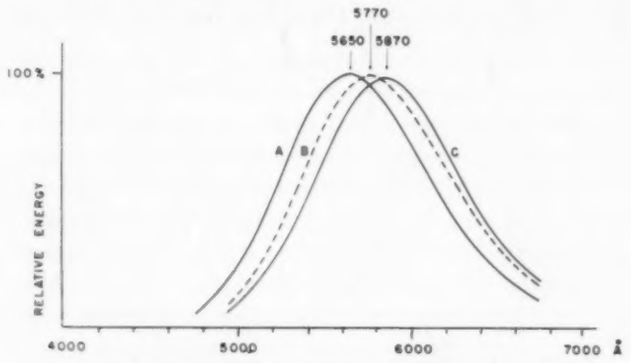

FIG. 5. Emission of ZnS (0.3% Cu, 0.69% Al) with different intensities of 3650 Å excitation. Approximate ratio of intensities A:B:C = 40:5:1.

0.69 per cent Al. An increase in the 3650 Å intensity, estimated at about fortyfold, caused the emission spectrum to move about 200 Å toward shorter wave lengths. The phosphor looked considerably greener when excited at close range, and more orange when excited at a greater distance from the BH4 lamp. This is readily explained with the postulate of two or more individual bands in the emission spectrum, the bands having different excitation sensitivities. As the intensity of the exciting radiation is increased, the longer wave length band appears to be approaching a state of saturation, while the intensity of the green band continues to build up at a regular rate. While the half width of the emissions does not change over the range of u.v. intensities used, it is not likely that the observed shift represents a mere displacement of a single band.

The strongest argument for multiple band emission, however, was found in the phosphorescent decay of these phosphors. Though not measured as yet, the decay was observed to consist of a very rapidly declining green emission and a far more slowly declining yellow-orange emission. The time constants for the two decays were estimated to differ by a factor of the order of 100.

DIGITIZED BY MICHIGAN LIBRARIES

In Fig. 3, the peak emission of the phosphor with 0.3 per cent Cu and 0.69 per cent Al is shown to be at 5740 Å. This is about intermediate compared with the results of Fig. 5 for the same phosphor. As the distance of u.v. source-phosphor-spectrograph slit was not changed while the curves for the phosphors of Fig. 3 were taken, the relative color changes due to phosphor composition as shown in that figure are approximately correct for the particular intensity of 3650 Å radiation used. The isolation of each sub-band as a function of the exciting energy and intensity remains to be undertaken.

The band at 5900 Å appears to be the longest wave length emission which the Zn(Al)S:Cu phosphor system with high Cu contents can furnish. The green band at 5150 Å represents the other extreme. Thus, one might expect that these two bands in different

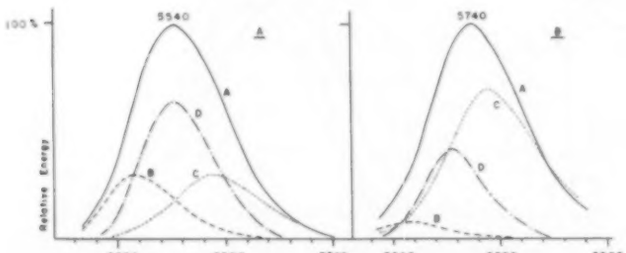

FIG. 6. Approximate intensity distribution of sub-bands in emission spectra of 3650 Å-excited ZnS phosphors with: A—0.3% Cu and 0.32% Al; B—0.3% Cu and 0.69% Al.

relative intensities should yield the observed emissions of the intermediate phosphors. This is not so. At least three bands are required to synthesize the observed emissions from simpler sub-bands.

The third band is obtained by subtracting the extreme bands (in intensities adjusted by trial to give the best fit) from the observed emission bands of the yellow phosphors. The remaining band peaks at 5550 Å, it has a normal shape, and it is always found at the same position. Its half width is slightly larger than that of the green band and slightly smaller than that of the orange band. This is shown in Fig. 6A where the reconstruction of the emission spectrum of phosphor *F* in Fig. 3 is indicated. The solid line represents the emission as recorded, from which the adjusted sub-bands *B* and *C* have been subtracted to leave the third band as the dashed line *D*. A slight discrepancy occurred only at the deep red end where the measurements were known to be less reliable (slightly too high).

Curve *B* in Fig. 6A is identical with curve *B* in Fig. 3, reduced to 30 per cent of its peak intensity; likewise, curve *C* in Fig. 6A is identical with curve *H* in Fig. 3, also reduced to 30 per cent of its peak intensity. This leaves the differential band *D* at 5550 Å as the most intense band of the three. The sum of the sub-bands B, C, and D gives curve *A*, the observed emission. In this particular phosphor, therefore, the relative intensity contribution of the three sub-bands is in the approximate ratio of 1:2:1.

While the construction of curve A in Fig. 6A may seem obvious due to the fairly symmetrical grouping and identical height of the sub-bands *B* and *C*, the emission curves of other intermediate phosphors such as *G* in Fig. 3 can be equally well reconstructed from the same three bands. In this case, however, the ratio of peak intensities for the 5150, 5550, and 5900 Å bands must be about 1:6:10 in order to obtain a good match. This is done by adjusting the 5150 Å band to 10 per cent of peak intensity and the 5900 Å

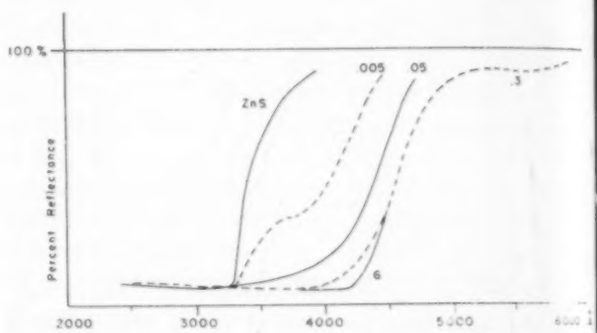

FIG. 7. Reflection spectra of H_2S-fired ZnS phosphors with constant mole ratio of Cu:Al = 1:5.4. Figures next to curves indicate per cent by weight of added Cu.

band to 70 per cent of peak intensity as shown in Fig. 6B. If the adjusted bands are subtracted from the recorded band, the remaining band at 5550 Å is identical in shape with the one obtained from curve *F* above. In this phosphor the band at 5900 Å is the dominant one. For this reason, the discrepancy at the deep red end becomes slightly worse.

It is curious that the relative intensities of the three sub-bands seem to be always so adjusted that the resulting emissions as observed with average intensities of exciting radiation present the picture of normally shaped single bands. There are no humps in the curves to indicate the beginning of resolution at either room or lower temperatures. It has not been possible so far to isolate the 5550 Å band for observation by itself.

The optically excited emission of the phosphors is due to a strong absorption band in the near u.v. which extends into the visible. This band, as obtained in reflection and shown in Fig. 7, is at the same position as the bands for Cu and Al alone. It is a great deal stronger, however, and increases in strength with increasing concentrations of both Cu and Al. A

complete absorption spectrum is shown specifically for the phosphor with 0.3 per cent Cu and 0.69 per cent Al. The absorption in the blue is responsible for the yellow body color of the phosphor. The excitation spectrum for these materials will not coincide with the absorption spectrum, as neither short u.v., such as 2537 Å radiation, nor blue light, such as the strongly absorbed 4200 Å radiation, lead to any noteworthy fluorescent response of the phosphors.

When excited by 5000-volt cathode rays with moderate beam currents, all Zn(Al)S:Cu phosphors with copper contents in excess of 0.05 per cent emitted substantially green luminescence, regardless of the amount of Al present, and regardless of their color with u.v. excitation. The bands were of normal shape. The peak positions shifted from 5100 Å for the phosphor with 0.05 per cent Cu to 5300 Å for the materials with up to 0.6 per cent Cu. Aluminum played only a minor role in broadening the spectrum, in contrast to the results obtained on the same phosphors with u.v. excitation. For phosphor *G*, for example, the shift of peak with u.v. excitation amounted to 700 Å and the broadening to about 40 per cent compared with phosphor *A*; with cathode ray excitation of the same phosphor sample, the shift of peak amounted to only 200 Å and the broadening to about 15 per cent.

Practically all Zn(Al)S:Cu phosphors fired in atmospheres of pure H_2S were nonresponsive to electroluminescent excitation. The only exceptions were materials prepared with molar deficiencies of Al which were fired at lower temperatures. This is discussed below. Unlike the ZnS:Cu phosphors described in the preceding paper, those prepared with additional Al did not respond to infrared stimulation.

In view of the different emission characteristics of the phosphors with u.v. and with cathode ray excitation one might suspect that the materials were not homogeneous so far as the fluorescent phase is concerned (i.e., disregarding the presence of free Al_2O_3). Conceivably, a shell of a certain composition and fluorescent response on each phosphor particle might surround a core of different composition and response. This was disproved, however, by subjecting the phosphors to slow and destructive dissolution in strong acid. The characteristic emissions of the phosphors under u.v. and under cathode ray excitation, respectively, persisted at all stages until the very last of the materials had been dissolved by the acid (again disregarding any Al_2O_3).

Trivalent Substituents other than Al

The introduction of other trivalent elements into H_2S-fired ZnS:Cu phosphors with higher copper contents has been explored to a considerable extent. While a large number of experimental results have been obtained, only a very brief and qualitative survey can be presented here. This introductory survey will be confined to only those compositions which appear to be of greater interest and novelty.

The trivalent elements may be expected to give results similar to aluminum, unless their ionic size is either much too small or much too large to permit easy entry into the ZnS lattice. The extremes in ionic radii of the trivalent group III elements are found in boron (0.2 Å) and lanthanum (1.15 Å), compared with aluminum (0.55 Å) and the next closest element, gallium (0.65 Å). Thus Kroeger and Dikhoff have found that the copper emission in ZnS phosphors with low Cu contents and any of the larger trivalent group III elements is the same position-wise and differs mainly intensity-wise.

At the higher Cu concentrations, such equivalence was no longer found. For example, phosphors with 0.1 per cent Cu and enough Ga to give mole ratios of 1:1 and 1:5 were practically devoid of any fluorescent response to either u.v., cathode ray, or electroluminescent excitation. They gave a very weak orange luminescence when excited at −196°C; this despite the fact that the materials were apparently triple sulfides like the compositions with aluminum. They were of light yellow body color, did not contain any appreciable amount of free copper sulfide, and did not hydrolyze with water or weak acetic acid.

Similarly, homogeneous materials were obtained with indium, yttrium, and lanthanum in place of aluminum, and with copper contents of 0.1 per cent. The body color of the samples with indium was a deep yellow. They gave a weak deep orange-red emission with a peak at about 6700 Å when excited by u.v. at room temperature, and a lighter and brighter emission at −196°C. With cathode ray excitation the emission was a weak deep orange. Yttrium, in equimolar amount and in excess of 0.1 per cent Cu, gave yellowish-brown body colors, a weak orange emission with 3650 Å excitation which became redder at low temperatures, and a fairly bright yellow-orange emission with cathode ray excitation. The fluorescence of the samples with La was a very weak green. Despite the low intensity of fluorescence, the phosphorescent decay was long and strong, especially in some samples made with high La contents.

While all these materials appeared to be built up according to the same principle which governed the formation of rather bright phosphors with aluminum substitution, the fluorescent response of these other materials was surprisingly poor. In particular, the lack of response in the case of gallium was of interest in view of the great chemical similarity between Ga and Al. Thallium probably does not form a trivalent sulfide at the firing temperatures in question, but

several group V elements, such as Bi or Sb, probably do. These elements, however, were ineffective in promoting the formation of triple sulfides with ZnS and Cu_2S.

The remaining group III elements, including especially a few of the rare earths, were again of considerable interest. Thus, triple sulfides with bright yellow and orange luminescence were obtained with scandium in equimolar amount and in excess, and with as much as 0.3 per cent Cu or more. The materials appeared to be homogeneous and contained all added Cu in nonextractable form. They were of light tan to deeper orange-brown body colors, the colors increasing in depth with increasing Cu and Sc contents and with increasing firing temperature. The yellow to orange luminescence was obtained with u.v. as well as with cathode ray excitation, the fluorescent color likewise deepening with higher activator concentrations and higher firing temperature. It was again found that a two-band or multiple emission was involved consisting of a green and at least one orange band. The phosphorescence was very strong in all samples with scandium.

Under u.v. excitation, the phosphors with scandium showed reasonably good temperature stability of the orange band, while the green band faded much more rapidly at elevated temperatures. Thus, all phosphors emitted orange light between 100 and 200°C. The phosphors also showed a strong thermoluminescent emission of both green and orange, the orange being stronger in the materials with high scandium contents.

The phosphors with scandium were of greatest interest, however, because of their strong infrared stimulability. The emitted light was of yellow to orange color in the brightest phosphors which were made with 0.05 per cent Cu and increasing amounts of Sc. However, and this seems even more interesting, the stimulated emission was also very strong in the phosphors made with as much as 0.3 per cent Cu. The usual activator concentrations in stimulable sulfide phosphors are in the parts per million range, higher concentrations leading to quenching. The phosphors with scandium were stimulable only when fired in H_2S. When prepared with NaCl flux in the usual manner, they showed no stimulability whatever, and they fluoresced green instead of yellow-orange.

Compared with the strontium sulfide infrared phosphors, the Zn(Sc)S:Cu materials were less bright in stimulation, but they showed much greater stability to atmospheric exposure. Thus, they were not attacked in over a week's contact with moist air or liquid water, indicating that the Sc_2S_3 that was formed appeared to have been incorporated in a stable solid solution in ZnS.

Similar results were obtained when cerium, praseodymium, or neodymium were used as the trivalent substituents. Praseodymium and neodymium produced orange luminescent colors in excitation and stimulation, while the colors of the phosphors with cerium were more concentration-dependent, ranging from green-yellow to orange with increasing Ce.

The emission spectra of phosphors with these three substituents showed the appearance of narrower, resolved bands, even with room temperature excitation. Cerium gave such bands near 4400, 5000, 5500, and 6700 Å. Praseodymium and neodymium gave even sharper bands approaching line emission in width, which were superimposed upon a continuous background of orange-red emission with peaks in the red. With Pr, the bands or lines were located at 5040, 5500, 6100 (multiplet), and 6700 Å. By far the strongest of the four was the one at 6700 Å, in a phosphor with 0.05 per cent Cu and 0.22 per cent Pr (mole ratio 1:2). The 6700 Å band towered sharply over the continuous background, with its peak intensity in the deep red. In the phosphors with neodymium, the bands or lines were located at 5050, 5410, 6050 (multiplet), and 6680 Å. The strongest band here was the one at 6050 Å in a phosphor with 0.05 per cent Cu and 0.23 per cent Nd (mole ratio 1:2). When excited at −196°C, the sharp bands did not change their position or half width; the continuous background, however, moved slightly toward longer wave lengths. It is evident that the narrow bands represent the characteristic emission of the rare earths, while the background represents the characteristic red emission of Cu discussed previously (3).

While the phosphors with 0.05 per cent Cu were brighter than the compositions with 0.3 per cent Cu, it was of interest that the latter products not only fluoresced at all, but were again responsive to infrared stimulation and in some cases to electroluminescent excitation.

The results on the combination of copper with the rare earths (at high concentrations) thus parallel the results which Kroeger and Dikhoff (1) obtained with the combination of silver with the rare earths (at low concentrations). The characteristic line emission is superimposed upon a continuous background in both cases. In this connection it is of interest to note that a corresponding system of phosphors with high silver and aluminum, etc., contents could not be developed. Phosphors with amounts of Ag that are equivalent to the 0.05 to 1 per cent range of Cu concentrations reported here did not fluoresce and did not appear to form homogeneous triple sulfides.

The storage ability of the phosphors with Ce was better than that of the materials with Sc, Pr, or Nd. After storage for 15 hours in the dark, the stimulated

light was about as bright as it was immediately following the excitation by u.v. While the introduction of the other trivalent elements had produced yellow to brown body colors of the phosphors, the H_2S-fired materials with Ce were pink to purple colored.

The remaining group III and rare earth elements produced little if any fluorescent response of interest, when used in conjunction with such relatively high concentrations of Cu as 0.05 to 1 per cent.

Phosphors Fired in Atmospheres of H_2S with Oxide Additions

Experimental

As mentioned before, the characteristics of some of the phosphors discussed changed markedly when they were fired in the presence of oxide additions to the H_2S firing atmosphere. These changes were especially noteworthy in the phosphors with aluminum substitution.

When the latter materials were fired in H_2S with small admixtures of air, water vapor, CO_2, SO_2, etc., the incorporation of copper sulfide became incomplete, regardless of the amount of Al present; the body color of the phosphors changed to the usual tan-gray characteristic of ZnS-ZnO:Cu phosphors; the yellow-orange emission substantially disappeared, leaving only the green emission; and the materials became strongly responsive to electroluminescent excitation within certain ranges of activator concentrations.

The phosphors were prepared as described previously, except for the addition of the oxide gases. For most of the compositions 1100°C proved again to be the optimum firing temperature. The relative brightness under u.v., cathode ray, and electroluminescent excitation was not the same for all phosphors. Since the phosphors were prepared with much higher Cu concentrations than those reported by Kroeger and Dikhoff (1) (for pure H_2S-firing), their brightness under u.v. excitation was not quite as high. Considering the large amount of Cu which was actually incorporated in the materials, however, their brightness was surprisingly high. Most of the discussion below will be devoted to the electroluminescent response which appears to be of greater interest in connection with these phosphors.

The admixture of oxide gases to the H_2S was simple only in the case of water vapor. When bubbled through water or dilute $Ba(OH)_2$ solution at room temperature, a mix of H_2S with about 3 per cent H_2O was conveniently obtained. To prepare mixtures with lower water contents, the gas mix was passed through traps cooled to lower temperatures to freeze out excess water. The vapor pressure of the ice formed was then assumed to determine the desired partial pressure of H_2O in the emerging gas mix. To obtain mixtures with more than 3 per cent H_2O, the gas was bubbled through heated water and the duct to the firing vessel was kept hot to prevent condensation.

For mixtures with air and CO_2, flowing currents of these gases were mixed with H_2S in a larger vessel and then led to the firing vessel after passing a trap cooled to -57°C. At this temperature, the vapor pressure of ice is 12 μ. Thus water was effectively removed to the extent of about 1 part in 65,000. The resultant mixture with such low water content acted as though it contained no water at all, i.e., the phosphors had the same characteristics as those fired in pure H_2S. The amounts of air and CO_2 that could be dosed reasonably well by this method ranged from 2 to 20 per cent.

When the phosphors were fired in atmospheres with large additions of oxide gases (10, 20 % or more), their electroluminescent response was a weak to medium bright blue, regardless of the nature of the gas. When the amounts of oxide additions were small, the response was a pure green, and varied in intensity mainly with the activator concentrations. Thus, there was no significant difference in color or brightness between the phosphors fired with air, water vapor, or other additions. Since water was so much easier to dose than the other gases, most of the experiments were carried out with this addition. It will be referred to as "wet firing."

All phosphors, whether prepared with molar deficiencies or excess of Al relative to Cu, contained free copper sulfide which was removed with NaCN. While the solubility of copper sulfide in ZnS was thus considerably lower than in the dry-fired phosphors, it was nevertheless larger than in the phosphors with Cu alone, and it was dependent upon the Al concentration, increasing slightly with increasing Al additions. The removal of copper sulfide from the fired products was necessary for the double purpose of increasing the brightness and reducing the conductivity of the phosphors, so as to allow their use in electroluminescent cells without an insulating material. The concentration of acid-insoluble Al_2O_3 was slightly higher than in the dry-fired materials.

The exact nature of the atmosphere to which the phosphors were exposed during the firing has not been determined. It is apparent that the addition of air or CO_2 to H_2S produces H_2O and SO_2 in certain concentrations. Since all of these gases were equally effective in producing the reported changes, it follows that it is the oxygen constituent of the gas mix which, regardless of its nature, produced the changes in characteristics compared with the phosphors fired in pure H_2S.

PRINCETON UNIVERSITY LIBRARIES

Wet-Fired Zn(Al)S:Cu *Phosphors*

The formation of Zn(Al)S:Cu phosphors with different emission and response characteristics is a fully reversible process. One type of phosphor could be readily converted into the other type, merely by refiring for a short time in the appropriate atmosphere. Thus a dry-fired phosphor with yellow body color, orange 3650 Å-response, and lack of electroluminescent response, gave a tan-gray colored product with green u.v. and green electroluminescent response on refiring in wet H_2S; this latter material, heated again in dry H_2S (without removal of the excess copper sulfide) reverted to the first type, which on further firing in H_2S plus air gave again the second type, etc.

TABLE I. *Effect of water vapor in firing atmosphere on electroluminescent response*

Water temp	Trap temp	Ratio $H_2O:H_2S$	Electrolum. response
°C	°C		
100	—	1:0	Faint blue
55	—	1:4.6	Bright green
25	—	1:33	Very bright green
25	−20	1:1000	Weak green
25	−42	1:10000	Very weak green
25	−57	1:65000	Dead

The best range for the preparation of bright green electroluminescent phosphors was about 1 to 20 per cent H_2O, and about 2 to 5 per cent of either air or CO_2 in H_2S. The effect of the concentration of water vapor upon the electroluminescent emission of a phosphor prepared with 0.3 per cent Cu and 0.35 per cent Al is shown in Table I.

It has been pointed out (3) that the H_2S-fired ZnS phosphors activated with Cu alone gave an orange emission with electroluminescent excitation. When fired with oxide additions, they luminesced mainly blue at both low and high frequencies. The addition of even very small amounts of aluminum to the phosphors changed their response completely, to a pure green, when they were fired in the presence of gaseous oxides. As little as 10 mole per cent of Al relative to Cu effected the color change to green and, at the same time, increased the brightness fourfold. Larger amounts of Al gave a greater brightness increase, as shown below. It is of particular interest and importance that the luminescence remained green over the entire frequency range of 60 to 15000 cps investigated. This is in contrast to the Destriau-type ZnS-ZnO:Cu phosphors and to the ZnS phosphors activated with Cu and Pb which change from green to blue at the higher frequencies (4).

The spectral emission of the wet-fired phosphors with aluminum was substantially invariant with composition under electroluminescent excitation. Their brightness, however, was a function of composition as well as firing temperature. This was found from several series of phosphors which were prepared with increasing amounts of Cu, each of them with a number of different Al concentrations, and each of these fired at different temperatures. The optimum firing temperature was about 1100°C. Phosphors fired at either 1000° or 1200°C were significantly less bright. The optimum copper content was about 0.15 per cent added Cu (with 0.05 % Al), although a much wider range of compositions gave nearly equally bright materials. The dependency of the brightness upon the Al concentration is shown in Fig. 8 which holds for both 60 and 5000 cps excitation of the

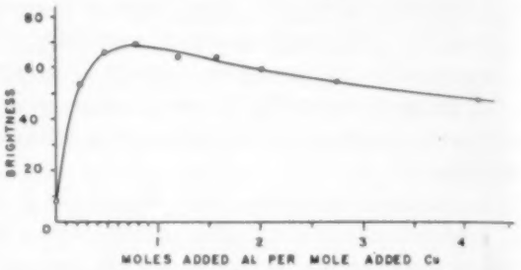

FIG. 8. Electroluminescent brightness as dependent upon Al concentration in phosphors prepared with 0.15% Cu. Excitation by 60 and 5000 cps currents.

phosphors in oil cells. The brightness ordinate is in arbitrary units. Curves of similar shape were obtained for Cu concentrations from 0.05 to 0.5 per cent added Cu, with peaks occurring at different levels of brightness.

The figure demonstrates the striking increase in electroluminescent brightness due to Al. This increase was obtained with very small amounts of Al, much less than the equivalent of added Cu, and it reached a maximum at a concentration of about 0.75 moles Al per mole added Cu. A plot of brightness vs. moles of Al per mole of retained Cu (after the NaCN wash) gave a similarly flat maximum at about 2 moles Al. Since 0.75 is known to be too low (not all added Cu was retained by the washed phosphors), and since 2 is too high (not all Al is incorporated as Al_2S_3 in the phosphors), the true mole ratio of Cu:Al for phosphors of optimum brightness must be in between, i.e., somewhere near 1:1. It does not follow, however, that all phosphors with equimolar Cu and Al contents are electroluminescent. This is discussed below.

With respect to the optical response of the wet-fired Zn(Al)S:Cu phosphors, it was already mentioned that their emission was bright green with 3650 Å excitation. This is shown in Fig. 9 for amounts of added Cu up to 0.3 per cent. There was no further change in emission with higher concentrations of Cu.

but the intensity of emission began to decline again. The range of colors obtained was a great deal narrower than that of phosphors of the same initial composition but fired in pure H_2S. It covered a total displacement of only about 170 Å by going from 0.05 to 0.3 per cent Cu or higher, compared with the 700 Å displacement for the dry-fired materials. This was not due to the lower amounts of Cu actually incorporated in the phosphors. Thus a dry-fired product with 0.3 per cent retained Cu emitted yellow-orange, whereas a wet-fired product with 0.3 per cent retained Cu emitted green light.

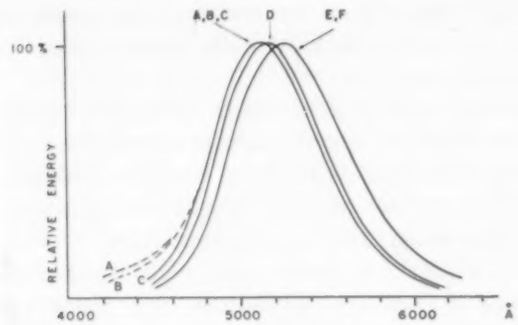

FIG. 9. Emission with 3650 Å excitation of Zn(Al)S:Cu phosphors fired at 1100°C in H_2S with 3% H_2O.

Curve	% Added Cu	% Added Al
A	0	1.7
B	0.005	0.0114
C	0.05	0.069
D	0.05	0.69
E	0.3	0.69
F	0.3	2.7

The typical blue band appeared again in low intensity in the phosphors with low Cu content. In comparing the curves for the phosphors with increasing concentrations of Cu and Al, it was found that practically all of the peak displacement was due to the increasing Cu content; Al contributed but little to the shift. The reflection (absorption) curves of the wet-fired phosphors presented about the same picture as those of the dry-fired phosphors shown in Fig. 2. An increase of the Cu content caused the absorption band to become stronger, while an increase of the Al content was relatively ineffective.

Under 5000-volt cathode ray excitation, identical emission bands were found, as already reported for the dry-fired phosphors of like composition. With increasing Cu concentration up to about 0.3 per cent, the peak of emission shifted from 5100 to about 5250 Å. The shape of the emission curves of the wet-fired Zn(Al)S:Cu phosphors was practically identical under all three forms of excitation, i.e., ultraviolet, cathode rays, and electroluminescence.

Wet-Fired Phosphors with Other Trivalent Cations

The phosphors with aluminum substitution underwent characteristic changes resulting from dry vs. wet firing. In surveying the effect of wet firing upon the phosphors with other trivalent substituents, it can be stated summarily that such striking changes were, in general, not observed. It was surprising to find that the electroluminescent response was hardly affected where it existed at all in the corresponding dry-fired materials, and that it was not as strikingly improved as with Al substitution. Again it was found that gallium in particular did not produce more than the faintest electroluminescent response.

With excitation by u.v., wet firing resulted generally in either slight or stronger shifts toward shorter wave lengths. In some cases, the shifts were accompanied by a change in brightness, in others, they were not. For example, the phosphors with indium, cerium, and praseodymium became dimmer as the emission shifted toward green-blue, while the phosphors with scandium became just slightly greener with little or no loss of brightness. Likewise, the infrared stimulability was generally affected adversely, and showed similar changes of color, except again in the samples with scandium whose stimulated light was slightly greener but almost as bright as with dry firing. In general, none of these phosphors was as interesting as the ones with aluminum substitution.

DISCUSSION

The results obtained on H_2S-fired ZnS phosphors with high copper and high trivalent cation contents are best explained with the premise that these materials are substantially true triple sulfides. So far, the x-ray diffraction patterns have shown that the materials with aluminum substitution have the structure, and very nearly the spacings, of hexagonal ZnS. Differentials in spacings between pure ZnS and the phosphors with as much as 0.3 per cent Cu and 0.69 per cent Al, for example, appear to be so small that refined analysis becomes necessary. Individual phases of CuS, Cu_2S, Al_2O_3 or Al_2S_3 have not been identified on the patterns obtained, despite the fact that Al_2O_3, for example, was found analytically. Other physical and chemical characteristics make it also most plausible to regard the phosphors as triple sulfides with monovalent Cu. Thus Kroeger's (1) original hypothesis that trivalent cations facilitate the incorporation of Cu in ZnS appears to have been even better substantiated with these materials of much higher activator concentrations than Kroeger investigated.

If the presence of free Al_2O_3 is disregarded in the phosphors prepared with molar excess of Al over Cu, the luminescent phase proper looks like a homogene-

ous product in which a single species of copper atoms appears to perform the dual role of base modifier and of activator. In contradiction with this conclusion, the complexity of the emission spectra leads to the opposite conclusion, namely, that two or more different species of Cu activator atoms must be present in these phosphors. This is concluded from the fact that the green emission is characterized by a different and independent excitation sensitivity, different temperature dependence, and different phosphorescent decay compared with the longer wave length emissions. It also follows from the fact that the emission spectra of phosphors of intermediate colors, such as green-yellow or yellow, cannot be built up additively from just two bands of extreme emission. A third sub-band is required to describe the observed emission fully.

The phosphors with the lower (0.05%) and higher (0.6% Cu) activator concentrations are considered to furnish two of the three sub-bands in nearly pure form. The remaining sub-band at 5550 Å could not be isolated individually.

The 5150 Å band is at the same position and of the same shape as the green emission band of conventional, hexagonal ZnS:Cu phosphors. It is suggested, therefore, that the same type of center which is operative in hexagonal ZnS:Cu phosphors, prepared with low concentrations of activator and coactivator, is also operative as an individual in the Zn(Al)S:Cu phosphors with much higher activator contents, furnishing the same green emission. This is the emission which is ultimately reached in pure form when these latter phosphors are excited at very low temperatures, or when they are excited by cathode rays at room temperature. The green emission would thus be due to only a small fraction of the number of Cu atoms in the phosphors, placed in the more common surroundings. The bulk of the Cu and Al atoms may be assumed to be aggregated in "insular" regions of higher than average concentration and thus nonrandom distribution throughout the phosphor crystals. The longer wave length emissions are then attributed to such "molecular island" complexes consisting of more nearly stoichiometric Zn_2AlCuS_4 groupings with much higher than average concentration of Cu and Al. Such complexes may be expected to be very temperature-sensitive, consistent with the observed rapid loss of fluorescent brightness which approaches zero at temperatures as low as 100°C.

The phosphors with electroluminescent response have a much simpler emission, which is due essentially to the same type of center operative in all ZnS:Cu phosphors with green emission. However, and speaking on submicroscopic scale, the phosphors are probably heterogeneous and of more complicated structure than the dry-fired materials. The tan-gray color of the wet-fired materials shows that the copper activator is present in some other association with the host lattice than in dry-fired phosphors of the same retained Cu content. The electroluminescent response is a direct consequence of the presence of oxides in the firing atmosphere, and its intensity depends upon the amount of these oxides. It thus seems reasonable to attribute the electroluminescent response to a solid oxide phase, providing barriers (5), which are distributed in extreme subdivision in or on the phosphor particles and in close physical contact with them. Speaking macrochemically, the "oxide" phase may be any of these possibilities: ZnO, Al_2O_3, CuS or CuO with divalent Cu, or their combinations.

Among these possibilities, it seems most plausible to associate the electroluminescent response with a separate phase of Al_2O_3. In the wet-fired phosphors, a certain amount of oxide should remain or form in accordance with the equilibrium $Al_2S_3 + H_2O \rightleftharpoons Al_2O_3 + H_2S$. Actually, the acid-insoluble Al_2O_3 content of wet-fired phosphors was found to be higher than that of dry-fired materials, as expected. However, the Al_2O_3 formed in wet firing must be considered to be in a different state than any unconverted oxide in dry-fired phosphors. The latter is a mere diluent and does not provide the type of boundaries necessary to make them responsive to electroluminescent excitation.

Thus, the following crude picture develops for the Zn(Al)S:Cu phosphors with high activator contents and with a molar excess of Al over Cu. When fired in dry H_2S, nearly all added Al is converted into Al_2S_3 which, together with all added Cu in the form of Cu_2S, forms a solid solution with ZnS, the ZnS being present in much larger amount than the compound Zn_2AlCuS_4 requires. Any nonconverted Al survives in the form of separate, diluent particles of Al_2O_3. The main phosphor phase can fluoresce, but it is not responsive to electroluminescent excitation as it is homogeneous and has no oxide barriers. The formation of triple sulfides probably continues beyond the concentrations of Cu and Al that were investigated here; however, these materials cease to be phosphors.

Upon firing in atmospheres with oxide additions, the Al additive survives in form of two functional phases: most of the Al is converted into sulfide which is necessary to hold relatively large amounts of Cu in solid solution in the base material; it is not essential for the electroluminescent excitation itself. A smaller but significant portion of the added Al survives as Al_2O_3 in extreme subdivision in or on the phosphors; it does not contribute to the solubility of Cu_2S, but it is essential to provide the heterogene-

ous barriers for the electroluminescent excitation of the phosphors. Since only a portion of the added Al is converted into Al_2S_3, not all of the added Cu can be taken into solid solution. The balance survives the firing as free copper sulfide, which can be washed out. Although the solubility of Cu_2S in the wet-fired phosphors is lower than in the dry-fired materials, it is appreciably higher than in the phosphors without aluminum.

It was mentioned before that some dry-fired phosphors did give a response to electroluminescent excitation. These were materials prepared with molar deficiencies of Al which were fired at lower temperatures. This may be explained on the basis of the picture outlined above. The temperatures were not high enough to effect the complete conversion of Al_2O_3 into Al_2S_3. The concentrations of Al and the temperature were too low to allow particle growth of free, diluent Al_2O_3 to occur. Thus, sufficient Al_2O_3 could remain in the phosphors in suitable subdivision to provide the heterogeneous barrier phase and the condition for the electroluminescent response of the phosphors.

The response of the Zn(Al)S:Cu phosphors is thus attributed to a small amount of oxide in the phosphors. A similar situation seems to exist in the Destriau-type ZnS-ZnO:Cu phosphors which are, in fact, prepared with a deliberate, although much larger, addition of oxide.

Acknowledgment

The writer wishes to express his thanks to Dr. F. J. Studer of the General Electric Research Laboratory for the u.v. reflection curves and the cathode ray excitation curves of the phosphors.

Any discussion of this paper will appear in a Discussion Section, to be published in the June 1954 issue of the Journal.

References

1. F. A. Kroeger and J. A. M. Dikhoff, *Physica*, **16**, 297 (1950).
2. H. C. Froelich, *J. Opt. Soc. Amer.*, **42**, 982 (1952).
3. H. C. Froelich, *J. Electrochem. Soc.*, **100**, 280 (1953).
4. J. F. Waymouth and C. W. Jerome, "Enlarged Abstracts," Electrochemical Society Meeting, p. 66, Philadelphia, 1952; *Sylvania Technologist*, **5**, 54 (1952).
5. K. Lehovec, C. A. Accardo, and E. Jamgochian, *Phys. Rev.*, **83**, 603 (1951); W. W. Piper and F. E. Williams, *Phys. Rev.*, **87**, 151 (1952).

Electrical Conductivity and Density of Molten Cryolite with Additives[1]

JUNIUS D. EDWARDS, CYRIL S. TAYLOR, LEE A. COSGROVE, AND ALLEN S. RUSSELL

Aluminum Research Laboratories, Aluminum Company of America, New Kensington, Pennsylvania

ABSTRACT

The electrical conductivities at 1000°C, expressed as per cent of the cryolite value, for cryolite containing 10 weight per cent of the following substances are: sodium fluoride 112, calcium fluoride 96, aluminum fluoride 91, and alumina 83. For pure sodium fluoride at 1000°C, conductivity is 5.52 $ohm^{-1}cm^{-1}$, compared to 2.80 $ohm^{-1}cm^{-1}$ for cryolite. Molar conductance decreases linearly with mole per cent sodium fluoride, aluminum fluoride, alumina, or calcium fluoride addition to cryolite. The activation energy for conductance, calculated from a plot of the Arrhenius equation, is about 4.3 kcal/mole for the systems of cryolite with sodium fluoride, aluminum fluoride, and alumina, as well as for pure sodium fluoride, but is slightly higher for the cryolite-calcium fluoride system. This value agrees reasonably with the 4.48 kcal/mole for pure chryolite. Densities in these systems change linearly with temperature, that for pure sodium fluoride following the equation $2.567-0.610 \times 10^{-3} t$. The stability of the complex $NaF \cdot Na_3AlF_6$ is indicated by a density maximum.

INTRODUCTION

The first paper (1) in this series reported the electrical conductivity of cryolite as measured by improved techniques. In the Hall process for electrolytic production of aluminum, the electrolyte, while largely cryolite, usually contains an excess of either sodium fluoride or aluminum fluoride, along with calcium fluoride and varying quantities of dissolved alumina. Consequently, the effect on conductivities and densities of these additives to cryolite has been measured over a considerable composition range.

Literature values for the electrical conductivity of cryolite were summarized in the earlier work (1). No values are available for the electrical conductivity of pure molten aluminum fluoride inasmuch as it sublimes before melting. Arndt and Kalass (2) listed the specific conductance of sodium fluoride at 1000°C as 3.15 ohm^{-1} cm^{-1}, and asserted that the equivalent conductances of sodium fluoride and of cryolite are nearly equal. In the temperature range of 1000°–1100°C, calcium fluoride and alumina are both solids and insulators.

EXPERIMENTAL

Materials.—Hand-picked crystals of pure Greenland cryolite were crushed to 20 mesh and any associated particles of galena were removed. Sodium fluoride was Baker's C.P. powder. Aluminum fluoride was distilled and was presumed to be pure, except for a 0.9 per cent loss on ignition at 600°C. The alumina was Alcoa A-14, a high purity, calcined product containing less than 0.2 per cent water with other impurities not exceeding 0.1 per cent. Calcium fluoride was hand-picked fluorspar, ground to a fine powder. These materials were heated for one hour

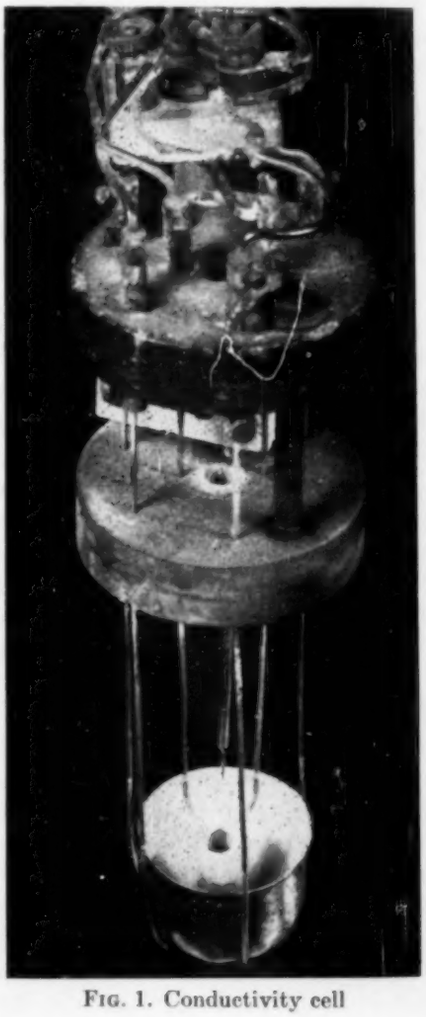

FIG. 1. Conductivity cell

[1] Manuscript received March 30, 1953.

in a platinum crucible at 400°C before weighing for each determination.

Electrical conductivities.—The procedure was to weigh out the desired mixture, grind the components together, and determine the resistance between hemispherical platinum electrodes immersed in the molten liquid. The cell pictured in Fig. 1 was immersed in a platinum crucible containing the stirred molten salt, with frequent adjustment to a fixed depth below the surface. The cell constant was taken as 0.0835 cm^{-1} as in the work with pure cryolite (1). Resistance was measured with a Kelvin bridge to eliminate errors from lead resistance. Frequencies from 600 to 4000 cycles/sec were employed and resistance vs. frequency$^{-\frac{1}{2}}$ was extrapolated to the infinite frequency value which has been used throughout this work to minimize polarization errors. Temperature was measured with a platinum, platinum-10 per cent rhodium thermocouple immersed a fixed distance in the molten salt.

Densities.—Density was determined with a platinum sinker (calibrated from the room temperature density and the coefficient of expansion of platinum) suspended from an analytical balance by a fine platinum wire. Equations for density as a function of temperature are given in Table I.

Definitions.—For a mixture of components A and B:

$$\text{Molar conductance} = \frac{(\text{mole wt}_A \times \text{mole fract}_A + \text{mole wt}_B \times \text{mole fract}_B)}{\text{density of melt}} \times \text{specific conductance of melt}$$

$$\text{Equivalent conductance} = \frac{(\text{eq wt}_A \times \text{wt fract}_A + \text{eq wt}_B \times \text{wt fract}_B)}{\text{density of melt}} \times \text{specific conductance of melt}$$

The equivalent weight of cryolite has been taken as one-third the formula weight (Na_3AlF_6), that of calcium fluoride as one-half the formula weight.

Polarization

There is no satisfactory criterion for knowing whether the additives to cryolite are causing appreciable errors in the extrapolation of resistance to infinite frequency. In the present work with the submerged platinum cell, the frequency dependence seemed to be unaffected to any major degree by the sodium fluoride, aluminum fluoride, calcium fluoride, or alumina additives, and the slopes of the resistance extrapolations against frequency$^{-\frac{1}{2}}$ were taken the same as for cryolite measured with the cell platinization in an equivalent state. As was the case in earlier experiments with pure cryolite, the platinum cell was platinized only at the start of the work. There was an erratic tendency for the slopes of the plots of resistance vs. frequency$^{-\frac{1}{2}}$ to increase as the work proceeded. Temperature changes in the range of these measurements, 1000° to 1080°C, had little influence on the slope of the frequency curves.

Table I. *Densities of cryolite with several additives*

Composition by weight	Density g/cm³	Range of measurement °C
100% Cryolite	3.032 - 0.937·10⁻³t*	1000–1080
5% NaF-95% cryolite	3.051 - 0.950·10⁻³t	996–1080
10% NaF-90% cryolite	3.024 - 0.920·10⁻³t	1007–1078
15% NaF-85% cryolite	3.016 - 0.910·10⁻³t	988–1080
20% NaF-80% cryolite	3.015 - 0.910·10⁻³t	978–1080
40% NaF-60% cryolite	2.867 - 0.790·10⁻³t	947–1074
100% NaF-0% cryolite	2.567 - 0.610·10⁻³t	1003–1076
5% Al_2O_3-95% cryolite	2.942 - 0.880·10⁻³t	1009–1093
10% Al_2O_3-90% cryolite	2.852 - 0.810·10⁻³t	976–1079
15% Al_2O_3-85% cryolite	2.753 - 0.720·10⁻³t	998–1085
5% AlF_3-95% cryolite	2.986 - 0.910·10⁻³t	1007–1086
8% AlF_3-92% cryolite	2.992 - 0.930·10⁻³t	1008–1094
5% CaF_2-95% cryolite	3.012 - 0.890·10⁻³t	992–1083
10% CaF_2-90% cryolite	3.027 - 0.870·10⁻³t	993–1084
15% CaF_2-85% cryolite	3.057 - 0.870·10⁻³t	997–1099
20% CaF_2-80% cryolite	3.060 - 0.840·10⁻³t	987–1085
40% CaF_2-60% cryolite	3.172 - 0.840·10⁻³t	1015–1096
5% Al_2O_3-10% CaF_2-85% cryolite	2.929 - 0.810·10⁻³t	1000–1080

* t in °C.

Conductivity of Cryolite with Additives

The specific conductances are plotted in Fig. 2 as per cent of the cryolite value vs. weight per cent of added sodium fluoride, calcium fluoride, aluminum fluoride, and alumina. To achieve maximum conductivity, the bath should contain an excess of

sodium fluoride, and it should have minimum amounts of alumina and calcium fluoride. Additional data on these systems are shown in Table II.

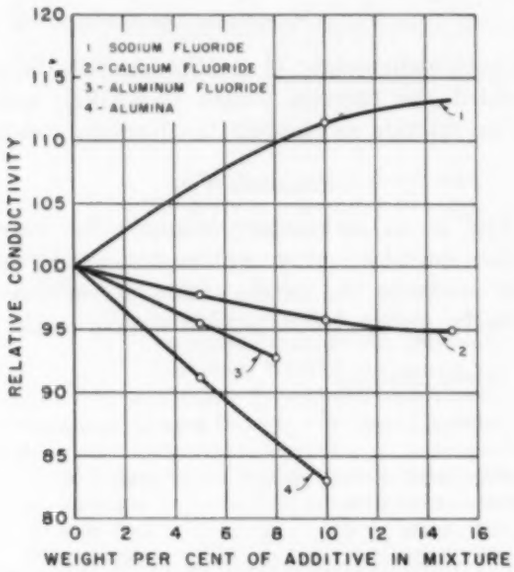

FIG. 2. Electrical conductivity of cryolite systems relative to pure cryolite.

at high concentrations in cryolite makes measurements on this system unreliable.

Pearson and Waddington (3), using the data of Batashev (4), found a linear decrease in molar conductance plotted against mole per cent on addition of either sodium fluoride or aluminum fluoride to cryolite. The authors' data and those of Vayna (5) plotted by this method give general confirmation of the linearity of these plots, although the absolute values throughout the system are altered (Fig. 3).

Equivalent conductance vs. mole per cent additive for the system cryolite-sodium fluoride has a slight break in the graph (not shown) at a concentration corresponding to the formula $NaF \cdot Na_3AlF_6$. For the system cryolite-aluminum fluoride, the long extrapolation of equivalent conductance gives a value of about 40 ohm^{-1} for the hypothetical pure molten aluminum fluoride.

The densities at 1000°C in the system sodium fluoride-aluminum fluoride show a maximum (Fig. 4) at a composition corresponding approximately to $NaF \cdot Na_3AlF_6$, in agreement with the data of Abramov and Kozunov (6) and of Lundina (7). However,

TABLE II. *Electrical conductivity of cryolite containing sodium fluoride, aluminum fluoride, alumina, and calcium fluoride*

Additive		Specific conductance			Energy of activation of conductance kcal/mole	Conductance 1000°C	
wt %	mole %	1000°C $ohm^{-1}cm^{-1}$	1040°C $ohm^{-1}cm^{-1}$	1080°C $ohm^{-1}cm^{-1}$		molar ohm^{-1}	equivalent ohm^{-1}
Cryolite							
0	0	2.79_9	2.90_1	2.99_7	4.48	281	94
Sodium fluoride							
10	35.7	3.12_2	3.23_2	3.33_3	4.30	223	100
16.67	50.0	3.18_9	3.30_1	3.40_8	4.30	191	99
40	76.9	3.85_5	3.99_8	4.13_5	4.30	150	109
100	100.0	5.51_8	5.74_4	5.95_3	4.30	118	118
Aluminum fluoride							
5	11.6	2.67_7	2.77_3	2.85_6	4.19	252	88
8	17.9	2.60_0	2.68_4	2.76_2	4.19	236	84
Alumina							
5	9.7	2.55_1	2.63_8	2.71_9	4.20	247	83
10	17.2	2.32_7	2.40_9	2.48_6	4.20	218	74
Calcium fluoride							
5	12.3	2.73_5	2.84_7	2.95_0	4.69	250	88
10	23.0	2.68_0	2.79_1	2.89_7	4.69	223	83
15	32.3	2.65_7	2.76_6	2.87_2	4.69	203	79
Alumina 5 wt %, 8.4 mole %—calcium fluoride 10 wt %, 22.0 mole %							
15	30.4	2.44_0	2.54_9	2.65_3	4.92	198	66

Sodium fluoride, aluminum fluoride.—For the systems cryolite-sodium fluoride and cryolite-aluminum fluoride, conductivity decreases continuously from sodium fluoride through cryolite toward aluminum fluoride. The extreme volatility of aluminum fluoride

Vayna's densities (8) at 1000°C show a maximum between pure cryolite and $NaF \cdot Na_3AlF_6$.

Alumina.—The molar conductances measured by Batashev (4), for the system cryolite-alumina, were extrapolated to zero conductivity at pure alumina

when plotted against mole per cent added alumina by Pearson and Waddington (3). The authors' values and Vayna's (5) for molar conductance vs. mole per cent added alumina are shown in Fig. 5 in comparison with these values. The evidence from the present work is that molar conductance falls off

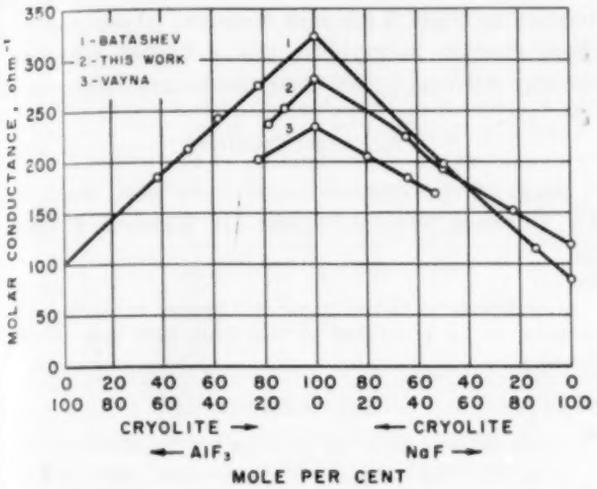

FIG. 3. Molar conductance of cryolite-aluminum fluoride and cryolite-sodium fluoride.

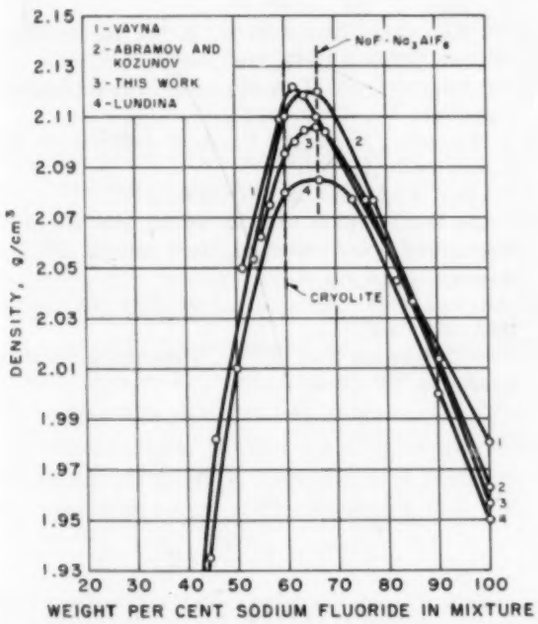

FIG. 4. Density of the system sodium fluoride-aluminum fluoride.

more rapidly than would be anticipated if the alumina were inert in this system.

The density at 1000°C of the cryolite-alumina system (Fig. 6) decreases with the first alumina additions, another indication of an interaction between alumina and cryolite, inasmuch as the density for hypothetical molten alumina at 1000°C would be much greater than that of cryolite. The density of molten alumina near its melting point (2040°C) was determined as 2.5 g/cm³ by Wartenberg and coworkers (9).

This system is particularly difficult to measure because of the slow solution of alumina in cryolite

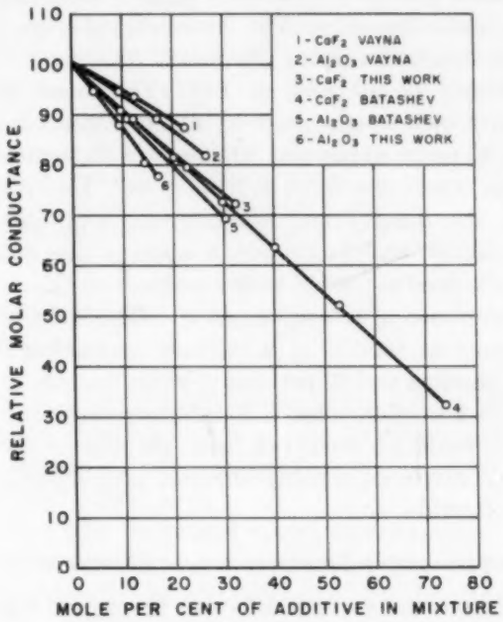
1 - CaF₂ VAYNA
2 - Al₂O₃ VAYNA
3 - CaF₂ THIS WORK
4 - CaF₂ BATASHEV
5 - Al₂O₃ BATASHEV
6 - Al₂O₃ THIS WORK
RELATIVE MOLAR CONDUCTANCE
MOLE PER CENT OF ADDITIVE IN MIXTURE

FIG. 5. Molar conductance of cryolite-calcium fluoride and cryolite-alumina relative to pure cryolite.

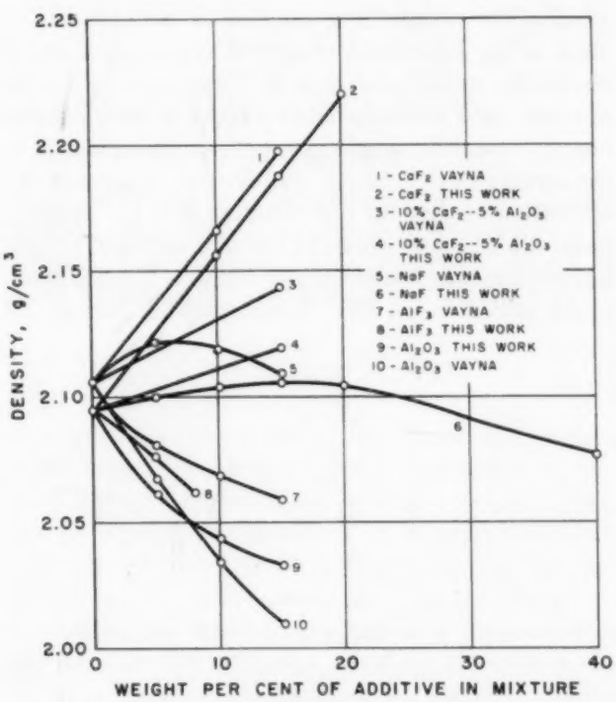
1 - CaF₂ VAYNA
2 - CaF₂ THIS WORK
3 - 10% CaF₂--5% Al₂O₃ VAYNA
4 - 10% CaF₂--5% Al₂O₃ THIS WORK
5 - NaF VAYNA
6 - NaF THIS WORK
7 - AlF₃ VAYNA
8 - AlF₃ THIS WORK
9 - Al₂O₃ THIS WORK
10 - Al₂O₃ VAYNA
DENSITY, g/cm³
WEIGHT PER CENT OF ADDITIVE IN MIXTURE

FIG. 6. Density of cryolite with additives

at high alumina concentrations, and the extrapolation of results from low alumina concentrations to pure alumina is subject to inaccuracies.

Calcium fluoride.—Pearson and Waddington (3) reported a linear decrease of molar conductance with

mole per cent calcium fluoride for the cryolite-calcium fluoride system. Vayna's (5) data are again in marked disagreement. The authors' values for this system are not quite linear (Fig. 5). Equivalent conductance plotted (not shown) against mole per cent also lacks linearity. The extrapolated equivalent conductance of calcium fluoride is 50 ohm^{-1}.

Density of the melt at 1000°C increases almost linearly with weight per cent added calcium fluoride (Fig. 6) up to 40 per cent, the limit of these measurements, where the value is 2.333 g/cm^3. Inasmuch as both the density and conductivity plots (on the equivalence basis) are ideal, it appears that calcium fluoride does not react with cryolite.

Calculation of ternary mixtures.—The specific conductance at 1000°C of a mixture containing 5 per cent alumina and 10 per cent calcium fluoride in cryolite is 2.44 ohm^{-1} cm^{-1}. It is interesting that this value would be predicted from the curves for the binary mixtures cryolite-alumina and cryolite-calcium fluoride.

Temperature Dependence of Conductivity

All the conductivity data can be plotted linearly as log equivalent conductance, Λ, against reciprocal absolute temperature, T, where $\Lambda = KE/d$, with K the specific conductance, E the equivalent weight (equivalent weight of a mixture is defined in this work as the equivalent weight of pure component A times the weight per cent of component A in the mixture, plus the equivalent weight of pure component B times the weight per cent of component B in the mixture, etc.), and d, the density. Values of the activation energy for conductance (10, 11) in kcal/mole, are listed in Table II for sodium fluoride, aluminum fluoride, alumina, and calcium fluoride separately added to cryolite. The activation energy appears to be consistent within the limits of error at 4.3 kcal/mole over the measured range of sodium fluoride, aluminum fluoride, and alumina compositions. With calcium fluoride addition, however, the value increases to 4.7 kcal/mole. This increase is in accord with the general rule that energies of activation increase with increased size of the cation. The ternary mixture, 5 per cent alumina, 10 per cent calcium fluoride in cryolite, has a higher activation energy, 4.9 kcal/mole, than the binary mixtures.

Acknowledgment

Some of the measurements have been made by Dr. L. Frank Maranville and Mr. Kenneth E. Martin.

Any discussion of this paper will appear in a Discussion Section, to be published in the June 1954 issue of the Journal.

References

1. J. D. Edwards, C. S. Taylor, A. S. Russell, and L. F. Maranville, *J. Electrochem. Soc.*, **99**, 527 (1952).
2. K. Arndt and W. Kalass, *Z. Elektrochem.*, **30**, 12 (1924).
3. T. G. Pearson and J. Waddington, *Discussions Faraday Soc.*, **1**, 307 (1947).
4. K. P. Batashev, *Legkie Metal.*, **5**, No. 10, 48 (1936).
5. A. Vayna, *Alluminio*, **19**, 215 (1950).
6. G. A. Abramov and P. A. Kozunov, *Trans. Leningrad Ind. Inst.*, No. 1, 60 (1939).
7. Z. F. Lundina, *Trans. All-Union Aluminium and Magnesium Inst.*, **13**, 5 (1936).
8. A. Vayna, *Alluminio*, **19**, 541 (1950).
9. H. von Wartenberg, G. Wehner, and E. Saran, *Nachr. Ges. Wiss. Göttingen, Math.-physik. Kl., Fachgruppen II, (N.F.)*, **2**, 73 (1936).
10. H. Bloom and E. Heymann, *Proc. Roy. Soc., London*, **188A**, 392 (1947).
11. J. O'M. Bockris and J. W. Tomlinson, *Research, London*, **2**, 362 (1949).

Correlation of Limiting Currents under Free Convection Conditions[1]

C. R. Wilke, M. Eisenberg, and C. W. Tobias

Department of Chemistry and Chemical Engineering, University of California, Berkeley, California

ABSTRACT

Limiting currents were measured for deposition of copper on plane vertical cathodes from unstirred solutions. Electrolyte composition ranged from 0.01 to 0.7 molal $CuSO_4$, 1.38 to 1.57 molal H_2SO_4, and 0 to 6.38 molal glycerol. Cathode heights varied from 0.25 to 3.0 in. Limiting current densities were from 0.4 to 108 ma/cm². A general correlation of the data may be represented by the equation: $Nu' = 0.673\ (ScGr)^{1/4}$, where Nu', Sc, and Gr are the mass transfer Nusselt, Schmidt, and Grashof numbers, respectively. This result is in good agreement with that predicted from the boundary layer theory for mass transfer by free convection.

Introduction

This paper is concerned with limiting rates of deposition of copper ions at a vertical cathode in an unstirred solution. In such a system, natural convection, or "spontaneous stirring," results from density changes which accompany concentration changes in the region of the electrode. The limiting process is controlled by the maximum rate of mass transfer of copper between bulk solution and the electrode surface. A more detailed discussion of mass transfer phenomena in electrochemical problems has been presented in an earlier paper (1).

Natural convection usually involves laminar motion of the fluid so that the over-all process requires consideration of the simultaneous action of molecular diffusion and convective flow. In steady-state free convection, the main resistance to mass transfer is associated with a relatively small region of fluid in the vicinity of the electrode, and the concentration of the bulk solution remains constant. It is convenient to describe the rate of transfer between any point on the electrode surface and the surrounding solution in terms of a mass transfer coefficient for free convection as given by the relation:

$$(N_D)_x = k_x(C_o - C_i) \qquad \text{(I)}$$

where: $(N_D)_x$ = local rate of mass transfer, gram moles/cm²-sec; k_x = local mass transfer coefficient at height x on the electrode surface; and C_o and C_i = concentration of reacting species in bulk solution and at electrode surface, respectively, gram moles/cm³.

The total local rate of mass transfer, excluding migration, is determined by the current density:

$$(N_D)_x = \frac{I_x(1 - t)}{n\mathbf{F}} \qquad \text{(II)}$$

where: I_x = current density at height x; n = valence charge of reacting ion; $\mathbf{F}$ = the Faraday; and t = transference number of reacting ion averaged over the mass transfer path.

To describe the rate of mass transfer per unit area averaged over the entire electrode, an average mass transfer coefficient may be defined by the equation:

$$N_D = k_L(C_o - C_i) = \frac{I(1 - t)}{n\mathbf{F}} \qquad \text{(III)}$$

where: N_D = average mass transfer rate, gram moles/cm²-sec; k_L = average mass transfer coefficient, cm/sec; and I = average current density, amp/cm², i.e., total current ÷ electrode surface area.

Limiting Current and Concentration Polarization

The mass transfer coefficient has a value characteristic of the system and current density under consideration, so that the average current density is given by rearrangement of equation (III):

$$I = \frac{n\mathbf{F}(C_o - C_i)k_L}{(1 - t)}. \qquad \text{(IV)}$$

The theoretical maximum current density is that which would reduce C_i to zero. This theoretical limiting current density cannot be fully reached in practice because of the development of electrode polarization associated with depletion of the reacting ions in the region of the electrode. This polarization is approximately equal to the emf of a concentration cell formed between two solutions containing the reacting ion at concentrations C_o and C_i, respectively. Thus:

$$\Delta E = \frac{RT}{n\mathbf{F}} \ln \frac{a_o}{a_i} \approx \frac{RT}{n\mathbf{F}} \ln \frac{C_o}{C_i} \qquad \text{(V)}$$

where ΔE = concentration polarization, volts. As the current density is increased toward the theoretical limit, the applied potential must increase as a

[1] Manuscript received April 6, 1953. This paper was prepared for delivery before the Philadelphia Meeting, May 4 to 8, 1952.

result of the polarization, so that, in general, before the theoretical maximum current can be reached, some competing electrode reaction such as hydrogen evolution occurs. However, C_i often can be reduced in practice to an essentially negligible value before the onset of a successive reaction. For example, in the deposition of a copper ion at 25°C, a concentration polarization of 0.087 volt will require the ratio C_i/C_o to be 10^{-3}. In view of the possibility of successive reactions, it is necessary to define the limiting current density as the maximum current density which may be utilized exclusively for the production of a desired electrode reaction.

Equations for prediction of mass transfer coefficients and general correlation of data may be developed by analogy to solutions of the corresponding problem of heat transfer to vertical surfaces by free convection. In another paper (2), the authors have applied the boundary layer equations of Squires (3), as outlined by Eckert (4), to the present mass transfer problem. This procedure leads to the following results in the form of dimensionless groups:

$$(Nu')_x = 0.508Sc^{\frac{1}{2}}(0.952 + Sc)^{-1/4}Gr^{1/4} \quad \text{(VI)}$$

where: $(Nu')_x$ = local Nusselt number for mass transfer; Sc = Schmidt number; and Gr = Grashof number.

The Nusselt, Schmidt, and Grashof numbers are given by

$$(Nu')_x = \frac{k_x x X_f}{D} \quad \text{(VII)}$$

where: k_x = mass transfer coefficient at height x, cm; x = vertical height on electrode surface, cm; D = effective diffusion coefficient of cupric ion, cm²/sec; X_f = "film factor" for diffusion of cupric ion analogous to film pressure factor in gases (5, 6), equal to the log mean volume fraction of nondiffusing species in the present case.

$$Sc = \frac{\mu}{\rho D} \quad \text{(VIII)}$$

where: μ = average liquid viscosity, g/cm-sec, and ρ = average liquid density, g/cm³.

$$Gr_x = \frac{g(\rho_o - \rho_i)\rho^2 x^3}{\rho_i \mu^2} \quad \text{(IX)}$$

where: ρ_o and ρ_i = fluid densities in bulk solution and at the electrode surface, respectively, g/cm³, and g = acceleration of gravity, cm/sec².

It is convenient to relate the density difference, $\rho_o - \rho_i$, to the concentration difference, $C_o - C_i$, by the specific densification coefficient, α, defined by the relation:

$$\alpha = \frac{\rho_o - \rho_i}{\rho_i(C_o - C_i)} \quad \text{(X)}$$

The specific densification coefficient does not vary greatly with concentration and, therefore, provides a convenient method for correlation of density data for use in these equations.

At the limiting current, assuming C_i to be negligible over the entire electrode, k_x varies inversely as the ¼ power of x. By integration over the electrode, the average mass transfer coefficient over height 0 to x can be related to the local value at height x by the equation:

$$k_L = 4/3k_x \quad \text{(XI)}$$

Assuming $X_f = 1$ and the number 0.952 negligible compared to Sc, equations (VII), (VIII), and (XI) may be combined to give the general equation for correlation of mass transfer coefficients in liquid systems:

$$Nu' = \frac{k_L x}{D} = 0.677\ (Sc\ Gr)^{1/4} \quad \text{(XII)}$$

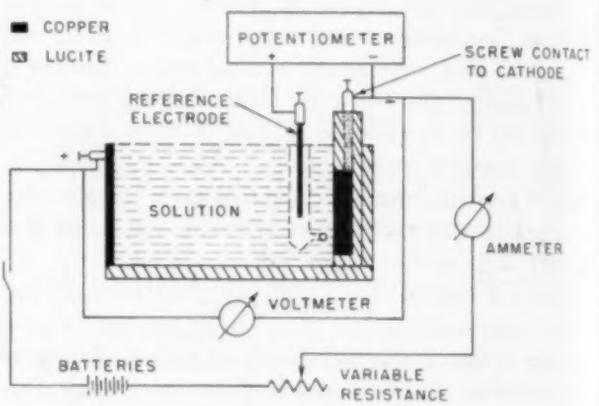

FIG. 1. Cell and circuit diagram

APPARATUS AND MATERIALS

The apparatus consisted essentially of an electrolytic cell for copper deposition and auxiliary equipment for measurement of total current and cathode potential relative to the bulk solution in the cell. Fig. 1 is a schematic diagram of the apparatus.

The cell was a rectangular container 7.6-cm wide and 10-cm high, formed of several sections of Lucite so that the distance could be varied between the cathode and anode located at opposite ends. Fig. 2 and 3 illustrate these features. A copper plate formed one of the end walls and served as anode. The copper cathodes were mounted in various Lucite holders as shown in Fig. 4. These holders permitted use of electrodes of four different heights: 0.634 cm, 2.54 cm, 3.75 cm, and 7.6 cm, and facilitated exchange of electrodes for repetition of the experiments. All cathodes were equal in width to the inner dimension of the cell, i.e., 7.6 cm. The sides of the cathodes were insulated with Glyptal lacquer so that only the side facing the anode conducted current. The cathode

circuit was completed by means of a contact screw, as indicated in Fig. 1. A fresh electrode was used for every limiting current determination, each electrode having been abrased and preplated by a standard procedure to assure uniformity of surface properties. Care was taken to obtain smooth alignment of the cathode surface with the vertical cell wall formed by the Lucite holder.

As reference electrode, a copper rod was immersed in a solution of the same composition as the bulk liquid in the cell and connected to the cell through a capillary of ½-mm outside diameter, located in the corner of the cell at the centerline of the cathode at a distance of 1 mm from the surface. Data were not corrected for the small error in potential caused by ohmic resistance of the solution between the capillary tip and the electrode.

Potentials between the cathode and the reference electrode, i.e., total cathodic polarization, were measured with a type K-2 potentiometer, and current was measured with a range of calibrated ammeters.

Fifteen different solutions of $CuSO_4$ in approximately 1.5M sulfuric acid were investigated. $CuSO_4$ concentration varied from about 0.01M to 0.74M, and H_2SO_4 varied from 1.38M to 1.57M. The electrolyte composition remained essentially constant in any one experiment. The cell liquid was analyzed frequently during the course of the study; Cu^{++} by the iodine-thiosulfate method, and $SO_4^{=}$ by standard gravimetric procedure. C.P. chemicals were used for preparation of all solutions.

Experimental Procedure for Limiting Current

The principal limiting current experiments are described below. Certain auxiliary experiments are discussed in a later section.

With the electrodes in place, the cell was filled with liquid to a depth of 10 cm, completely covering the cathode in all cases. Current was then passed through the cell and increased in small increments until the limiting current was attained, and usually increased further to the point of hydrogen evolution. Potential readings and new current settings were made at intervals of approximately 1 minute. These time intervals permitted the current and potential to reach essentially steady-state conditions at each rheostat setting, as demonstrated in preliminary experiments. Current-potential measurements were made with each electrode and electrolyte composition, and repeated three or four times, using freshly prepared cathodes. Reproducibility of successive limiting current determinations was within 1–2 per cent. The limiting current density for each experimental condition was determined by plotting the average current density over the electrode vs. potential, as determined by the reference electrode, and observing the "plateau" where the current density became essentially independent of po-

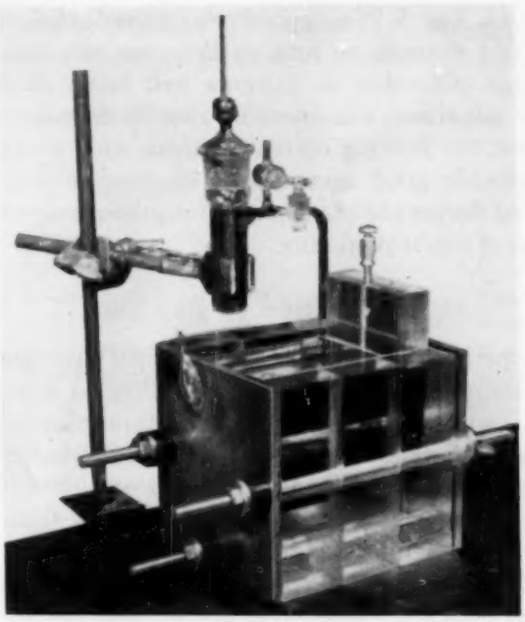

Fig. 2. Assembled cell and reference electrode

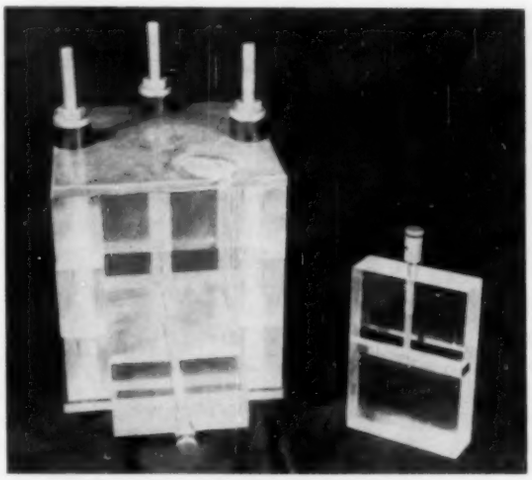

Fig. 3. Cell resting on end, anode at top

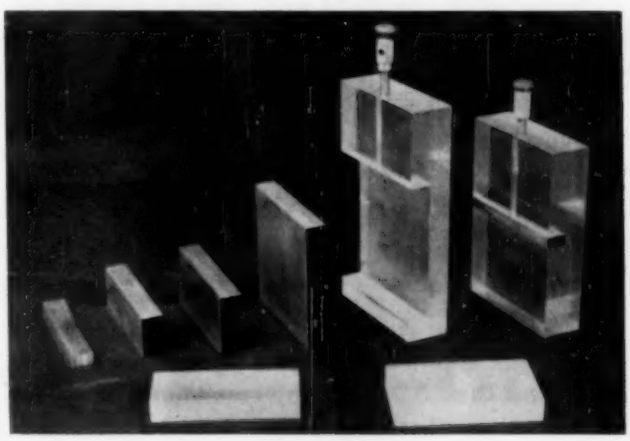

Fig. 4. Various cathodes and holders

tential. Fig. 5 is a typical current-potential curve for two consecutive runs on the same solution. Although potentials at currents well below limiting were not always consistent for runs on different electrodes, the limiting current plateaus were always in reasonably good agreement. Temperature was observed during the experiments for subsequent evaluation of liquid properties.

Correlation of Results

Experimental data for the principal experiments are summarized in Table I. According to equation (XII) and related theory, the Nusselt number should be a unique function of the Schmidt-Grashof number product for all electrode heights and electrolyte compositions. The procedure for obtaining these dimensionless groups is outlined briefly.

Mass transfer coefficients.—Average mass transfer coefficients were calculated by substitution of ex-

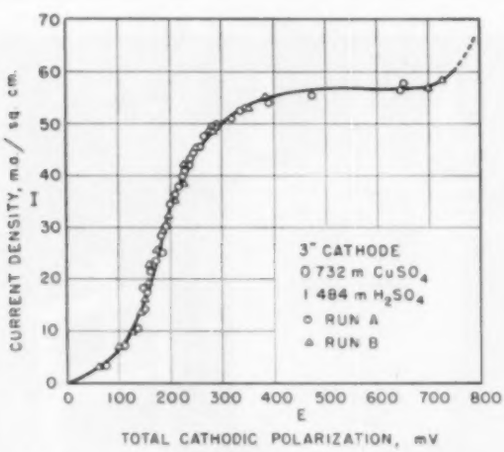

Fig. 5. Typical current potential curve

perimental quantities in equation (III), assuming C_i to be negligible compared to C_o, and t for cupric ion to be zero. Estimates based on ionic mobilities at infinite dilution and corrected for concentration by comparison with similar systems indicated that the average value of t over the boundary layer probably did not exceed 0.015 for even the most concentrated $CuSO_4$ solutions. In absence of a rigorous theory for treating transference over the present concentration profiles further refinement of the analysis did not seem justified.

Film factor for cupric ion.—Due to the small volume of the cupric ion, (X_f) in equation (VII) was never less than 0.997 for the maximum concentrations and was, therefore, assumed unity in all calculations.

Diffusion coefficients.—The effective diffusion coefficient for cupric ion was assumed to be the value for $CuSO_4$ since sulfate was the only anion present. Numerical values were based on the experimental data of Gordon and Cole (7) corrected for temperature, viscosity, and ionic strength of the solution. Hydrogen ion and sulfate ion were assumed to diffuse as sulfuric acid since the cupric ion concentration was relatively small in all cases. Sulfuric acid diffusivities were derived from data of Gordon (8) and Thovert (9), utilizing temperature and viscosity corrections in a similar manner to the procedure for $CuSO_4$. Diffusion coefficients and viscosities entering the final correlation were evaluated at the arithmetic mean composition between the bulk solution and electrode-solution interface. Numerical values are given in Table I.

Interfacial composition.—The cathode reaction and migration effects result in a net movement of sulfuric acid toward the interface. Eventually, a steady state is reached in which acid is transported away from the electrode by convective mass transfer at the same rate it is carried toward the electrode. The concentration difference thus developed between the electrode and bulk solution is expressed by the relation:

$$It_{H^+} = k_{H_2SO_4}(C_i - C_o)_{H_2SO_4} \qquad \text{(XIII)}$$

where t_{H^+} = transference number for hydrogen ion, and $k_{H_2SO_4}$ = mass transfer coefficient for sulfuric acid. According to equation (XII), the mass transfer coefficients for the various species vary as the $^3/_4$ power of the respective diffusion constants for any given electrode and solution. Therefore, the mass transfer coefficients for H_2SO_4 were calculated from the relation

$$k_{H_2SO_4} = \left[\frac{D_{H_2SO_4}}{D_{CuSO_4}}\right]^{3/4} \cdot k_{CuSO_4} \qquad \text{(XIV)}$$

From the known bulk solution sulfuric acid concentration, the electrolyte composition at the interface could be calculated for each experiment. Trial and error procedure was required in the solution of equations (XIII) and (XIV) since the average film composition, and, hence, the diffusion constant, was not known in advance.

Viscosities.—Viscosities were measured with an Ostwalt viscosimeter for sulfuric acid and copper sulfate solutions over the range of temperature and composition of interest. Results for pure sulfuric acid solutions were in agreement with the data of Vinal and Craig (10).

Densities.—Densities were measured with a special pycnometer of large volume for various solutions covering the range of compositions used in the experiments. A general correlation of α values for $CuSO_4$ and H_2SO_4 in water and aqueous glycerol solutions was developed which permitted the calcu-

lation of the density difference between bulk solution and the electrode-solution interface for each experiment. This procedure is outlined in detail elsewhere (11). Density data based on these α values are presented in the data tables pertaining to the various experiments.

General correlation.—Using the mass transfer coefficients and property values developed as discussed above, the Nusselt, Schmidt, and Grashof groups were evaluated for each experiment as presented in Table I. Fig. 6 is a log-log plot of the Nusselt group vs. the Schmidt-Grashof product. All of the data

TABLE I. *Experimental data and results for deposition of copper from* $CuSO_4$-H_2SO_4 *solutions on vertical electrodes*

Run No.	Electrode height, in.	$CuSO_4$ molarity	H_2SO_4 molarity	Lim. current density ma/cm²	Mass transfer coefficient × 10⁴ cm/sec	Temp, °C	Avg. viscosity centipoise	Avg. density g/cm³	Avg diffusion coefficient × 10⁵ cm²/sec	$\Delta C_{H_2SO_4}$ moles/liter	$\rho_o - \rho_i$ g/cm³	Nu'	Sc	$Gr \times 10^{-6}$
1	0.25	0.01002	1.530	0.602	0.3113	24.7	1.197	1.0898	0.628	0.0031	0.00139	31.43	1749	0.00264
2	0.25	0.0270	1.561	2.12	0.4068	23.7	1.220	1.0919	0.615	0.0083	0.00371	41.94	1817	0.00680
3	0.25	0.0498	1.498	4.20	0.4370	23.0	1.260	1.0933	0.593	0.0153	0.00675	46.72	1943	0.01167
4	0.25	0.0688	1.523	6.44	0.4850	23.7	1.242	1.0924	0.604	0.0209	0.00926	50.91	1882	0.01641
5	0.25	0.0813	1.501	7.67	0.4890	23.7	1.229	1.0918	0.610	0.0247	0.0109	50.82	1845	0.01969
6	0.25	0.0966	1.508	9.63	0.5010	23.7	1.263	1.0968	0.594	0.0301	0.0133	53.47	1939	0.22290
7	0.25	0.189	1.573	20.69	0.5671	23.7	1.300	1.1034	0.580	0.054	0.0248	62.00	2031	0.04078
8	0.25	0.247	1.465	27.55	0.5778	20.5	1.396	1.1056	0.533	0.071	0.0319	68.73	2369	0.04575
9	0.25	0.376	1.450	48.68	0.6710	22.5	1.400	1.1150	0.537	0.103	0.0478	79.25	2338	0.06936
10	0.25	0.467	1.471	66.45	0.7373	22.5	1.438	1.1282	0.525	0.123	0.0594	89.01	2428	0.08345
11	0.25	0.624	1.424	92.44	0.7675	26.0	1.385	1.1328	0.522	0.156	0.0791	88.13	2215	0.1211
12	0.25	0.660	1.502	94.65	0.7435	21.5	1.576	1.1406	0.480	0.160	0.0845	98.21	2878	0.1006
13	0.25	0.732	1.484	108.2	0.7658	23.7	1.559	1.1447	0.490	0.174	0.0938	99.09	2779	0.1151
14	0.25	0.739	1.384	105.3	0.7376	23.7	1.536	1.1397	0.495	0.177	0.0941	94.47	2773	0.1186
15	1.00	0.0113	1.522	0.495	0.2270	22.9	1.218	1.0906	0.613	0.0035	0.00157	94.06	1822	0.1852
16	1.00	0.0270	1.561	1.46	0.2802	24.9	1.186	1.0913	0.635	0.0083	0.00371	112.1	1711	0.4625
17	1.00	0.0498	1.498	2.76	0.2872	21.0	1.317	1.0942	0.536	0.0153	0.00675	129.6	2138	0.6867
18	1.00	0.0813	1.501	5.00	0.3187	20.4	1.320	1.034	0.561	0.0247	0.0109	144.3	2152	1.101
19	1.00	0.189	1.573	13.05	0.3578	20.5	1.392	1.1050	0.536	0.0540	0.0249	169.5	2350	2.295
20	1.00	0.247	1.465	17.58	0.3688	20.1	1.404	1.1058	0.528	0.071	0.0319	177.4	2405	2.910
21	1.00	0.376	1.450	28.8	0.3969	19.4	1.495	1.1168	0.498	0.103	0.0479	202.4	2688	3.924
22	1.00	0.467	1.471	44.9	0.4982	24.0	1.390	1.1272	0.546	0.123	0.0593	231.7	2258	5.733
23	1.00	0.660	1.502	66.3	0.5252	25.0	1.466	1.1375	0.523	0.160	0.0844	255.0	2464	7.437
24	1.00	0.732	1.484	74.65	0.5284	21.3	1.654	1.1465	0.458	0.174	0.0939	293.1	3150	6.597
25	1.50	0.0113	1.522	0.45	0.2063	22.4	1.231	1.0910	0.605	0.0035	0.00137	127.9	1865	0.5839
26	1.50	0.0270	1.561	1.29	0.2476	25.5	1.171	1.0911	0.645	0.0082	0.00371	143.9	1664	1.528
27	1.50	0.0305	1.522	1.53	0.2599	22.0	1.265	1.0920	0.588	0.0094	0.00418	165.8	1970	1.476
28	1.50	0.0498	1.498	2.60	0.2705	22.5	1.276	1.0936	0.584	0.0153	0.00675	173.7	1998	2.351
29	1.50	0.0813	1.501	4.58	0.2919	20.0	1.331	1.0936	0.556	0.0247	0.0109	196.9	2188	3.485
30	1.50	0.189	1.573	12.05	0.3304	20.4	1.395	1.1051	0.535	0.054	0.0249	231.6	2359	7.354
31	1.50	0.247	1.465	16.6	0.3486	22.3	1.345	1.1046	0.557	0.071	0.0319	234.7	2186	10.18
32	1.50	0.376	1.450	26.2	0.3610	20.0	1.474	1.1168	0.506	0.103	0.0478	267.6	2608	12.99
33	1.50	0.467	1.471	39.5	0.4383	22.7	1.432	1.1280	0.527	0.123	0.0594	311.9	2409	17.41
34	1.50	0.660	1.502	49.2	0.3863	19.0	1.700	1.1417	0.441	0.160	0.0846	328.5	3376	17.93
35	1.50	0.732	1.484	66.8	0.4728	23.7	1.558	1.1448	0.490	0.174	0.0937	361.8	2777	23.85
36	3.00	0.0113	1.522	0.397	0.1820	22.3	1.231	1.0909	0.605	0.0035	0.00157	228.7	1865	4.860
37	3.00	0.0270	1.561	1.07	0.2053	24.8	1.190	1.0914	0.633	0.0082	0.00371	246.5	1722	12.31
38	3.00	0.0305	1.522	1.24	0.2107	22.4	1.256	1.0918	0.593	0.0094	0.00418	270.0	1940	12.46
39	3.00	0.0498	1.498	2.09	0.2175	21.2	1.310	1.0942	0.567	0.0153	0.00675	291.5	2117	18.59
40	3.00	0.0813	1.501	3.55	0.2263	20.4	1.320	1.0934	0.561	0.0247	0.0109	306.5	2152	29.48
41	3.00	0.189	1.573	9.91	0.2717	20.4	1.395	1.1051	0.535	0.054	0.0249	385.9	2359	61.22
42	3.00	0.247	1.465	14.05	0.2947	22.1	1.351	1.1048	0.554	0.071	0.0319	404.3	2207	84.03
43	3.00	0.376	1.450	20.7	0.2853	19.0	1.504	1.1171	0.494	0.103	0.0478	438.8	2725	103.9
44	3.00	0.467	1.471	29.7	0.3295	18.0	1.612	1.1308	0.461	0.123	0.0595	543.2	3092	114.9
45	3.00	0.660	1.502	44.1	0.3462	22.8	1.546	1.1396	0.491	0.160	0.0844	535.9	2763	179.7
46	3.00	0.732	1.484	56.6	0.4003	27.2	1.429	1.1422	0.540	0.174	0.0937	563.3	2317	235.1

Note: Transference numbers of H^+ varied from 0.75 to 0.81.

correlate very satisfactorily in the manner indicated by the theory to a straight line corresponding to the equation:

$$Nu' = 0.673(ScGr)^{1/4}. \qquad \text{(XV)}$$

The constant 0.673 was evaluated by averaging the constants calculated for individual experiments, assuming the Schmidt-Grashof product to enter as the ¼ power. Such close agreement between equation (XV) and equation (XII) is no doubt fortuitous, but, nevertheless, the result appears to be a very encouraging indication of the general validity of the methods employed.

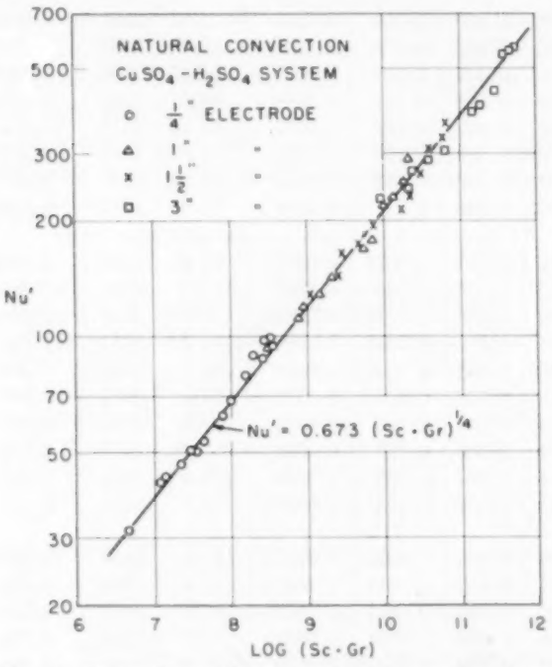

FIG. 6. General correlation of free convection data

DISCUSSION

Comparison of Results with other Theories and Experiments

Diffusion layer theory.—As originated by Nernst (12), this theory assumes transfer of ions to occur by diffusion through a "diffusion layer" of thickness B' defined for dilute solutions by the relation:

$$N_D = \frac{C_o - C_i}{B'} D. \qquad \text{(XVI)}$$

The diffusion layer is thus a hypothetical layer of stagnant fluid by means of which the total rate of mass transfer by all mechanisms acting over the actual mass transfer path may be expressed by an equivalent rate equation for pure diffusion. This concept has been widely used in the chemical engineering literature, with B' usually designated as the "effective film thickness." From equations (III), (XV), and (XVI), the diffusion layer thickness is given by:

$$B' = 1.48x(ScGr)^{-1/4}. \qquad \text{(XVII)}$$

Equation (XVII) indicates that B' is not constant, but varies with electrode height, electrolyte composition, and other factors which influence the Schmidt-Grashof number product. For the experimental results obtained in this study, B' ranged, in agreement with the theory, from 0.0064 cm to 0.0332 cm. Some authors (13, 14) have recommended use of an average value of 0.05 cm for B' in unstirred systems, a procedure which is theoretically unsound and which may be very seriously in error, as indicated by the present results.

Analogy to the Schmidt-Pohlhausen-Beckmann development for heat transfer (15).—As recommended for electrochemical systems by Agar (16) this theory gives the result:[2]

$$Nu' = 0.525(ScGr)^{1/4}. \qquad \text{(XVIII)}$$

Although the numerical coefficient in this equation disagrees with that derived from more exact theories and the present experimental result, the essential form of the equation is the same for large values of Sc. The disagreement is to be expected since the original solution of the differential equations by Pohlhausen was based upon Beckmann's experimental result for heat transfer to air from vertical plates. The numerical coefficient of equation (XVIII) can be considered applicable only to systems with Schmidt or Prandtl numbers of numerical value near to the Prandtl number for air, i.e., about 0.73.

Equations of Levich.—Levich (17) has developed an approximate solution to the differential equations for the free convection boundary layer which may be put into the form of equation (XII) as follows:

$$Nu' = 0.51(ScGr)^{1/4}. \qquad \text{(XIX)}$$

Again, although the exact numerical coefficient differs, this theory leads to an equation of the same general form as those previously described.

Equations of Wagner.—A detailed treatment of the free convection problem in relation to electrode processes has been presented by Wagner (18). Wagner uses the method of the boundary layer, assuming that the boundary layers for velocity and for diffusion of the various ionic species do not necessarily coincide. By assuming certain functions for the distribution of velocity and concentration between the electrode and point of maximum velocity, equations are developed to apply specifically to the system $CuSO_4$-H_2SO_4-H_2O. This result may be expressed in the following form for comparison with equation (XII):

$$Nu' = 0.805(ScGr)^{1/4}. \qquad \text{(XX)}$$

[2] Inspection of the equations as presented by ten Bosch indicates that the coefficient of equation (XVIII) should be 0.518.

As a consequence of assuming the boundary layer thickness for diffusion of H^+ to be greater than for diffusion of Cu^{++}, Wagner obtains an expression for calculation of the density difference between bulk solution and the electrode surface which differs from the result obtained in this paper. Direct comparison of the methods is, therefore, complicated.

When α may be assumed constant at an average value for each species, equations (IV) and (XIII) to (XV) lead to the following result for the average limiting current density over an electrode of height x_o:

$$I = \frac{0.673nF\Delta C_o}{x_o(1 - t_{Cu^{++}})} \cdot \left[\frac{gx_o^3D^3\Delta C_o(\alpha_{CuSO_4} - \alpha_{H_2SO_4}t_{H^+}[D_{CuSO_4}/D_{H_2SO_4}]^{3/4})}{\mu^2}\right]^{1/4} \quad \text{(XXI)}$$

Equation (XXI) may be compared directly with equation (XLVI) of Wagner's paper. Limiting current data for deposition of copper from 0.1M $CuSO_4$ in 1.0M H_2SO_4 are presented by Wagner for three electrodes of heights 1, 4, and 16 cm. These observations are given in Table II, along with values calculated by the method of Wagner, and calculated by equation (XXI) above. Equation (XXI), in conjunction with physical properties evaluated by the correlations developed for this paper, gives a very satisfactory prediction of the measurements, with an average deviation of 3.9 per cent between calculated and observed values. Use of physical properties recommended by Wagner, however, leads to a much less satisfactory result. The principal disagreement with respect to physical data lies in the values of the diffusion coefficient for $CuSO_4$ and in the densification coefficients for $CuSO_4$ and H_2SO_4, as indicated in Table II.

TABLE II. *Limiting current densities at copper cathodes in 0.1M $CuSO_4$ + 1.0M H_2SO_4 at 25°C*

Electrode height, cm	Average limiting current density, amp/cm²			
	Experimental result (18)	Calculated[1] equation (XXI) (physical properties, this study)	Calculated[2] equation (XXI) (physical properties of Wagner)	Calculated, Wagner
1	0.0103	0.0099	0.0083	0.0094
4	0.0067	0.0070	0.0058	0.0066
16	0.0052	0.0050	0.0041	0.0047

[1] $D_{CuSO_4} = 0.657 \times 10^{-5}$ cm²/sec; $\alpha_{CuSO_4} = 143.6$ cm³/mole; $\alpha_{H_2SO_4} = 51.9$ cm³/mole.

[2] $D_{CuSO_4} = 0.5 \times 10^{-5}$ cm²/sec; $\alpha_{CuSO_4} = 166$ cm³/mole; $\alpha_{H_2SO_4} = 68$ cm³/mole.

Equations of Keulegan.—Keulegan (19) presents the differential equations for motion and diffusion in the boundary layer for mass transfer in a manner similar to that used by Pohlhausen (15) for heat transfer. An approximate solution is developed by assuming the distribution of velocity and concentration to be arbitrarily selected sine functions of distance through the boundary layer perpendicular to the electrode surface. The resulting solution may be extended into the general form corresponding to equation (XV) as follows:

$$Nu' = 0.628(ScGr)^{1/4}. \quad \text{(XXII)}$$

Keulegan compares density reductions between bulk solution and the electrode for deposition of copper and nickel, calculated by equations based on this theory, with experimental results determined in freezing experiments by Brenner (18). The agreement obtained between calculation and theory is sufficient to constitute a strong indication of the correctness of the concepts which have been assumed in the boundary layer theory. Keulegan's presentation does not consider effects of migration and resultant increase in concentration of acid at the electrode on the developed density difference between the interface and bulk solution; however, the resultant error is not sufficient to alter the general agreement of the theory with the interpretation of Brenner's experiments.

Equations of Ostrach for heat transfer.—An excellent comprehensive treatment of heat transfer by free convection to vertical plates has been presented by Ostrach (19). The convection-diffusion equations are developed to give differential equations of the form used by Pohlhausen. By use of an IBM Card Programmed Electronic Calculator, solutions of these differential equations were obtained for various values of Prandtl number to give useful tabular functions from which Nusselt numbers, temperature, and velocity distributions can easily be obtained. These equations are adaptable to the mass transfer problem by substitution of Schmidt number for Prandtl number. For the average mass transfer Nusselt number over a plate of height x_o, the result of Ostrach may be expressed as follows:

$$\frac{Nu'}{(Gr)^{1/4}} = 0.943\, f(Sc) \quad \text{(XXIII)}$$

where $f(Sc)$ is a function of the Schmidt number, tabulated by Ostrach as the function $-H'(O)$ of Prandtl number. Equations (VI) and (XI) give:

$$\frac{Nu'}{(Gr)^{1/4}} = \frac{0.677(Sc)^{1/2}}{(0.952 + Sc)^{1/4}}. \quad \text{(XXIV)}$$

A comparison of numerical values of equations (XXIII) and (XXIV) for various Sc, using $f(Sc)$ from the tables of Ostrach, indicates that satisfactory agreement is over the range of Schmidt numbers above 0.73, with the two methods almost coinciding in the region of high Schmidt numbers such

as usually prevails in liquid systems. Both of these methods indicate equations of the simple form of equation (XVIII) to be theoretically inadequate over an extended range of Schmidt numbers for mass transfer or of Prandtl numbers for heat transfer.

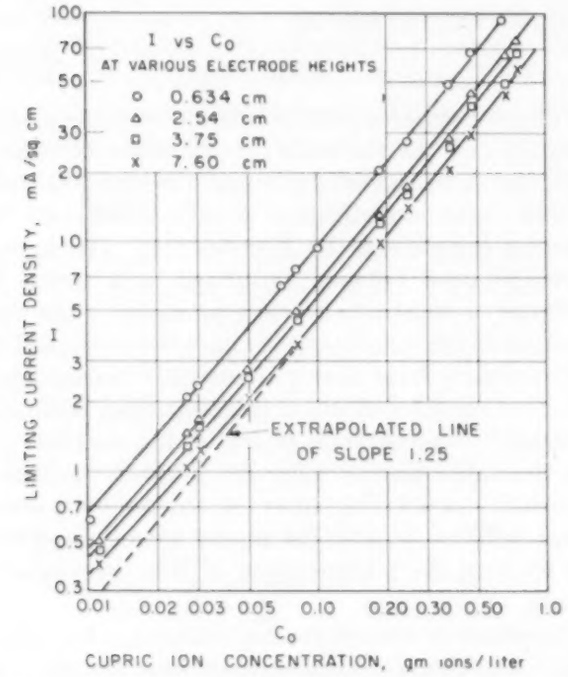

FIG. 7. Variation of limiting current with bulk cupric ion concentration.

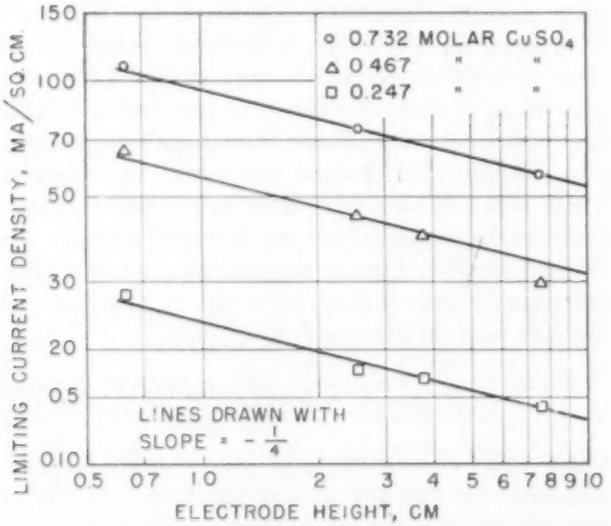

FIG. 8. Effect of electrode height on average limiting current density.

This limitation of equation (XVIII) has apparently been overlooked by ten Bosch, Agar, and others, who have postulated its application for all Prandtl and Schmidt numbers. A detailed discussion of these equations and comparisons with experimental heat transfer data is given by Ostrach.

Effect of Experimental Variables on Limiting Current Density

Bulk concentration of reacting species.—Equation (XXI) indicates the effect of all variables on the limiting current density when α may be assumed constant. If variation of other properties with electrolyte composition is not significant for a given system, the limiting current density should vary with the $\frac{5}{4}$ power of the bulk concentration of reacting species. In Fig. 7, limiting current densities for the present experiments are plotted against concentration of cupric ion in the bulk electrolyte. A straight line of slope $\frac{5}{4}$ passes through the data very well at concentrations greater than 0.1M. However, at lower concentrations, the relationship breaks down, due to failure of the assumption of constancy of α and other properties. Thus it may be concluded that limiting current density may vary as the $\frac{5}{4}$ power of concentration in certain cases, but that the rule is not universal.

Electrode height.—According to equation (XXI), the average limiting current density over an entire electrode should vary inversely as the $\frac{1}{4}$ power of total electrode height. This relationship is substantiated in Fig. 8, which is a log-log plot of current density vs. electrode height for three different $CuSO_4$ concentrations. As a further consequence of this relationship, the total current passing to an electrode increases as the $\frac{3}{4}$ power of electrode height.

Effect of Free Convection on Limiting Current Distribution

Equation (XXI) gives the local value of limiting current density at height x on a given electrode when the total height x_e in the equation is replaced by local height x and the numerical constant is reduced to 0.508. According to this result, the local current density varies inversely as the $\frac{1}{4}$ power of distance from the bottom of the electrode. This effect has been demonstrated by Wagner (18), who measured the current distribution for deposition of copper. Fig. 9 shows the theoretical current distribution for one of the present experiments. To investigate the extent of nonuniformity of current distribution at current densities below the limiting value, two experiments were conducted in which copper was deposited at a steady state rate of 19.5 ma/cm^2 on an electrode of 7.6 cm height. After a given run, the fresh metal deposit was stripped off, and its weight per 1 cm^2 measured as a function of position on the electrode. This, in turn, permitted the calculation of local current density. At heights above 2 cm, the current distribution was fairly uniform. At lower heights, a significant distortion of current distribu-

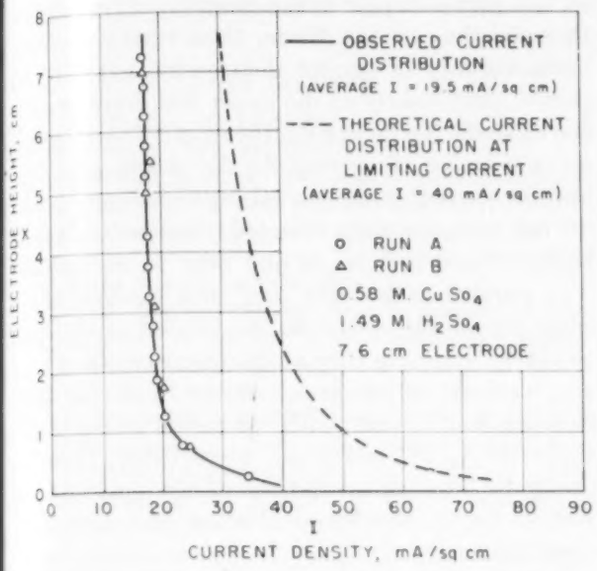

FIG. 9. Current distribution in free convection

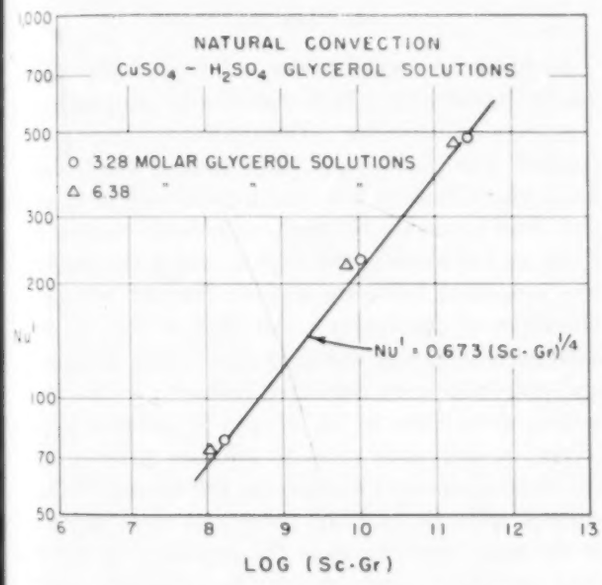

FIG. 10. Comparison of data for glycerol solutions with general correlation.

SPECIAL EXPERIMENTS

In order to illustrate certain additional features of the problem and to test further the general application of the correlation a number of special experiments were conducted as follows.

Copper Deposition from Aqueous Glycerol Solutions

In order to obtain a greater variation in properties of the electrolyte, particularly a variation in viscosity and diffusion coefficient, various H_2SO_4-H_2O solutions were prepared containing glycerol in amounts ranging from 3.28 to 6.38 moles/liter. This increased the viscosity of the liquid and reduced the diffusion constant, respectively, by a factor of ten. Limiting current data were obtained for ¼-in., 1-in., and 3-in. electrodes in the manner previously described. Table III presents the experimental results. Fig. 10 shows the comparison of Nu' as a function of $ScGr$ for these solutions with the line obtained in the general correlation, Fig. 6. This agreement is believed to be very satisfactory and an encouraging indication of the general validity of the correlation.

Study of Full-End Electrodes

In the preceding experiments, the electrodes were placed in Lucite holders and centered approximately midway between the floor of the cell and upper surface of the electrolyte. It seemed desirable, therefore, to study an electrode extending over the entire end-wall of the cell, since this arrangement represents the opposite extreme in cell geometry. Accordingly, the entire Lucite end of the cell was replaced by a copper plate which served as the cathode. Limiting current measurements were made with liquid filling the cell at various levels from 2.5 cm to 10.0 cm. Experimental results are compared with the general correlation in Fig. 11. Although the best line through the data might be placed a few per cent below th

TABLE III. *Data and results for copper deposition from* $CuSO_4$-H_2SO_4-*glycerol solutions on vertical electrodes*

Run No.	Electrode height, in.	$CuSO_4$ molarity	H_2SO_4 molarity	Glycerol molarity	Lim. C.D. ma/cm²	Mass transfer coeff. × 10⁵	Temp, °C	Avg viscosity centipoise	Avg density g/cm³	Avg diffusion coeff.[1] × 10⁵ cm²/sec	$\Delta C_{H_2SO_4}$ moles/l	$\rho_o - \rho_i$ g/cm³	Nu'	Sc	$Gr \times 10^{-8}$
47	0.25	0.3679	0.751	6.38	9.32	0.1313	23.4	10.02	1.1983	0.113	0.153	0.0472	73.67	73,976	0.001437
48	0.25	0.5702	1.145	3.28	35.5	0.3226	22.5	4.254	1.1755	0.264	0.204	0.0719	77.47	13,708	0.01204
49	1.00	0.3679	0.751	6.38	7.12	0.1003	23.5	9.991	1.1983	0.114	0.153	0.0472	224.4	73,784	0.09284
50	1.00	0.5702	1.145	3.28	25.5	0.2317	21.5	4.392	1.1762	0.255	0.204	0.0719	230.8	14,643	0.7272
51	3.00	0.3679	0.751	6.38	4.58	0.0645	22.1	10.596	1.1992	0.106	0.153	0.0472	462.5	83,357	2.215
52	3.00	0.5702	1.145	3.28	18.65	0.1695	22.9	4.197	1.1752	0.268	0.204	0.0719	480.6	13,326	21.29

[1] Measured in diaphragm cell (23).

vection persists at current densities well below limiting in these systems.

line based on Fig. 6, the deviation is not very significant. It may, therefore, be concluded that the posi-

tion of the electrode with respect to the floor of the cell or with respect to the liquid surface is relatively unimportant insofar as limiting current is concerned.

Position of Electrode Relative to Floor of Cell

To observe further the effect of variation in electrode location, additional experiments were conducted with two electrodes 0.634 and 2.54 cm in height, respectively. In a series of runs, these electrodes were each placed at distances of 0, 1.3, 3.2, and 5.7 cm from the cell floor with the cell filled to a depth of 7.6 cm. Several solutions ranging from 0.042 to 0.732 in $CuSO_4$ molarity were used in these tests. For a given electrode and solution, variations in the observed limiting currents from the average for the series never exceeded 1.5 per cent over the range of electrode positions.

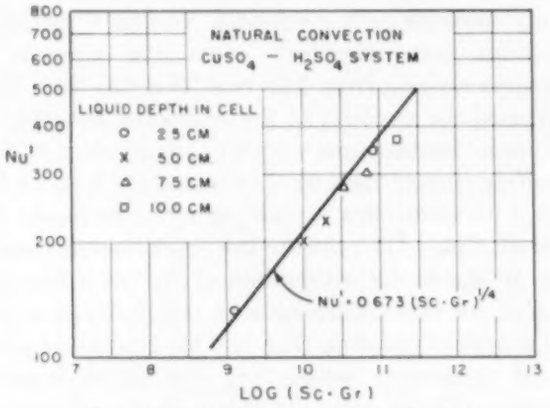

FIG. 11. Data for full-end electrodes

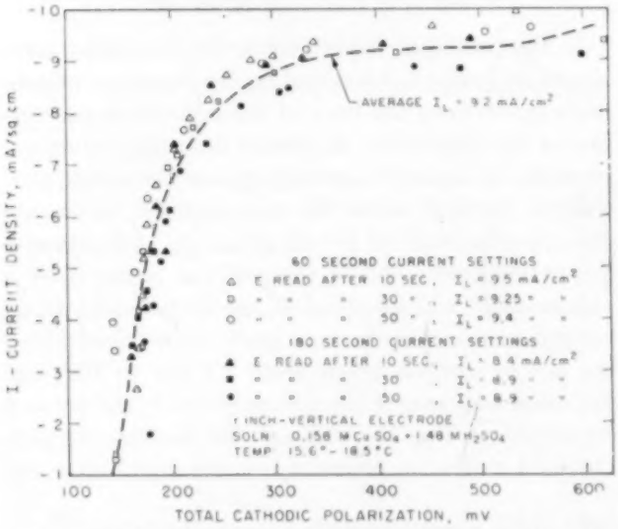
I - CURRENT DENSITY, mA/sq cm
AVERAGE I_L = 9.2 mA/cm²
60 SECOND CURRENT SETTINGS
E READ AFTER 10 SEC., I_L = 9.5 mA/cm²
30 " , I_L = 9.25 " "
50 " , I_L = 9.4 " "
180 SECOND CURRENT SETTINGS
E READ AFTER 10 SEC., I_L = 8.4 mA/cm²
30 , I_L = 8.9 " "
50 , I_L = 8.9 " "
1 INCH-VERTICAL ELECTRODE
SOLN 0.158 M $CuSO_4$ + 1.48 M H_2SO_4
TEMP 15.6° - 18.5 °C
TOTAL CATHODIC POLARIZATION, mV

FIG. 12. Effect of time intervals between current settings and potential reading and between successive current settings upon the limiting current.

Effect of Window Baffles between Anode and Cathode

In the majority of experiments, the electrolyte between anode and cathode presented a larger cross section perpendicular to the direction of current flow than did the cathode. Under these conditions, some nonuniformity of current distribution might be expected, particularly at the upper and lower edges of the cathode. To determine the extent to which such nonuniformity of current density might affect the limiting current data, several experiments were conducted using specially designed window-type Lucite baffles placed parallel to and near to the cathode. Two parallel baffles were used with windows of the same size as the electrode and located at the same elevation. Limiting current data were obtained for a 1-in. cathode at various elevations in the cell filled to a depth of 7.6 cm, with the baffles placed at distances of ¼ in. and 1 in., respectively, from the electrode. Limiting current results obtained with and without baffles were identical within limits of experimental accuracy.

Variation in Technique of Obtaining Current-Potential Curves

In order to establish the validity of the experimental techniques which was finally adopted, various ways of obtaining current-potential curves were studied. The objective of these studies was to determine any effect on the limiting current of altering the time intervals between successive current settings, and of altering the time at which the potential was measured following a given current setting. In one series of experiments, the time of electrolysis at each current setting was held constant at 60 seconds, and potentials were measured following each current setting at intervals of 10, 30, and 50 seconds, respectively, in successive runs. In another series of runs, the electrolysis time was held at 180 seconds between current settings, and the potentials were measured at the same intervals as in the preceding series. The data for these runs, giving six different current-potential curves for identical electrolyte compositions and electrodes, are shown in Fig. 12. The maximum deviation of the limiting currents from the average value of 9.22 ma/cm² is 3.2 per cent. Irreproducibility of polarization of copper cathodes should be expected in view of results of other studies (22). However, the limiting current density appears to be independent of the initial shape of the current-potential curve, in agreement with the concept of mass transfer being the controlling process at the limiting current point.

ACKNOWLEDGMENT

The authors wish to acknowledge the support of the Office of Naval Research. Appreciation is due Mr. Richard Stein for assistance with experimental measurements.

Any discussion of this paper will appear in a Discussion Section, to be published in the June 1954 issue of the JOURNAL.

REFERENCES

1. C. W. TOBIAS, M. EISENBERG, AND C. R. WILKE, *J. Electrochem. Soc.*, **99**, 359*C* (1952).
2. C. R. WILKE, M. EISENBERG, AND C. W. TOBIAS, To be published in *Chemical Engineering Progress*.
3. S. GOLDSTEIN, "Modern Developments in Fluid Dynamics," Squires' method, pp. 641–643, Oxford University Press, New York (1938).
4. E. R. G. ECKERT, "Introduction to Transfer of Heat and Mass," pp. 158–163, McGraw Hill Book Company, New York (1950).
5. C. R. WILKE, *Chem. Eng. Progr.*, **46**, 95 (1950).
6. O. A. HOUGEN AND K. M. WATSON, "Chemical Process Principles, III," 1st ed., p. 977, John Wiley and Sons, Inc., New York (1947).
7. A. R. GORDON AND A. COLE, *J. Phys. Chem.*, **40**, 733 (1936).
8. A. R. GORDON, *J. Chem. Phys.*, **7**, 89 (1939); **8**, 423 (1940).
9. G. THOVERT, Landolt-Boernstein Tabellen I, p. 248.
10. G. W. VINAL AND D. N. CRAIG, *Bur. Standards J. Research*, **10**, 781 (1933).
11. M. EISENBERG, C. W. TOBIAS, AND C. R. WILKE, To be published.
12. W. NERNST, *Z. physik. Chem.*, **47**, 52 (1904).
13. J. N. AGAR AND F. P. BOWDEN, *Proc. Roy. Soc. London*, **169A**, 206 (1938).
14. S. GLASSTONE, "An Introduction to Electrochemistry," pp. 448–52, D. Van Nostrand Company, New York (1942).
15. M. TEN BOSCH, "Die Wärmeübertragung," III Auflage, pp. 160–167, Julius Springer, Berlin (1936).
16. J. N. AGAR, *Discussions Faraday Soc.*, **1**, 31 (1947).
17. B. LEVICH, *Acta Physicochim. U.S.R.R.*, **19**, 125 (1944).
18. C. WAGNER, *J.* (*and Trans.*) *Electrochem. Soc.*, **95**, 161 (1949).
19. G. H. KEULEGAN, *J. Research Natl. Bur. Standards*, **47**, 156 (1951).
20. A. BRENNER, *Ann. Proc. Tech. Sessions, Am. Electroplaters' Soc.*, p. 28 (1941).
21. S. OSTRACH, *Natl. Advisory Comm. Aeronaut.*, Tech. Note 2635, Lewis Flight Propulsion Laboratory, Cleveland, Ohio, February 1952.
22. L. L. SHREIR AND J. W. SMITH, *J. Electrochem. Soc.*, **98**, 193 (1951).
23. PIN CHANG, Ph.D. Thesis, University of California (in preparation, 1953).

Thermodynamics of the Acid Weston Cell and the Acid Clark Cell[1]

CARL WAGNER

Department of Metallurgy, Massachusetts Institute of Technology, Cambridge, Massachusetts

ABSTRACT

The dependence of the potential of the saturated Weston cell on the concentration of sulfuric acid is calculated thermodynamically in satisfactory accord with experimental results. In the case of the Clark cell, the observed dependence of the potential on the concentration of sulfuric acid is somewhat greater than the calculated value. A modified acid Weston cell is suggested in order to eliminate the dependence of the potential on acid concentration.

THERMODYNAMICS OF THE ACID WESTON CELL

Most Weston cells are prepared with a small amount of sulfuric acid in order to prevent hydrolysis of mercurous sulfate (1). Presence of sulfuric acid lowers the electromotive force. According to Obata (2), the electromotive force E of a Weston cell saturated with $CdSO_4 \cdot 8/3H_2O$ decreases linearly with the concentration of sulfuric acid according to the empirical equation

$$\delta E/\delta c = -0.855 \cdot 10^{-3} \text{ volt/(equivalent } H_2SO_4\text{/liter)} \quad \text{(I)}$$

where c is the concentration of H_2SO_4 in equivalents per liter. Measurements made by Vosburgh (3) confirm equation (I). Ishibashi and Ishizaki (4) have obtained the slightly different relation

$$\delta E/\delta c = -0.833 \cdot 10^{-3} \text{ volt/(equivalent } H_2SO_4\text{/liter)}. \quad \text{(II)}$$

The dependence of the electromotive force on the concentration of sulfuric acid may be derived from thermodynamic considerations as is shown in the following:

The virtual cell reaction for passing two faradays ($=2\mathbf{F}$) across the Weston cell

Cd amalgam | electrolyte saturated with $CdSO_4 \cdot 8/3H_2O, Hg_2SO_4$ | Hg may be written as

$$\text{Cd (amalgam)} + Hg_2SO_4\,(s) + 8/3H_2O \text{ (electrolyte)} = Hg(l) + CdSO_4 \cdot 8/3H_2O\,(s). \quad \text{(III)}$$

Hence the electromotive force E equals

$$E = -[F_{Hg} + F_{CdSO_4 \cdot 8/3H_2O} - \bar{F}_{Cd} - F_{Hg_2SO_4} - (8/3)\bar{F}_{H_2O}]/2\mathbf{F} \quad \text{(IV)}$$

where the molar free energies of liquid mercury and $CdSO_4 \cdot 8/3H_2O$ (s) and the partial molar free energies of Cd and H_2O are denoted by F and $\bar{F}$ with the corresponding subscripts, respectively. Addition of H_2SO_4 to the electrolyte decreases $\bar{F}_{H_2O}$ and thus, according to equation (IV), also decreases the potential E.

The components of the electrolyte, H_2O, $CdSO_4$, and H_2SO_4, will be denoted as 1, 2, and 3, and their numbers of moles by n_1, n_2, and n_3, respectively. Presence of Hg_2SO_4 in the electrolyte is disregarded, since its concentration is relatively low. The Gibbs-Duhem equation reads

$$[n_1 d\bar{F}_1 + n_2 d\bar{F}_2 + n_3 d\bar{F}_3 = 0]_{P,T}. \quad \text{(V)}$$

If the solution is saturated with $CdSO_4 \cdot 8/3H_2O$, the sum $\bar{F}_2 + (8/3)\bar{F}_1$ is constant, i.e.,

$$[d\bar{F}_2 + (8/3)\, d\bar{F}_1 = 0]_{P,T}. \quad \text{(VI)}$$

Upon combining equations (V) and (VI), it follows that

$$d\bar{F}_1 = -\frac{n_3/n_1}{1 - (8/3)(n_2/n_1)}\, d\bar{F}_3. \quad \text{(VII)}$$

If H_2SO_4 is added to the electrolyte, the following reaction takes place

$$H_2SO_4 + SO_4^{--} = 2HSO_4^-. \quad \text{(VIII)}$$

In view of the large excess of cadmium sulfate in the saturated solution, the activity of SO_4^{--} and the activity coefficient of HSO_4^- are virtually constant for small additions of H_2SO_4. Consequently, the activity of H_2SO_4 is essentially proportional to the square of its concentration. Thus, if $n_3 \ll n_1$,

$$d\bar{F}_3 = 2RT\, d \ln (n_3/n_1). \quad \text{(IX)}$$

Substitution of equation (IX) in equation (VII) yields

$$d\bar{F}_1 = -\frac{2RTd(n_3/n_1)}{1 - (8/3)(n_2/n_1)}. \quad \text{(X)}$$

Upon combining equations (IV) and (X), it follows that

$$dE = -\frac{8}{3}\frac{RT/\mathbf{F}}{1 - (8/3)(n_2/n_1)}\frac{dn_3}{n_1}. \quad \text{(XI)}$$

[1] Manuscript received January 7, 1953.

According to Hulett (5) and Cohen and Sinnige (6) one liter of a solution saturated with $CdSO_4 \cdot 8/3\ H_2O$ at 25°C contains 3.36 mole $CdSO_4$ and 50.8 mole H_2O. Hence

$$\frac{n_3}{n_1 - (8/3)n_2} = \frac{\frac{1}{2}c}{50.8 - (8/3)3.36} = 0.0120c \quad \text{(XII)}$$

where c is the concentration of H_2SO_4 in equivalents per liter.

Substitution of equation (XII) in equation (XI) yields for 25°C

$$(\delta E/\delta c)_{c=0} = -0.82 \cdot 10^{-3} \text{ volt/(equivalent } H_2SO_4\text{/liter)} \quad \text{(XIII)}$$

in close accordance with equations (I) and (II).

Uhlig (7) has pointed out that a cadmium amalgam electrode reacts with acid, $Cd + 2H^+ = Cd^{++} + H_2$, and thus the potential of a cadmium electrode is slightly more noble than the true equilibrium potential. This effect increases with increasing acid concentration but is only of the order of a microvolt and therefore insignificant in comparison to the shift of the equilibrium potential calculated in equation (XIII).

Thermodynamics of the Acid Clark Cell

The effect of sulfuric acid on the electromotive force of the Clark cell

Zn amalgam | electrolyte saturated with $ZnSO_4 \cdot 7H_2O$, Hg_2SO_4 | Hg

may be calculated in a similar way. Since the solid salt contains 7 moles H_2O per mole $ZnSO_4$, the analogue to equation (XI) is

$$dE = -\frac{7RT/\mathbf{F}}{1 - 7(n_4/n_1)} \frac{dn_3}{n_1} \quad \text{(XIV)}$$

where (n_4/n_1) is the molar ratio of $ZnSO_4$ and H_2O in the electrolyte.

According to Hulett (5), a solution saturated with $ZnSO_4 \cdot 7H_2O$ at 25°C contains 3.36 mole $ZnSO_4$ and 52.7 mole H_2O. Hence,

$$\frac{n_3}{n_1 - 7n_4} = \frac{\frac{1}{2}c}{52.7 - 7 \times 3.36} = 0.0171c. \quad \text{(XV)}$$

Substitution of equation (XV) in equation (XIV) yields for 25°C

$$\delta E/\delta c = -3.1 \cdot 10^{-3} \text{ volt/(equivalent } H_2SO_4\text{/liter)} \quad \text{(XVI)}$$

whereas Hulett (5) found experimentally

$$\delta E/\delta c = -4.1 \cdot 10^{-3} \text{ volt/(equivalent } H_2SO_4\text{/liter).} \quad \text{(XVII)}$$

The difference between the calculated and the experimental value may be due to the reaction between zinc amalgam and acid, whereby the potential of the zinc amalgam electrode is shifted to a slightly more noble potential (8). For the Clark cell this effect is far more significant than for the Weston cell since the single electrode potential of a zinc amalgam electrode is 0.4 volt less noble than that of a cadmium amalgam electrode and, accordingly, the rate of hydrogen evolution and dissolution of metal is about 1000 times greater.

Suggestion of a Modified Acid Weston Cell

At either side of the saturated Weston cell there are four phases, viz., two metallic phases, solid $CdSO_4 \cdot 8/3H_2O$, and aqueous solution at the negative electrode; and liquid mercury, solid $CdSO_4 \cdot 8/3H_2O$, solid Hg_2SO_4, and aqueous solution at the positive electrode. In the acid Weston cell there are five components, e.g., Hg, Cd, $CdSO_4$, H_2O, and H_2SO_4. Hence, applying the Gibbs phase rule to either half cell (9, 10), there are three degrees of freedom, e.g., temperature, pressure, and the activity of sulfuric acid.

To obtain the greatest possible stability of the potential at a given temperature, it seems desirable to reduce the number of degrees of freedom to two so that the electromotive force is determined by only two independent variables, i.e., temperature and pressure. To this end, one may add K_2SO_4 as a new component and two other phases, e.g., the solid salt $3CdSO_4 \cdot K_2SO_4 \cdot 5H_2O$ described by Benrath and Thömessen (11) and a solid acid potassium sulfate, possibly $KHSO_4$. Cells of this type although without $KHSO_4$ have been investigated by Vosburgh, Derr, Cooper, and Pettengill (12). Eventually, however, the rather high hydrogen concentration in cells involving solid $KHSO_4$ may cause too high a rate of hydrogen evolution at the cadmium amalgam electrode, which is undesirable in the first place because of an irreversible potential change according to Uhlig (7), and in the second place because of the dependence of the potential on total pressure. According to Cohen and Sinnige (6) the potential of the saturated Weston cell increases by 6 microvolts when the pressure is increased by one atmosphere.

As an alternative possibility for reducing the number of degrees of freedom, one may add an organic acid as a new component and two other phases, e.g., solid acid HX and solid salt CdX_2 or its hydrate. Eventually, 1- or 2-naphthalinesulfonic acid may be suitable, but at the present no definite proposal can be made.

Acknowledgment

The author is indebted to Dr. H. H. Uhlig for stimulating discussions.

Any discussion of this paper will appear in a Discussion Section, to be published in the June 1954 issue of the JOURNAL.

REFERENCES

1. G. W. VINAL, "Primary Batteries," p. 200, J. Wiley & Sons, New York (1950).
2. J. OBATA, *Proc. Math. Phys. Soc. Japan*, (3) **2**, 232 (1920).
3. W. C. VOSBURGH, *J. Am. Chem. Soc.*, **47**, 1265 (1925).
4. Y. ISHIBASHI AND T. ISHIZAKI, *Researches Electrotech. Lab. Tokyo*, No. 318 (1931).
5. G. A. HULETT, *Phys. Rev.*, (1) **27**, 337 (1908).
6. E. COHEN AND L. R. SINNIGE, *Z. physik. Chem.*, **67**, 513 (1909).
7. H. H. UHLIG, *J. Electrochem. Soc.*, **100**, 173 (1953).
8. C. WAGNER AND W. TRAUD, *Z. Elektrochem.*, **44**, 391 (1938).
9. P. H. J. VAN GINNECKEN AND H. R. KRUYT, *Z. physik. Chem.*, **77**, 744 (1911).
10. W. C. VOSBURGH, *J. Am. Chem. Soc.*, **49**, 78 (1927).
11. A. BENRATH AND C. THÖNNESSEN, *Z. anorg. allgem. Chem.*, **203**, 405 (1933).
12. W. C. VOSBURGH, P. F. DERR, G. R. COOPER, AND B. PETTENGILL, *J. Am. Chem. Soc.*, **61**, 2687 (1939).

UNIVERSITY OF MICHIGAN LIBRARIES

Technical Note

Iron Contamination of Storage Batteries[1]

E. Willihnganz

Research Laboratories, Gould National Batteries, Depew, New York

Introduction

Small amounts of iron are present in all lead-acid storage batteries. The raw materials usually contain iron, and the manufacturing is carried out in iron equipment. The amount of iron present in the battery is usually estimated by analyzing the electrolyte, and the amount so found is usually less than 0.01 per cent.

The exact amount which a battery can tolerate without damage has not been accurately determined. Gilette (1) found that when 0.01 per cent was added to the electrolyte, there was no perceptible influence, but that 0.10 per cent caused a high rate of self-discharge. Vinal (2) found that there was a perceptible influence on self-discharge when 0.012 per cent was added to the electrolyte.

Vinal's tests were carried out under rather special conditions. He used single plates, suspended them in a large excess of acid, and followed changes by weighing the plates while suspended in the acid.

In view of the limited nature of this information, it was decided to redetermine the effect of iron under conditions which more closely conform to actual battery practice.

Experimental

For this test, a series of 67 test batteries was prepared. These were standard 100-amp-hr, 15-plate, six-volt automobile units prepared from commercial materials. The separators were a commercial type, consisting of a polystyrene bonded diatomaceous earth, supported on a glass mat and having a conventional ribbed surface and a glass mat facing the positive plates. After the first charge, usually described as the formation, the cells were drained, rinsed with a solution of reagent grade sulfuric acid to remove most of the dissolved iron, and then filled with reagent grade acid which had been adjusted to a specific gravity of 1.270. They were then charged to secure thorough mixing of the acid, and the iron content of the electrolyte determined. This averaged 0.007 per cent on several typical cells.

Ferrous sulfate was then added to some of the cells in accurately measured amount to adjust the iron content of the electrolyte to the desired value. Thirteen batteries of each of five iron contents were prepared.

Duplicate batteries were then given each of the customary performance tests according to the specifications of the Society of Automotive Engineers as published in 1952 (3). Three different laboratories carried out the tests, using either four or five batteries of each of the five iron contents.

Results

The averaged results are summarized in Table I for three significant iron contents. In general, iron affected the performance in two ways. Most obviously, it shortened the battery life when the battery was given repeated cycles of charge and discharge. At 0.1 per cent by weight of added iron, the life was seriously reduced.

The rate of self-discharge was also affected by iron content. At 0.1 per cent added iron, the rate of self-discharge was measurably greater than that of a battery with no added iron. When the self-discharge was measured in terms of a loss of specific gravity, 0.1 per cent iron increased the loss 1.5 times. When the residual capacity was measured, the loss was only 1.15 times.

Where less than 0.1 per cent of iron was added to the electrolyte, no definite harmful effects were observed. Tests were run at 0.00, 0.012, 0.020, 0.030, and 0.100 per cent iron. The results of the first four iron contents are substantially identical, so that of these only the 0.00 and 0.030 per cent results are tabulated. Although it appears that there is some effect at the latter level, the differences are within the expected variation of experimental results and are not considered significant.

[1] Manuscript received February 24, 1953.

TABLE I. *Effect of iron*

Iron content, % of electrolyte*	0.000	0.030	0.100
Self-discharge—28-day loss in sp gr @ 80°F			
Laboratory A	0.033	0.032	0.053
Laboratory B	0.041	0.046	0.057
Laboratory C (% residual capacity)	70	72	66
20-hr capacity, amp hr @ 5 amp @ 80°F			
Laboratory A	103.8	100.7	96.5
Laboratory B	100.6	99.4	96.6
Laboratory C	101	100.0	95.0
SAE life, cycles, 4 charge-discharge cycles per day			
Laboratory A	—	—	—
Laboratory B	360	360	214
Laboratory C	453	417	123
Overcharge life, weeks @ 9 amp			
Laboratory A	8	8	7
Laboratory B	6	6	6
Laboratory C	6	7	7
Cold test capacity, min at 300 amp			
Laboratory A	4.41	3.93	3.67
Laboratory B	3.8	3.40	3.70
Laboratory C	3.58	3.55	3.63
5-Sec voltage, at start of cold test			
Laboratory A	4.38	4.44	4.39
Laboratory B	4.48	4.41	4.40
Laboratory C	4.38	4.32	4.22
End of charge volts			
Laboratory A	7.53	7.53	7.56
Laboratory B	—	—	—
Laboratory C	7.36	7.30	7.25

* Grams Fe per 100 g electrolyte. Added as an equivalent amount of $FeSO_4 \cdot 7H_2O$.

TABLE II. *Iron summary as percentage of electrolyte*

Added to acid	0.000	0.030	0.100
Total in cell	0.007	0.037	0.107
Found in acid			
Found—after 3 cycles	0.009	0.025	0.130
after 60 days stand	0.007	0.018	0.045
after cycle life test	0.006	0.021	0.077
after overcharge life test	0.004	0.007	0.034
Found in lead peroxide after overcharge life test			
(Calculation to % in acid)	—	0.030	—

Iron Analyses

Although carefully weighed amounts of ferrous sulfate were added to the test batteries, analysis of the electrolyte for iron gave low results. The missing iron was found in the lead peroxide upon dismantling the test cells. The results are summarized in Table II.

Discussion

Two aspects of the action of iron are important. First, there is the practical matter of the iron tolerance of a battery; and second, there is the technical question of why iron affects battery performance.

The mechanism of the action of iron in the storage battery can be discussed only briefly. Vinal has shown that iron is oxidized at the positive plate to the ferric state, and this diffuses to the negative plate where it is reduced and returned to the positive plate. The net result is a transfer of an electrical charge between the plates without the passage of an external current, and constitutes self-discharge. On this basis, the contribution of iron to self-discharge should be proportional to the iron content of the electrolyte.

The appearance of iron in the positive active material is certainly evidence that ferric iron is dissolved in, or is adsorbed by, lead peroxide.

The effect on SAE life is interesting since, in this test, life is limited by the shedding, or sloughing off, of the positive active material. During periodic charge-discharge cycles, the lead peroxide is converted to crystalline lead sulfate and back to lead peroxide repeatedly. During this process, the active material gradually softens, and finally drops to the bottom of the battery as a finely divided lead peroxide sediment. Since iron accelerates this process considerably, it seems probable that iron is adsorbed on the peroxide crystals, and prevents fresh peroxide formed during charge from attaching itself firmly to the underlying lead peroxide.

The effect of large amounts of iron on the 20-hr rate capacity can be explained by the same mechanism. This test capacity is usually limited by the rate at which acid can reach the interior of the positive plate. Since iron reduces the capacity, it probably influences the plate structure to retard diffusion. In view of the structural differences postulated in connection with the SAE cycling life test, it is anticipated that iron would gradually reduce the capacity measured at the 20-hr rate.

The test data are not sufficiently precise to establish this gradual deterioration of capacity, but they are at least suggestive of such a deterioration.

On the basis of the above tests, it is concluded that iron is harmless to the automobile battery when 0.037 per cent is present initially in the electrolyte, but that 0.10 per cent is somewhat harmful. Further, it is concluded that an analysis of the electrolyte is not a reliable method of measuring the iron content of the battery since part of the iron is removed from

UNIVERSITY OF MICHIGAN LIBRARIES

the electrolyte by the lead peroxide of the positive plate.

To avoid uncertainty, it appears desirable to consider the total iron content of the cell, that is, both the electrolyte iron and the iron in the lead peroxide. The above results can be expressed by saying that the battery can tolerate a total iron content equal to 0.037 per cent of the weight of acid, but to test the cell it is necessary to analyze both acid and lead peroxide.

This conclusion is based on the standard bench testing of automotive batteries only. It manifestly cannot be applied to specialty batteries, or special service conditions, such as calcium alloy telephone batteries where self-discharge offers a different kind of problem, or industrial truck batteries where shedding rates must be controlled more carefully than in automobile batteries.

REFERENCES

1. H. Gilette, *Trans. Am. Electrochem. Soc.*, **41**, 217 (1922).
2. G. W. Vinal, "Storage Batteries," p. 135, John Wiley & Sons, Inc., New York (1940).
3. Hand Book, Society of Automotive Engineers, 29 West 39th St., New York, N. Y. (1952).

FUTURE MEETINGS OF
The Electrochemical Society

Chicago, May 2, 3, 4, 5, and 6, 1954

Sessions on

Electric Insulation, Electronics, Electro-Organic Chemistry, Industrial Electrolytics, Theoretical Electrochemistry

Headquarters at the La Salle Hotel

* * *

Boston, October 3, 4, 5, 6, and 7, 1954

Headquarters at the Statler Hotel

* * *

Cincinnati, May 2, 3, 4, and 5, 1955

Headquarters at the Sheraton-Gibson Hotel

* * *

Pittsburgh, October 9, 10, 11, 12, and 13, 1955

Headquarters at the William Penn Hotel

Papers are now being accepted for the meeting to be held in Chicago. Five copies of each abstract (not exceeding 75 words in length) are due at the Secretary's Office, 216 West 102nd Street, New York 25, N. Y., *not later than January 15, 1954.* Complete manuscripts should be sent in triplicate to the Managing Editor of the JOURNAL at the same address.

UNIVERSITY OF MICHIGAN LIBRARIES